LUND
UNIVERSITY

HOST UNIVERSITY: Lund University

FACULTY: Faculty of Engineering

DEPARTMENT: Division of Fire safety Engineering

Academic year 2022-2023

COMBUSTIBILITY STUDY OF RESIN FOR WARM MAGNET COILS USED AT CERN

Juan Carlos Lopez Santiago

Supervisors:

Konrad Wilkens Flecknoe-Brown, Lund University

Dan Madsen, Lund University

Patrick Van Hees, Lund University

Darko Perović, CERN

Master thesis submitted in the Erasmus+ Study Programme

International Master of Science in Fire Safety Engineering

Combustibility study of resin for warm magnet coils used at CERN

Juan Carlos Lopez Santiago

Fire Safety Engineering
Lund University
Sweden

Report 5696, Lund 2023

Master Thesis in Fire Safety Engineering

Combustibility study of resin for warm magnet coils used at CERN

Juan Carlos Lopez Santiago

Report 5696
ISRN: LUTVDG/TVBB—5696--SE

Number of pages: 88
Illustrations: 91

Keywords
Epoxy resin, MCC, TGA, LIFT, Magnetic coils, Radiation, Aging.

Abstract
CERN is the world's largest particle physics laboratory, housing multiple accelerators that rely heavily on magnetic coils. These coils are integral to the generation of powerful magnetic fields essential for particle accelerator experiments, detectors, and other equipment. At CERN, a range of magnetic coils are utilized, many of which are custom-made and located in various research facilities both above and below ground. However, these magnetic coils include epoxy resins, making them susceptible to fire hazards. Given the unique nature of CERN, a thorough engineering approach is required for fire safety design. Therefore, understanding the flammability characteristics of the epoxy resin used in magnetic coils is therefore crucial for ensuring proper fire safety measures at CERN.

The focus of this thesis is to investigate and gain a deeper understanding of the fire risk and fire behaviour associated with the epoxy resins used in magnetic coils at CERN that operate at ambient temperatures. In the first part of the thesis, the key factors that impact the flammability of epoxy resins and composites have been identified and their effects are well understood. Literature shows that the mechanical properties of epoxy resins can degrade due to radiation and aging, which represents a potential ignition source.

The second section of the thesis involves conducting four standardized tests on three representative epoxy resins used at CERN. Two of the epoxy resins are from magnetic coils that have been exposed to radiation environments for a considerable amount of time. These tests include micro-combustion calorimetry, cone calorimetry, lateral ignition and flame spread testing, and thermogravimetric analysis combined with Fourier transform infrared spectroscopy. The tests evaluate the ignition behavior, fire spread behavior, and flammability properties of the epoxy resins.

Fire Safety Engineering
Lund University
P.O. Box 118
SE-221 00 Lund
Sweden

http://www.brand.lth.se

Telephone: +46 46 222 73 60

Disclaimer

This thesis is submitted in partial fulfilment of the requirements for the degree of *The International Master of Science in Fire Safety Engineering (IMFSE)*. This thesis has never been submitted for any degree or examination to any other University/programme. The author(s) declare(s) that this thesis is original work except where stated. This declaration constitutes an assertion that full and accurate references and citations have been included for all material, directly included and indirectly contributing to the thesis. The author(s) gives (give) permission to make this master thesis available for consultation and to copy parts of this master thesis for personal use. In the case of any other use, the limitations of the copyright have to be respected, in particular with regard to the obligation to state expressly the source when quoting results from this master thesis. The thesis supervisor must be informed when data or results are used.

Read and approved,

Juan Carlos Lopez Santiago

June 5, 2023

Abstract

CERN is the world's largest particle physics laboratory, housing multiple accelerators that rely heavily on magnetic coils. These coils are integral to the generation of powerful magnetic fields essential for particle accelerator experiments, detectors, and other equipment. At CERN, a range of magnetic coils are utilized, many of which are custom-made and located in various research facilities both above and below ground. However, these magnetic coils include epoxy resins, making them susceptible to fire hazards. Given the unique nature of CERN, a thorough engineering approach is required for fire safety design. Therefore, understanding the flammability characteristics of the epoxy resin used in magnetic coils is therefore crucial for ensuring proper fire safety measures at CERN.

The focus of this thesis is to investigate and gain a deeper understanding of the fire risk and fire behavior associated with the epoxy resins used in magnetic coils at CERN that operate at ambient temperatures. In the first part of the thesis, the key factors that impact the flammability of epoxy resins and composites have been identified and their effects are well understood. Literature shows that the mechanical properties of epoxy resins can degrade due to radiation and aging, which represents a potential ignition source.

The second section of the thesis involves conducting four standardized tests on three representative epoxy resins used at CERN. Two of the epoxy resins are from magnetic coils that have been exposed to radiation environments for a considerable amount of time. These tests include micro-combustion calorimeter, cone calorimeter, lateral ignition and flame spread testing, and thermogravimetric analysis combined with Fourier transform infrared spectroscopy. The tests evaluate the ignition behavior, fire spread behavior, and flammability properties of the epoxy resins.

Resumen

El CERN es el laboratorio de física de partículas más grande del mundo, albergando múltiples aceleradores de partículas que dependen en gran medida de bobinas magnéticas. Estas bobinas son parte integral de la generación de poderosos campos magnéticos esenciales para experimentos de aceleradores de partículas, detectores y otros equipos. En el CERN, se utiliza una variedad de bobinas magnéticas, muchas de las cuales están hechas a la medida y ubicadas en varias instalaciones de investigación tanto en la superficie como en el subsuelo. Sin embargo, estas bobinas magnéticas incluyen resinas epoxi, lo que las hace susceptibles a riesgos de incendio. Dada la naturaleza única del CERN, se requiere un enfoque de ingeniería completo para el diseño de seguridad contra incendios. Por lo tanto, comprender las características de inflamabilidad de la resina epoxi utilizada en las bobinas magnéticas es fundamental para garantizar las medidas de seguridad contra incendios adecuadas en el CERN.

El enfoque de esta tesis es investigar y obtener una comprensión más profunda del riesgo de incendio y el comportamiento del fuego asociado con las resinas epoxi utilizadas en bobinas magnéticas en el CERN que operan a temperatura ambiente. En la primera parte de la tesis, se identificaron los factores clave que afectan la inflamabilidad de las resinas epoxi y los compuestos epoxi, y se comprenden bien sus efectos. La literatura muestra que las propiedades mecánicas de las resinas epoxi pueden degradarse debido a la radiación y el envejecimiento, lo que representa una fuente potencial de ignición.

La segunda sección de la tesis involucra la realización de cuatro pruebas estandarizadas en tres resinas epoxi representativas utilizadas en el CERN. Dos de las resinas epoxi provienen de bobinas magnéticas que han estado expuestas a entornos de radiación durante un tiempo considerable. Estas pruebas incluyen el calorímetro de micro combustión, calorimetría de cono, prueba de ignición lateral y propagación de llama, y análisis termogravimétrico combinado con espectroscopia infrarroja transformada de Fourier. Las pruebas evalúan el comportamiento de ignición, el comportamiento de propagación del fuego y las propiedades de inflamabilidad de las resinas epoxi.

Contents

List of Figures

List of Tables

1 Introduction

The European Council for Nuclear Research (CERN) is the world's largest particle physics laboratory. Their primary is to understand the fundamental composition of the universe by colliding subatomic particles, revealing insights into particle interactions and the structure of the universe. Due to the distinct nature of CERN, the fire safety approach must consider the advanced accelerators and detectors and their flammability characteristics.

CERN accommodates a remarkable array of accelerators that depend heavily on a diverse range of magnetic coils. Two distinct types of magnet coils are in operation, one set functions under ambient temperatures, while the other set operates under superconductive conditions (i.e 1.9 K or -271.3°C). The magnets operating under ambient temperatures are commonly referred to as 'warm magnets' and constitute the central focus of the ongoing thesis project. These coils are essential for generating magnetic fields that steer and focus particle beams. The custom-made coils incorporate epoxy resins as electrical insulators, which pose a potential fire hazard.

To ensure the safety and well-being of personnel and equipment at CERN, it is imperative to gain a deep understanding of the flammability characteristics associated with the epoxy resins used in the magnetic coils. This knowledge becomes the foundation for implementing fire safety measures and developing robust protocols to prevent and mitigate any potential fire incidents.

1.1 Objectives

The objectives of the current thesis are the following:

1. Conduct a comprehensive analysis of the flammability characteristics of the representative epoxy resins that are commonly used at CERN in warm magnetic coils.
2. Investigate the potential effects of radiation damage on the flammability properties of the epoxy resins used in the warm magnetic coils at CERN.
3. Evaluate the level of fire risk associated with the flame spread that may arise from the epoxy resins used in the warm magnetic coils at CERN.
4. Evaluate the correlation between results obtained from tests conducted on different scales, ranging from micro-scale tests to bench-scale tests, and understand the scalability of different parameters relevant to the analysis, such as heat release rate, heat of combustion, and soot yield.
5. Determine if any studies exist on the impact of aging on the fire performance of the epoxy resins used in the warm magnetic coils at CERN.

1.2 Thesis outline

The following action steps will be undertaken to achieve the objectives:

1. Conduct a literature review to identify the main chemical components that affect the characteristics of epoxy resin composites, the effects of radiation on epoxy resin, the

main factors that influence the flammability of epoxy resins and collect information of fire incidents related to magnetic coils and epoxy resins to identify possible source of ignition and preventive measures.
2. Perform experiments on representative epoxy resins and epoxy resin composites using the micro combustion calorimeter (MCC), the cone calorimeter, the lateral ignition and flame spread test (LIFT) and the thermogravimetric analysis (TGA) coupled to a Fourier transform infrared spectroscopy (FTIR).
3. Analyze the results obtained the experiments, provide recommendations to CERN based on the results of the experiments, propose potential avenues for future research to extend the current thesis and further investigate the topic and conclude.

1.3 Limitations

While the current project achieved several important objectives, there were limitations that should be acknowledged when evaluating the flammability of the magnetic coils. These limitations may affect the conclusions that can be drawn, as well as the certainty and accuracy of the results. Therefore, it is important to interpret our results with caution and consider potential areas for improvement in future research.

One significant limitation in assessing the flammability of the magnetic coils is the absence of standardized test methods for materials with their specific geometry, weight, and size. To address this limitation, smaller samples were cut from the magnetic coils to meet the sample requirements of the standardized test methods that were conducted. An example of sample preparation using segmented components was demonstrated in the LIFT experiments, where magnetic coils were cut into segments and assembled in the sample holder to represent a "straight" connected piece. While testing a representative portion of the magnetic coil material allows for initial insights into its flammability, it is crucial to acknowledge that the behavior at a larger scale may differ due to the material's complexity and the impact of external factors. Therefore, the results obtained from testing smaller samples may not be fully representative of the overall flammability of the magnetic coils, and caution must be exercised when interpreting the results. It is important to consider the limitations of the testing methodology to ensure that the conclusions drawn are valid and accurate.

A second important limitation to consider is the restricted availability of magnetic coils provided by CERN for testing. Due to the difficulty in obtaining more magnetic coils that have been exposed to the working environment of CERN, the tests had to be carefully planned to ensure that the magnetic coils provided were enough for the research. As a consequence of this, the number of repetitions for each test was also limited. This limitation impacts the statistical significance of the results obtained and may have affected the accuracy and reliability of the conclusions drawn from the data. This limitation meant that only three samples of epoxy resin were tested, and it is assumed that the tested epoxy resins are the most representative.

A third important limitation of this project is that it can only be assumed that the shape and size of the magnetic coils sent by CERN are representative of the multiple types

of magnetic coils used at CERN. This assumption implies that the results and conclusions drawn from the project are only valid for the material, size, and shape of the tested magnetic coils, and may not be completely applicable to other types of magnetic coils used at CERN or elsewhere. Therefore, caution must be exercised when extrapolating the results to other materials and geometries.

Finally, it is important to acknowledge a limitation encountered during the development of this thesis project, which relates to the unknown exact composition, age, and irradiation history of the epoxy resins under investigation. Understanding these factors would have provided valuable insights into the flammability characteristics of the epoxy resins, allowing for a more comprehensive analysis of their fire properties.

2 Literature review

Epoxy resins are versatile and widely used in many industrial applications due to their excellent mechanical, thermal and chemical properties (Ellis et al., 1993). However, their flammability remains a significant safety concern. This comprehensive literature review provides valuable insights into previous research conducted on the flammability of epoxy resins. It not only sheds light on the key chemical components that influence the properties of epoxy resin composites but also investigates the effects of radiation on epoxy resin behavior. Additionally, it identifies the primary factors that play a role in determining the flammability of epoxy resins.

Furthermore, this literature review includes an examination of the flammable characteristics of epoxy resins commonly employed as insulation in magnetic coils or similar applications. It also compiles information on fire incidents associated with magnetic coils and epoxy resins, aiming to identify potential sources of ignition and propose preventive measures to mitigate fire risks.

Additionally, the properties of epoxy resins can be influenced by various factors, including exposure to radiation and aging, which can lead to degradation and deterioration of their mechanical and physical properties. Therefore, understanding the effects of radiation and aging on epoxy resins is crucial for improving the durability and reliability of epoxy-based materials. In this literature review, an overview of the effects of radiation and aging on epoxy resins and their composites will also be provided, highlighting the current understanding of the mechanisms involved in these processes and the potential approaches to mitigate their negative impacts.

The relevant literature review was primarily sourced through a search conducted on Google Scholar (scholar.google.com/), the portal web JSTOR (www.jstor.org), the University of Edinburgh's scientific search engine (ed.primo.exlibrisgroup.com) and Lund University's scientific search engine (www.lub.lu.se/en/find/lubsearch). The words used included "Epoxy resin" "flammability study" "radiation effect", "aging of polymers" "flammability", "cone calorimeter tests", "micro combustion calorimeter", "thermogravimetric analysis", "lateral ignition and flame spread test", "chemical composition", "polymers" "epoxy composite" "polymer composite" "failure of epoxy resins" and their combination. In cases where specific assumptions were required, additional sources were purposefully searched.

2.1 Composition of epoxy resin and epoxy composites

Before delving into the topic at hand, it's crucial to grasp the concept of "epoxy resin" and its various constituents. The term "epoxy resin" can refer to the two forms of a resin (Ellis et al., 1993):

1. Unmodified prepolymers that contain reactive epoxy groups or
2. Cured resins where all the epoxy groups may have reacted.

Unmodified prepolymers containing reactive epoxy groups are typically produced by mixing epichlorohydrin with hydroxyl-containing compounds such as phenols or alcohols

(Oyanguren & Williams, 1992). Bisphenol A (BPA) is the most commonly used monomer to synthesize and manufacture unmodified prepolymers. The reaction of BPA with a large excess of epichlorohydrin yields Bisphenol A diglycidyl ether, which is also referred to as BADGE or DGEBA (Ellis et al., 1993). BADGE is a type of Bisphenol A epoxy polymer or Bisphenol A epoxy resin (Ellis et al., 1993) (Brugner & Jonnatti, 1983). It is worth noting that the properties of BADGE can vary depending on the number of structural units, denoted by the variable n. Therefore, different types of BADGE exist.

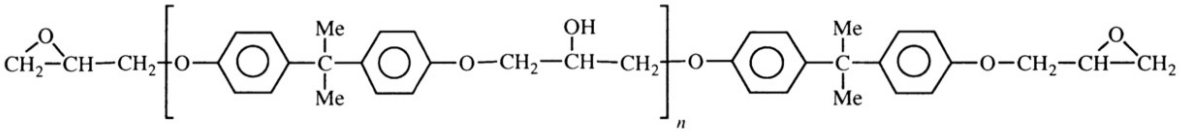

Figure 1: Structure formula of Bisphenol A diglycidyl ether.

To transform the liquid unmodified polymer into a solid state, it needs to be combined with a curing agent, also known as a hardener or crosslinking agent. A diverse range of curing agents is available, with amines, carboxylic acids, and anhydrides being the most prevalent. The final properties of the epoxy resin are determined by the reactivity of the epoxy rings in the unmodified prepolymer, and the curing agent used. For instance, when BADGE is cured with carboxylic acid anhydrides, the resulting epoxy resin is ideal for electrical insulation applications (Ellis et al., 1993).

Cured epoxy resins may also contain various additives to modify their properties and characteristics. These additives may include (Ellis et al., 1993):

1. Diluents
2. Fillers
3. Resinous modifiers
4. Flexibilisers/plasticising additives
5. Elastomeric modifiers
6. Thermoplastics
7. Promoters or accelerators

In addition to unmodified prepolymers and curing agents, fillers play a crucial role in the makeup of epoxy resins. By altering the properties of the resin, fillers can improve mechanical strength, thermal characteristics, electrical conductivity, and viscosity. In electrical applications, fillers such as mica, quartz, and silica are often added to increase the dielectric strength and thermal conductivity of the epoxy resin (Ellis et al., 1993).

Epoxy resins are a popular choice for producing composite materials, commonly known as epoxy composites, which are reinforced with fibrous materials. The selection of fiber reinforcement type and form is dependent on the desired properties of the final product. Typically, continuous sheets of aramid, carbon, or glass fibers are used. These materials are integrated with the resin to form a strong, stiff, and lightweight composite that displays anisotropic behavior. The resulting composite has exceptional strength-to-weight and stiffness-to-weight ratios, making it ideal for a wide range of applications (Ellis et al., 1993).

Epoxy resins are a type of polymer that undergo decomposition rather than melting when exposed to high temperatures. This is due to their chemical structure, which is made up of highly crosslinked chains that are unable to flow or reorganize at high temperatures. When heated, the epoxy resin will break down into smaller molecules and ultimately undergo thermal degradation, resulting in the release of various volatile compounds (Dao et al., 2013) (Ellis et al., 1993).

2.2 Combustibility study of epoxy resins

During the literature review, previous research papers and reports on flammability studies were consulted to gain insights into the expected behavior of epoxy resin and epoxy composites. The purpose was to compare possible results from different test methods and to gain a better understanding of the materials.

First, it would be important to understand the influence of non-flammable materials used as reinforcement in epoxy composites. In the study by Scudamore et al. (1991), various plastic materials were tested using the cone calorimeter to investigate their burning behavior. Among these materials were two epoxy resin samples: one consisting of epoxy resin alone, and the other containing fiber laminates comprising 69% glass. The pure epoxy resin sample was 11 mm thick and had a density of 1195 kg/m^3, while the reinforced epoxy resin had the same thickness and a higher density of 1917 kg/m^3. However, the exact composition of the epoxy resin used in the study was not specified. The samples were subjected to heat fluxes ranging from 20 to 50 kW/m^2. The experimental findings indicate that the glass-reinforced epoxy resin started emitting pyrolysis gases at a quicker pace than the pure epoxy resin sample. Furthermore, the glass-reinforced epoxy resin showed sharp peaks immediately after ignition, which could be attributed to the presence of a resin-rich layer on the surface. Additionally, it is possible to observe from the results shown in table 1 that the glass-reinforced epoxy resin exhibited a lower peak and mean heat release rate.

A different trial, which yielded comparable outcomes, was performed by Dao et al. (2013). Samples of BADGE-based epoxy composites with an amine-type hardener and varying content of carbon fiber laminates (56 and 59 vol%) were tested by Dao et al. (2013) in a cone calorimeter using a heat flux range of 14-75 kW/m^2. These types of epoxy resins are commonly used in hydrogen storage cylinders. The square samples measured 100 $\pm$ 0.5 mm on each side and were 10.1 $\pm$ 0.5 mm thick. The samples with a composition of 56 vol% carbon fiber had a weight of 174.2 $\pm$ 2.8 g, while those with a composition of 59 vol% carbon fiber weighed 148.7 $\pm$ 1.8 g. Table 2 illustrates that composites with higher carbon fiber content have lower thermal response parameter and thermal inertia values. Additionally, the table indicates that the ignition time is shorter for composites with higher carbon fiber content. As per Dao et al. (2013), the lower thermal response and inertia in composites with higher carbon fiber content can be attributed to the fact that carbon fiber is a thermally thick material. When the composite is heated, the carbon fiber surface heats up faster than the epoxy resin, and as the carbon fiber content increases, more heat is transferred from the carbon fiber to the epoxy resin. This leads to the release of a sufficient amount of flammable gases for flaming ignition with less energy.

Description	Heat flux (kW/m^2)	Epoxy resin	Epoxy resin reinforced with glass
Time of ignition (s)	20	252, 507, 253	380, 271,309
	30	153, 181, 181	102,125,132
	40	98,97,106	69, 74, 82, 75
	50	60, 60, 65	68, 62, 40
Mean peak heat release rate (kW/m^2)	20	392	164
	30	453	161
	40	560	172
	50	706	202
Mean effective heat of combustion (MJ/kg)	20	25	27
	30	25	28
	40	25	28
	50	25	27
Mean heat release rate (kW/m^2)	20	286	82
	30	323	86
	40	391	98
	50	426	102

Table 1: Characteristic parameters of two epoxy resin types using cone calorimeter (Scudamore et al., 1991)

Additionally, a higher carbon fiber content results in the release of more pyrolysis gases for a similar heat flux, causing a reduction in ignition time.

Description	59 Vol%	56 Vol%
Critical heat flux - CHF (kW/m^2)	14	18
Temperature of ignition at 40 kW/m^2 (°C)	300	240
Time of ignition at CHF (s)	1500	830
Time of ignition at 20 kW/m^2 (s)	659 ± 32	750 ± 30
Time of ignition at 75 kW/m^2 (s)	29 ± 2	33 ± 2
Thermal response parameter ($kWs^{\frac{1}{2}}/m^2$)	370	435
Thermal inertia (kW^2s/m^4K^2)	2.25	5.07

Table 2: Characteristic parameters of carbon fiber/epoxy composites based on bisphenol A and amine as hardener (Dao et al., 2013)

Investigating the effect of fillers on the flammability of epoxy resins, McBride (1991) subjected two epoxy composite samples sourced from different manufacturers, utilized as electrical insulation in cast coil transformers, to TGA. The researchers then analyzed the pyrolysis gases using a chromatogram. The first sample tested by McBride (1991) was a bisphenol A-based epoxy reinforced with fiberglass fibers, without any filler. When subjected to TGA, the sample was heated at a rate of 10°C/min under nitrogen atmosphere and began pyrolyzing at 300-350°C, with complete decomposition observed at 475°C. In an oxygen and nitrogen atmosphere, the sample began decomposing at 250°C and underwent oxidation between 350-435°C. Approximately 85% of its weight was pyrolyzed, while the remaining 15% underwent oxidation between 535°C-580°C. The second sample was

also bisphenol A-based epoxy reinforced with fiberglass fibers, but this time with quartz powder as an added filler to enhance its strength. During TGA analysis, conducted with a heating rate of 10°C/minute under nitrogen atmosphere, the sample lost half of its mass at 420°C, with the remaining half corresponding to the filler. When tested under an air atmosphere, the sample began decomposing at 250°C, followed by a first oxidation step between 330-420°C with a weight loss of 40%, and a second oxidation step between 450-500°C with a weight loss of 15%. Although the precise composition of the epoxy resins is not specified, it is apparent that the initial decomposition temperature and the temperature at which the highest mass loss rate occurred were nearly identical and remained unchanged. The only discernible difference was in the amount of residual mass after decomposition. However, it is crucial to note that these results were obtained from micro-scale samples, and the impact of scale-up on the flammability of epoxy resins may vary.

A TGA study using air atmosphere was carried out by Tarrio-Saavedra et al. (2008), in which various samples of diglycidyl ether of trimethylolpropane based epoxy resin were tested with m-xylylenediamine as a curing agent. The samples had different filler loadings, ranging from 10% to 50% by weight of silica. The study found that the TGA parameter values remained relatively unchanged with varying filler content, including the initial decomposition temperature and the temperature of maximum rate of mass loss, indicating that the filler content had little effect on the results. The primary distinction lies in the tendency of epoxy residue to increase after the initial degradation step, primarily attributed to the higher silica content.

The thermal decomposition of epoxy composites is generally discussed in the works of Mouritz and Gibson (2007) and Dao et al. (2013). According to these sources, the first stage of decomposition occurs when the epoxy resin is exposed to a high external heat flux, which causes the release of volatile gases, solid carbonaceous char, and soot particles, mainly due to mechanism of random chain scission. During this phase, volatile substances are generated which can combine to create a flammable mixture that is capable of igniting in the presence of an external ignition source. The next phase follows after ignition, during which the rate of mass loss sharply rises, and the epoxy-based compounds decompose to create gaseous species and carbon char. During the thermal degradation of epoxy resins, it is possible for some epoxy resins to undergo a transition state where they produce liquid compounds, which depend on the chemical composition of the epoxy resin. If solvent monomers are used in the curing process, they may contribute to the formation of liquid compounds. Furthermore, the layer of carbon char reduces the transfer of heat to the epoxy resin and inhibits the release of pyrolysis gases, resulting in a decrease in the rate of mass loss. During the third phase, the remaining epoxy resin is decomposed and ignited. Mouritz and Gibson (2007) points out that during the fast mass loss phase, the volatile gases may accumulate, causing the char layer to foam and swell.

The pyrolysis of epoxy resins can release toxic gases, as demonstrated in an experiment conducted by McBride (1991). The study analyzed the pyrolysis gases from samples of Bisphenol A epoxy resin using a chromatogram. Four toxic gases - benzene, toluene, ethylbenzene, and phenol - were detected, with a higher concentration observed in a nitrogen atmosphere since these gases were not able to oxidize. However, it was found

that the concentration of these toxic gases remained below the threshold limit value (TLV) established by the Occupational Safety and Health Administration (OSHA). In addition, other volatile hydrocarbons and hardeners used in the curing process were also identified in the pyrolysis gases.

Compound	Concentration (mg/g)			
	Air atmosphere		Nitrogen atmosphere	
Benzene	3.1	1.2	7.8	1.24
Toluene	0.65	0.26	1.9	0.86
Ethylbenzene	0.12	0.25	0.15	0.13
Phenol	2.8	4.3	10.0	-

Table 3: Concentration of toxic pyrolysis gases of two bisphenol A based epoxy resins (McBride, 1991)

A similar result was obtained by Brugner and Jonnatti (1983), who determined experimentally the combustion products of BADGE using a gas chromatograph-mass spectrograph. Two types of samples of 0.25 g were tested, one cured sample of BADGE, and the other one made of cured sample of BADGE but with 64.6% copper, 20% glass fiber reinforcement and 0.4% quintex paper to simulate a real transformer coil assembly. For both types of samples, four toxic compounds were found: toluene, ethylbenzene, benzene, and phenol.

In another study conducted by Brugner and Jonnatti (1983), similar results were obtained. The study investigated the combustion products of BADGE using a gas chromatograph-mass spectrograph. Two types of samples, each weighing 0.25 g, were tested. The first sample consisted of cured BADGE, while the second was made of cured BADGE with 64.6% copper, 20% glass fiber reinforcement, and 0.4% quintex paper to simulate a real transformer coil assembly. In both sample types, the presence of four toxic compounds was detected: toluene, ethylbenzene, benzene, and phenol.

Description	Value
Phenol (ppmw)	26
Toluene (ppmw)	2.6
Ethylbenzene (ppmw)	2
Benzene (ppmw)	1.5

Table 4: Concentration of toxic pyrolysis products of two bisphenol A based epoxy resins (Brugner & Jonnatti, 1983). ppmw = Part per million by weight.

In their study, McBride (1991) examined the behavior of epoxy composites when subjected to an external flame source, electric arc, or short circuit in epoxy encapsulated transformer coils. The coils tested were 0.91 m (36 in) in length, had an internal diameter of 0.58 m (23 in), and an external diameter of 0.45 m (18 in) in height. The conductors were made of aluminum and covered with fiber glass and epoxy resin, which had a total thickness of 0.64 cm ($\frac{1}{4}$ in) over the winding. The first test involved exposing the coils to different electric arc durations, and the study found that the coil self-extinguished within a short period of time. In the second test, a short circuit was induced for a duration of 2 seconds, which resulted in burning a thin layer of the epoxy resin surface. However, a

layer of soot was formed, which protected the resin below from ignition. To investigate the behavior of epoxy composites under external fire conditions, McBride (1991) conducted a third series of experiments where the coil was subjected to three different external flame sources. These included an oxyacetylene cutting torch from below, a wood placed below, and a propane flame applied from the side of the coil. In all three cases, the flames from the epoxy resin extinguished shortly after the external heat source was removed. The study concluded that in case of a transformer coil being exposed to an external fire, the epoxy resin would burn, but it would not significantly contribute to the fire size. This is due to the composition of the coil, which includes epoxy resin, "non-flammable fillers", insulating materials such as fiberglass, and metal coils that dissipate and conduct heat. However, it is important to note that the methods used in this study are not standardized, so the results should only be considered qualitative.

As reported by McBride (1991), transformer coils, which are type of magnetic coils, are susceptible to ignition from two primary sources. The first source is internal failure within the transformer coil, which can generate a hot spot that exceeds the design limits of the transformer, resulting in the formation of an electric arc that can ignite surrounding materials. The second source of ignition is an external heat source that the transformer may be exposed to. It is essential to recognize both of these potential ignition sources and take appropriate precautions to reduce the risk of a transformer coil fire. The investigation indicates that the most prevalent internal failure in transformer coils is stress cracking, which occurs due to the thermal expansion of conductors enclosed in epoxy resin. The research discovered that the relative thermal expansion rate of pure epoxy resin is approximately 70 x 10^{-6} $°C^{-1}$, whereas the expansion coefficient for glass-reinforced epoxy resin is approximately 45 x 10^{-6} $°C^{-1}$ and for aluminum, it is approximately 23 x 10^{-6} $°C^{-1}$. The study found that stress cracking is the most common internal failure in transformer coils due to the thermal expansion of conductors encapsulated in epoxy resin. The relative thermal expansion rate of pure epoxy resin is higher than the conductor, which can lead to stress cracking. To prevent this, it is important to consider the expansion rates when designing and manufacturing transformer coils.

In the following part of this section, there is a compilation of various test data on epoxy resin and epoxy compounds, which will be compared with the results obtained from our project.

Zhang et al. (2011) conducted an experiment where samples manufactured by mixing 100 g of BADGE with 12 g of m-phenylenediamine as a curing agent were tested. The mixture was cured at 80°C for 2 hours and then post-cured at 150°C for an additional 2 hours before testing. To conduct the TGA test, the researchers heated 10 mg samples of the epoxy resin mixture at a rate of 20 K/min in a nitrogen atmosphere, ranging from 40°C to 800°C. For the cone calorimeter test, they tested three samples of the same mixture, each with dimensions of 100 x 100 x 3 mm, using a heat flux of 50 kW/m^2. The results of both tests are presented in table 5.

Hurley et al. (2015) provides a range of critical heat flux values for ignition of epoxy resins with unknown composition, ranging from 13 to 20 kW/m^2. Additionally, the critical heat flux for ignition of epoxy resin reinforced with glass fiber falls between 10-15 kW/m^2 as reported in the same handbook.

Description	Value
Onset temperature at 5% weight loss by TGA (°C)	372
Temperature at maximum weight loss rate by TGA (°C)	479
Residues at 800°C by TGA (%)	11.6
Time of ignition in cone calorimeter (s)	45
Peak heat release rate in cone calorimeter (kW/m^2)	855
Total heat released in cone calorimeter (MJ/m^2)	118

Table 5: Characteristic parameters of bisphenol A with amine as curing agent. TGA was conducted in nitrogen atmosphere (Zhang et al., 2011).

A research conducted by Y. Xu et al. (2020), specimens composed of Araldite LY 1564 SP-based epoxy resin that was reinforced with carbon laminates underwent testing using a cone calorimeter. The forming process of the specimens differed, with some manufactured through vacuum bagging and others through autoclaving. The specimens had an average thickness of 2.5 ± 0.3 mm and were prepared using Hardener XB 3487 in a mass ratio of 100:34. The calculated critical heat flux was 14.48 kW/m^2 for the vacuum bag-formed samples and 20.56 kW/m^2 for the autoclave-formed ones. The theoretical heat of combustion was 33.27 MJ/kg for the vacuum bag-formed samples and 43.82 MJ/kg for the autoclave-formed samples.

	Carbon/epoxy composites with vacuum bag as forming processes					Carbon/epoxy composites with autoclave as forming processes				
External heat flux (kW/m^2)	30	35	55	75	80	30	35	55	75	80
Peak HRR 1 (kW/m^2)	442	451	532	582	636	99	150	218	229	266
Peak HRR 2 (kW/m^2)	—	—	—	—	—	96	131	141	153	177
Av-HRR (kW/m^2)	63.84	64.38	81.41	84.22	86.61	24.78	39.44	42.39	55.72	59.5
EHC (MJ/kg)	31.59	31.98	32.69	31.92	33.6	34.88	34.26	36.32	35.2	36.07

Table 6: Heat release rate data obtained from the cone calorimeter at various levels of radiant heat flux (Y. Xu et al., 2020).

In a study by Wang and Zhang (2019), the cone calorimeter was used to analyze specimens consisting of epoxy resin with Araldite LY1564SP and HardenerXB3487 as the curing agents. The researchers estimated a critical heat flux of ignition of 12.12 kW/m^2 for the specimens. The specific curing process is unknown.

The following points summarize the key results of this section:

- The reinforcement of epoxy resins with glass fiber or carbon fiber reduces the time of ignition.
- The effects of the filler on the flammability of the epoxy resin are not significant when it is tested in micro-scale tests like TGA.

Thermal radiation intensity (kW/m^2)	Heat release rate (kW/m^2)		
	Peak	Average value (300 s)	Peak time (s)
25	605.9	83.7	83
30	643.7	86.1	67
35	699.6	88.4	53
40	745.9	91.3	42
50	890.2	96.6	37
55	960.1	105.2	30

Table 7: Peak heat release rate, and the average heat release rate of the first 300 s of the specimen under various thermal radiation intensities (Wang & Zhang, 2019).

- When subjected to the combustion process, epoxy resins undergo decomposition and generate volatile gases, solid carbonaceous char, and soot particles. It is worth noting that certain types of epoxy resins may also experience a transition phase during combustion, during which liquid compounds are produced.
- Phenol, toluene, ethylbenzene, and benzene are among the toxic gases that are typically produced as a result of the pyrolysis of epoxy resins.
- Transformers, a type of magnetic coils, are susceptible to ignition from both internal failures and external heat sources. The most frequent cause of internal failure is thermal expansion, which can lead to mechanical failure, resulting in a short circuit that could potentially start a fire.
- According to the collect records, the common range of the critical heat flux of ignition of epoxy resin is between 12.12 and 20.56 kW/m^2.

2.3 Effect of radiation on epoxy resin

Radiation can be broadly classified into two types: ionizing radiation and non-ionizing radiation. Ionizing radiation causes atoms and molecules to be ionized, that is, electrons are removed from the atom or molecule leaving it with an electrical charge, while non-ionizing radiation does not (Wood & Karipidis, 2017). Ionizing radiation includes particle beams such as alpha-particles, beta-particles and neutron particles, as well as electromagnetic waves such as gamma radiation.

In terms of the effects of radiation on polymers, there are two primary types: transient effects and permanent effects. Transient effects refer to changes that occur in response to radiation exposure, such as an exponential decrease in electrical resistance in plastic and elastomeric materials, which returns to normal after the exposure to irradiation ends (Schönbacher & Van de Voorde, 1975). Permanent effects, on the other hand, are changes that result from damage mechanisms caused by radiation exposure, such as cross-linking, chain scission, gas evolution, oxygen and radical evolution (Spindel, 1993). These effects can be long-lasting and significantly alter the properties of the polymer material.

The effects of radiation on polymers, including both transient and permanent changes, are influenced by several factors such as the composition of the polymer, the type of radiation, and the presence of oxygen in the environment. The content of oxygen in the

atmosphere can have a significant impact on the degradation of polymers, as it reacts with primary free radicals generated by radiation exposure, leading to the formation of secondary radicals and accelerating the degradation process (Guarino et al., 2001). In polymers, such as epoxy resins, permanent effects caused by radiation exposure are primarily due to cross-linking and chain scission (Kacem et al., 2019) (Guarino et al., 2001). Cross-linking occurs when two separate chains of the polymer become linked together, resulting in a stiffer and more brittle material. In contrast, chain scission involves the separation of bonds within the polymer chains, leading to a softer and weaker material (Guarino et al., 2001). These mechanisms are illustrated in figure 2.

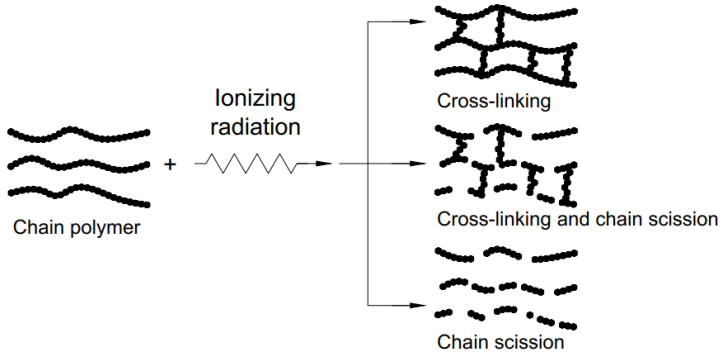

Figure 2: Main damaging mechanisms of epoxy resins due to ionizing radiation: Cross-linking and chain scission (Spindel, 1993) (Ovsik et al., 2020).

According to Spindel (1993), mechanical failure is the primary mode of failure in polymers due to mechanical stress. However, the effects of irradiation can lead to the degradation of thermal and electrical properties, but only after the mechanical properties of polymers have already begun to deteriorate. It is also suggested that the application of a mechanical load is often the cause of electrical failure that would not have occurred otherwise, therefore, the evaluation of strenght of polymers is critical. To compare the effects of radiation on epoxy composites, researchers often evaluate the interlaminar shear strength (ILSS). This measure provides insight into the material's ability to resist thermal and mechanical stresses and can indicate the extent of damage caused by radiation exposure (Wu et al., 2013).

In a study conducted by Wu et al. (2013), the effects of gamma irradiation at 77 Kelvin on an epoxy composite were investigated. The composite was made up of epoxy resin based on diglycidyl ether of bisphenol F, cured using diethyl toluene diamine, with IPBE as a modifier agent, and reinforced with glass fiber. It is important to note that the ionizing radiation dose used in the International System of Units (SI) is the Mega Grays (MGy). The results of the study showed that at radiation doses below 5 MGy, the interlaminar shear strength (ILSS) of the tested material was only slightly reduced. This was because the effect of cross-linking and chain scission on the epoxy resin was proportional. However, at higher doses of 10 MGy, the ILSS of the composite decreased significantly, and the stiffness of the material decreased. This indicated a decrease in Young's modulus and a prevalence of chain scission over cross-linking. This conclusion was confirmed by using DSC, which showed a slight decrease in the glass transition temperature of the epoxy resin as the dose was increased. Chain scission breaks chemical bonds, causing

a reduction in the glass transition temperature, whereas cross-linking causes different chains to join, increasing the glass transition temperature. Further analysis using FTIR spectroscopy showed an increase in the carbonyl groups released by the epoxy resin after being exposed to higher radiation doses, particularly at 10 MGy. This indicates that irradiation leads to a higher oxidative reaction damage.

In a similar experiment, Debré et al. (1997) tested BADGE-based epoxy resin with diaminodiphenylmethane (DDM) as a hardener in an air atmosphere. Multiple samples were irradiated with different doses up to 2 MGy and tested using dynamical mechanical analysis (DMA) coupled with FTIR. The results showed that there were no changes in the composition of the inner layers of the epoxy resin, and the only effect observed was a higher level of radio-oxidation on the surface, as a function of the radiation dose. In another study, Longiéras et al. (2007) irradiated different samples of BADGE-based epoxy resins with aliphatic amine as a hardener in both oxygen atmosphere and in an helium atmosphere. The results were similar to those obtained by Wu et al. (2013) and Debré et al. (1997); chain scission governed the degradation of the epoxy resin at high radiation doses in any atmosphere. However, the radio-oxidation process only affected the surface due to the low oxygen diffusion coefficient of epoxy resins when it was tested in the oxygen atmosphere.

When it comes to the flammability of materials, there has been limited research conducted to understand the effects of radiation. Schönbacher and Van de Voorde (1975) conducted a study where two types of polymers commonly used as cable insulating materials were examined: thermoplastics and elastomers. Specifically, the study focused on five different materials: polyvinylchloride (PVC), polyethylene (PE), chlorosulfonated polyethylene (CSPE), ethylene propylene rubber (EPR), and silicon rubber (SIR). The materials were subjected to neutron and gamma radiation doses ranging from $5x10^7$ to $5x10^8$ rad (0.5 MGy and 5 MGy), and their flammability was tested using the oxygen index test according to ASTM D2863. This test determines the minimum concentration of oxygen required in a nitrogen mixture to sustain combustion of a sample. The results of the study showed only small increase in the oxygen index of the different materials, indicating that there was not a significant change in their flammability properties after exposure to radiation. However, although the standard oxygen index test is a useful tool for comparing the relative flammability and ranking of polymers and composite materials, it has limitations. One significant limitation is that it does not measure the ease of ignition of a sample, as the ignition conditions are not clearly defined in the standards. Therefore, this test is not an accurate representation of fire behavior under realistic conditions. However, it is still commonly used in quality control applications due to its precision (Weil et al., 1992). Additionally, Schönbacher and Van de Voorde (1975) observed that the process of radiation-induced embrittlement in insulating structures can lead to cracks or flakes in the insulation, which can cause electrical circuits to fail through either an open or short circuit.

It is possible to conclude the following from the literature review regarding the effects of radiation on epoxy resins:

- There are no specific papers specifically addressing the effects of long-term radiation exposure on polymers. Most research in this field has focused on the effects of

radiation on polymers at varying doses over short periods of time. However, the conditions at CERN, where some magnetic coils have been operating for many years, differ from the typical testing scenarios.

- When epoxy resins are exposed to radiation doses below 5 MGy in an air atmosphere over a relatively short period of time, the degradation caused by cross-linking and chain scission is proportional, and the material's strength is typically not affected. However, it is unclear whether the continuous degradation over long periods of time would eventually lead to a degradation of its mechanical properties, as no studies have been conducted to investigate this possibility.
- Although mechanical failure is the primary mode of failure in polymers used in radioactive environments, it is crucial to acknowledge that degradation of their electrical and thermal properties may also occur after the mechanical properties have already begun to deteriorate.
- The potential degradation of epoxy composites under continuous exposure to the working conditions at CERN over several years is currently unknown. However, this degradation could potentially lead to electrical failure in the magnet coils, which could in turn serve as an ignition source.

2.4 Effect of aging in polymers

Epoxy resins and epoxy composites are highly versatile materials that are employed in various applications, thanks to their excellent mechanical, thermal, and chemical properties. However, long-term exposure to harsh environmental conditions, such as high temperature, can cause the epoxy resin to age and gradually degrade (Odegard & Bandyopadhyay, 2011) .

This aging process is marked by an increase in mass density due to a decrease in the free volume present in the molecular structure, as well as a decrease in molecular configurational energy. As the aging process continues, the specific volume and molecular energy of the material gradually decreases until they reach a state of equilibrium (Odegard & Bandyopadhyay, 2011). The aging of a physical material such as epoxy resin can be quantified using the enthalpy change dh = du + $p$dv, where the therm du represents the change in internal energy, and the second term $p$dv represent the change in volume, and both will depend on the initial conditions of the epoxy resin (Montserrat, 1994).

The degradation of epoxy resins over time can have a significant impact on their overall thermo-mechanical properties. This can result in a reduction in the material's strength, thermal stability, and chemical resistance. Although there is a small increase in elastic modulus due to aging, the ultimate tensile strength of the material decreases under tension. This decrease in tensile strength can lead to the embrittlement of the resin, which can make it more susceptible to the growth of microcracks at lower loads. There is also a reduction in the thermal expansion coefficient caused by the increase in density of the epoxy resin (Odegard & Bandyopadhyay, 2011).

Kong (2005) observed that the physical aging of composite materials produces a similar effect on their properties as it does on neat epoxy resins. However, it has been

observed that the load-transfer characteristics of fiber reinforced composites generally remain unaffected by the aging process. In other words, the material's ability to distribute loads and resist deformation under stress typically remains intact even as it ages.

Regarding the change of flammability of polymers due to aging, Xie et al. (2010) conducted TGA+FTIR and MCC analyses to evaluate the quality of PVC sheaths in both newly installed and decade-old cables. The results indicate that at temperatures above 550 K, the mass loss rate of the older cables was higher compared to the new ones. However, for lower temperatures, the mass loss rates were similar in both cases, suggesting that the sheath material retains its performance over time to a significant extent. The results also show that the emission of hydrochloric acid, toxic gases released during the pyrolysis of PVC, is faster for the old PVC. The MCC also shows a higher peak HRR for old material than new one.

It is possible to draw the following conditions:

- The thermo-mechanical properties of epoxy resins are degraded by the aging process, caused by the reduction of the free volume and molecular energy of the material.
- In general, the combustion and pyrolysis of old PVC is more intense in comparison to new one.
- Therefore, it can be assumed that polymers with similar properties may exhibit a similar increase in flammability over time, based on the behavior of PVC.
- Aging-induced degradation of epoxy resins can lead to the formation of microcracks, cracks, or other failure modes, which can cause open or short circuits in magnetic coils, potentially leading to ignition.

3 Methodology

This section provides a comprehensive description of the samples to be tested and their preparation for each test method. It also outlines the various test methods that were conducted, including the main steps involved in the experimental processes and the calculation procedures. In section 4, the nomenclature and dimensions of each sample that underwent individual testing, as well as the comprehensive results and discussion for each test are provided.

In total, four different test methods were conducted as part of the current project:

1. Microscale combustion calorimeter
2. Cone calorimeter
3. Lateral ignition and flame spread test
4. Thermogravimetric analysis + Fourier-transform infrared spectroscopy

3.1 Samples

CERN is an unparalleled facility in the world that extensively employs warm magnetic coils, particularly in its accelerators. These coils are distinctive in their design, making it a unique challenge to evaluate any potential hazards posed by the epoxy resins used in their construction. To address this issue, a decision has been made to examine two representative epoxy composites gathered from two coils that were dismantled from an operational accelerator at CERN. Furthermore, samples of pure epoxy resin that were recently manufactured were also tested. Throughout this thesis, the following names will be utilized:

1. Magnetic coil type 1
2. Magnetic coil type 2
3. Fresh epoxy resin

The quadruple magnetic coil that the magnetic coil type 1 was previously a part of has a ring-shaped structure, as shown in figure 3. With an approximate length of 80 cm and an average cross-section of 6.5 cm x 1.5 cm, this coil is engineered to precise specifications. To begin with, each coil (1) is wrapped with a 0.1 mm layer of polyamide, followed by a 0.4 mm layer of glass fiber tape, as per its specifications (2). The cross section of coils are arranged and wrapped together, as observed in figure 3, using a 0.5 mm layer of glass fiber (3). Afterward, the entire coil is impregnated with epoxy resin to enhance its strength and durability. The cross section of the epoxy resin type 1 can be seen in figure 4. The upper layer of the glass fiber wrapping each individual coil appears brown, while the glass fiber used to wrap the cross-section is transparent and coated with hard transparent epoxy resin. The finishing texture is smooth. Furthermore, to achieve the final dimensions of the magnetic coil, a filler was added to its cross-section (4). The chemical composition of this filler is unknown, but it was also impregnated with epoxy resin. The filler had a smooth surface and a green color.

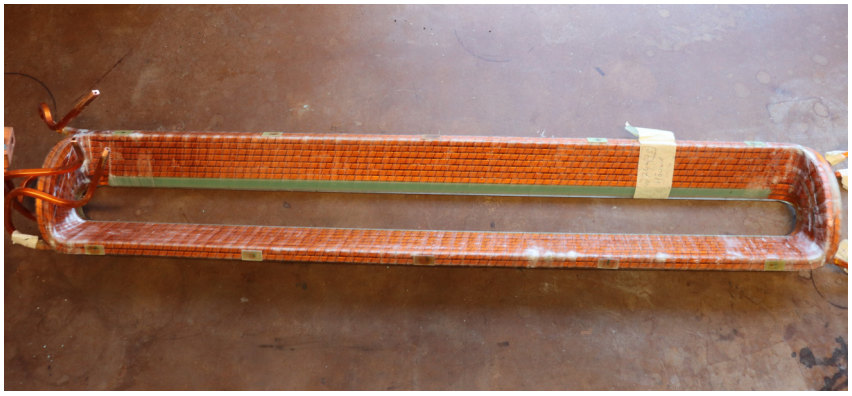

Figure 3: Magnetic coil type 1

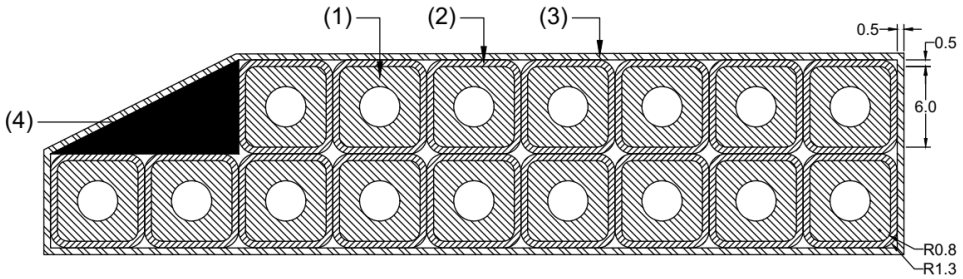

Figure 4: Magnetic coil type 1. Sketch of cross section. (1) Metallic core, (2) polyamide and glass fiber tape, (3) glass fiber tape and (4) filler.

Magnetic coil type 2 was previously a part of a dipole main assembly magnetic coil, which, like the magnetic coil type 1, has a ring-shaped structure, as observed in figure 5. The longest two sections of this coil are bent with different radius of curvature, with the upper section having a radius of 96 cm and the lower section having a radius of 91 cm. The entire assembly is approximately 117 cm long and 59 cm wide, with an average cross-section of around 10 cm x 6.4 cm, as shown in figure 7. As per its corresponding specification, each individual coil (1) is wrapped with glass fiber tape (2), and then the cross-section is wrapped once again with glass fiber (3). The upper layer of the wrapping surrounding each coil appears light yellow. However, the glass fiber wrapping around the cross-section is transparent and coated with a hard, transparent epoxy resin. The finishing texture is uneven, with small accumulations of epoxy resin spread across its entire surface.

It is important to outline that the exact composition of epoxy resin used in the magnetic coil type 1 and type 2 are unknown, and both have been operating in radiation environments at CERN for a substantial period of time.

For this project, additional samples of fresh epoxy resin were cast specifically for testing purposes. Unlike the epoxy resin used in magnetic coils type 1 and type 2, this particular epoxy has never been exposed to CERN's accelerator working environment. As per the Polymer laboratory at CERN, this specific type of polymer is widely used in magnet coils at CERN and hence, considered as a representative sample. This epoxy resin is based on a solvent-free unmodified bisphenol A epoxy resin (commercially known as Araldite F) that was cured using a modified carboxylic anhydride (commercially known

as Hardener HY 905). Additionally, it contains a low viscous, solvent-free polyglycol as a flexibilizer (commercially known as DY 040) and a solvent-free tertiary amine as an accelerator (commercially known as DY 061). The ratio of bisphenol A epoxy resin to hardener is 1:1, while the ratios of flexibilizer to epoxy resin and accelerator to epoxy resin are 1:10 and 1:100, respectively. The epoxy resin was cured for 6 hours at 80°C, followed by 10 hours at 130°C. Its color is brown, and the surface is completely smooth.

During the initial stages of this project, it was impossible to determine or make assumptions about the similarity or identity of the composition between the fresh epoxy resin and the epoxy resin utilized in magnet coils of type 1 and type 2.

Figure 5: Two magnetic coils type 2

Figure 6: Magnetic coil type 2. Zoom in of accumulation of epoxy resin

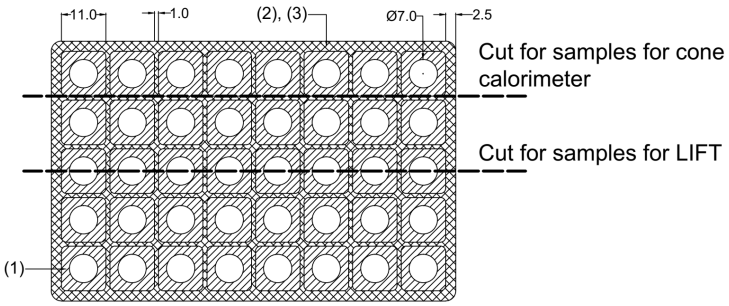

Figure 7: Magnetic coil type 2. Sketch of cross section. To prepare the samples for the cone calorimeter, a cut was made at the location shown in the figure. (1) Metallic core and (2), (3) glass fiber tape

The microscale combustion calorimeter (MCC), cone calorimeter, and thermogravimetric analysis (TGA) coupled with Fourier-transform infrared spectroscopy (FTIR) tested magnetic coil type 1, magnetic coil type 2, and fresh epoxy resin. However, the lateral ignition and flame spread test (LIFT) requires a larger sample size, and thus, it was not feasible to test the fresh epoxy resin using this method.

For the MCC and TGA + FTIR tests, only the epoxy resin collected from the magnetic coil type 1 and type 2 samples were tested, without including the metallic core or glass fiber tape. Conversely, for the cone calorimeter and LIFT tests, a section of the magnetic coils type 1 and type 2 were cut and tested. These samples included both the metallic coil and the epoxy composite, consisting of the epoxy resin and the glass fiber tape. Their respective nomenclature is included in the table 8.

Material	Nomenclature for MCC and TGA + FTIR	Nomenclature for cone calorimeter and LIFT
Magnetic coil type 1	Epoxy resin type 1	Epoxy composite type 1
Magnetic coil type 2	Epoxy resin type 2	Epoxy composite type 2
Fresh epoxy resin	Fresh epoxy resin	Fresh epoxy resin

Table 8: Sample nomenclature for each individual test method

The sample identification tags used in this project will use a three digit code as shown in figure 8.

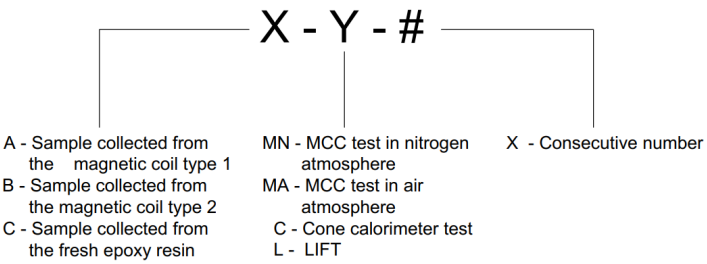

Figure 8: Sample identification tag convention

3.2 Experimental setup

Due to the unique size of the whole magnetic coils, there are currently no standardized experiments with repeatable results that can be used to assess their flammability. Therefore, the current project involves conducting four test methods using smaller scale samples. These tests include MCC, cone calorimeter, and LIFT, which were conducted at Lund University's fire safety laboratory. The TGA + FTIR tests were conducted at the Danish Institute of Fire and Security Technology, with the assistance of Dr. Abhishek Bhargava.

3.2.1 Microscale combustion calorimeter

The microscale combustion calorimeter (MCC) is a testing method used to determine the flammability of small size samples and follows the standard ASTM D7309. It is possible to conduct two pyrolysis modes in the MCC, Method A and Method B. In Method A, the sample is heated up at a specified heating rate and the pyrolysis gases are removed from the specimen chamber using nitrogen as a purge gas. Afterward, the gases are combined with an excess of oxygen and burned completely in a combustor with a high temperature of approximately 900°C. This method measures the heat of combustion of the volatile gases, but it does not measure the heat released by char. Method B follows a similar process to Method A, with the main difference being that the sample is heated up in an atmosphere composed by a mixture of oxygen and nitrogen. Under oxidative pyrolysis conditions, the pyrolysis gases and the solid carbonaceous char residue are also oxidized, meaning the heat of combustion considers both the specimen gases and char, and that

the results are comparable to the values obtained using the bomb calorimeter (ASTM, 2021).

As part of the current project, both test methods were used to evaluate the three materials. Method A is widely used in fire assessments as it is deemed more representative of fire behavior, as there is no oxygen between the flame and the fuel (McKenna et al., 2019). However, Method B was also used to assess the epoxy resin's resistance to thermal oxidation during exposure to fire, which was of interest.

The MCC test method has several advantages over other fire test methods, such as the cone calorimeter. One significant advantage is that the results obtained from the MCC test are not impacted by the physical behavior of the tested material, such as melting, dripping, swelling, shrinking, delamination, or char formation. Additionally, the MCC test results are not much influenced by factors such as sample size, orientation, external heat flux, ignition source, boundary conditions, or ventilation rate (ASTM, 2021). However, using this test method is only possible to analyze small samples, which can restrict their applicability when working with larger or bulk materials. This limitation may pose challenges when attempting to study the combustion behavior of materials that cannot be easily downsized or replicated in small quantities. For instance, when analyzing epoxy composites, bench-scale tests would be more suitable as they allow for a more representative evaluation of their combustion characteristics.

Below are the values obtained using Method A. However, the results reported in the section 4.1 were based on the net pyrolyzed sample mass. The decision to use net pyrolyzed sample mass was made because it was observed that the epoxy resin of magnetic coil type 2 contains a non-flammable filler material, meaning the total initial sample mass was greater than for other epoxy resins. Normalizing the results using the net pyrolyzed sample mass facilitates comparison between the three samples.

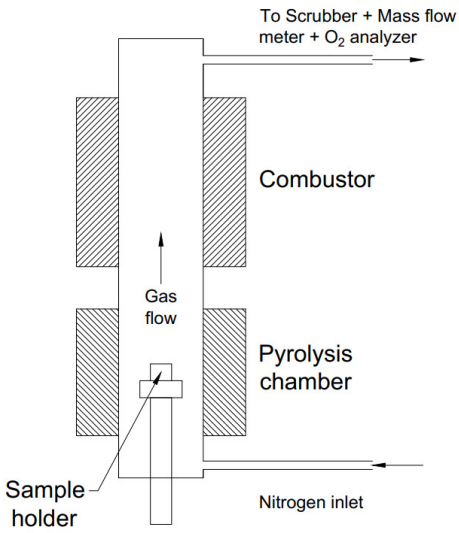

Figure 9: Sketching diagram of MCC

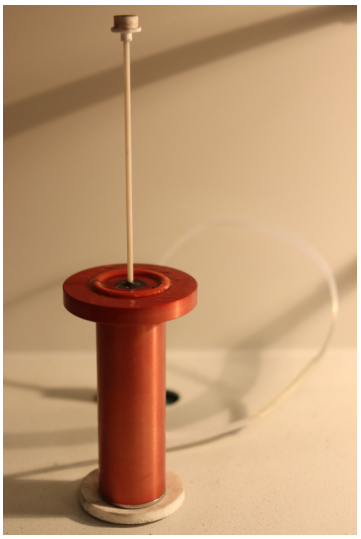

Figure 10: Sample holder of MCC

Below are the key measurements that can be derived from the MCC tests using both methods (ASTM, 2021):

- Specific heat release at time t - It is the net heat released divided by the initial sample mass. These values are presented as a curve $\left[\frac{W}{g}\right]$
- Peak heat release rate - It is the maximum heat release rate recorded during the test $\left[\frac{W}{g}\right]$
- Heat release capacity - It is the maximum specific heat release rate divided by the corresponding heating rate. It is recognized for its effectiveness in predicting the flammability of a material and its propensity to ignite (Q. Xu et al., 2018) $\left[\frac{J}{gK}\right]$
- Peak heat release temperature - It is the temperature corresponding to the maximum heat release rate $[K]$
- Specific heat release - It is the total amount of heat released during the complete burning process of the sample, estimated by calculating the area under the heat release curve $\left[\frac{kJ}{g}\right]$

3.2.2 Cone calorimeter

The cone calorimeter test used in the present project follows the standards ISO 5660 - Part 1 and part 2. During this test, the specimen undergoes controlled exposure to irradiance with an external igniter until sustained flaming occurs. To retain the heat, the samples are covered in aluminum foil and positioned atop a layer of mineral wool within a specimen holder, which in turn is mounted over a weighing device to record the mass during the test. To determine the heat release rate, the oxygen consumption in the combustion product stream is measured by analyzing the oxygen concentration, the carbon monoxide, the carbon dioxide and the flow rate. This data is then used to calculate the amount of heat released by the specimen during the combustion process (ISO, 2002). An illustration of the cone calorimeter at Lund University can be seen in figure 11.

Figure 11: Illustration of cone calorimeter at Lund University

The cone calorimeter at Lund University can accommodate a maximum capacity of 50 kW/m^2. Therefore, the standard irradiance levels of 50, 30, 20 and 15 kW/m^2 were used for the current project.

In an ideal scenario, a square sample that is representative of the actual product being studied and measuring up to 100 mm x 100 mm, with a thickness of no more than 50 mm, is preferred for testing. However, due to the limited width of magnetic coils type 1 and type 2, it was not possible to use samples with such dimensions. For the epoxy resin type 1, a section was cut from the ring-shaped magnetic coil and tested, resulting in the sample holder being partially filled. For the magnetic coil type 2, the cross-sectional area was thicker than the maximum dimensions that the sample holder could accommodate, hence, it was cut transversely to fit into the sample holder. Moreover, the samples of fresh epoxy resin used in this study were manufactured by CERN with dimensions that closely match the ideal dimensions for testing in the cone calorimeter.

It is crucial to mention that the cone calorimeter results are often normalized by dividing them by the exposed area of the sample to the external heat flux, which may not necessarily be equal to the total area of the sample. The total area of a sample for this test is recommended to be 100 cm^2, but due to the retainer frame of the sample holder covering a portion of the sample, the maximum exposed area is approximately, 88.4 cm^2. However, the surface area of some samples used in this study was even smaller than the exposed area of ideal samples. To account for this, the actual exposed area of each sample was manually calculated, taking into consideration the dimensions of the retainer frame of the sample holder. They are provided in the tables 15, 16 and 17.

Below are the key measurements that can be derived from the cone calorimeter test:

1. Heat release rate by oxygen consumption $\left[\frac{kW}{m^2}\right]$
2. Total heat released $\left[\frac{MJ}{m^2}\right]$
3. Peak heat released $\left[\frac{kW}{m^2}\right]$
4. Mass loss rate $\left[\frac{g}{s}\right]$
5. Mass lost during test $[g]$
6. Mean effective heat of combustion $\left[\frac{MJ}{kg}\right]$
7. Time to ignition $[s]$
8. Smoke production rate $\left[\frac{m^2}{s \cdot g}\right]$
9. Total smoke production $\left[\frac{m^2}{g}\right]$

By conducting experiments with a material at three or more distinct irradiance flux levels and using the Cone Calorimeter method with equation 1, it is possible to establish an equation that relates the external heat flux $q_e^{''}$ and the time to ignition t_{ig}, and to estimate the theoretical critical heat flux of ignition. This can be achieved by plotting $q_e^{''}$ versus $\frac{1}{\sqrt{t_{ig}}}$ and performing a linear regression on the resulting data. The resulting equation can be used to predict the ignition behavior of the material under different external heat flux conditions (Quintiere, 2016) (Hurley et al., 2015).

$$\frac{1}{\sqrt{\mathrm{t_{ig}}}} = \frac{2}{\sqrt{\pi}\sqrt{\mathrm{k}\rho\mathrm{c_p}}} \cdot \frac{\mathrm{q_e^{''}}}{\mathrm{T_{ig}} - \mathrm{T_\infty}} \tag{1}$$

where:

- t_{ig} is the time of ignition $[s]$
- k is thermal conductivity $\left[\frac{W}{mK}\right]$
- ρ is density $\left[\frac{kg}{m^3}\right]$
- c_p is the heat capacity $\left[\frac{J}{kgK}\right]$
- $q_e^{''}$ is the external heat flux $\left[\frac{W}{m^2}\right]$
- T_s is the surface temperature $[K]$
- T_∞ is the ambient temperature $[K]$

The equation under consideration is applicable for thermally thick solids that are exposed to high heat fluxes. The equation emphasizes the crucial role played by thermal inertia ($k\rho c_p$) in controlling the ignition of a solid material. As this term appears in the denominator of the equation, it implies that there is an inverse relationship between thermal inertia and time to ignition. In other words, materials with lower thermal inertia will ignite more quickly than those with higher thermal inertia when exposed to the same heat flux conditions. However, it is worth noting that the theory underlying this equation assumes that thermal inertia remains constant regardless of changes in temperature. These three parameters that contribute to thermal inertia do vary with temperature, which can impact the accuracy of the predictions made by the equation. Additionally, it should be noted that while the equation approximates the time to ignition as the pyrolysis time, the time to ignition is the sum of the pyrolysis time, mixing time, and induction time.

Moreover, the applicability of the equation is limited to low heat fluxes where the heating time may become excessively long and the assumption of a thermally thick solid may not be valid. Therefore, it is important to consider the limitations of the equation and ensure that the experimental conditions fall within its range of validity to obtain accurate predictions.

3.2.3 Lateral ignition and flame spread test

The Lateral ignition and flame spread test (LIFT) follows the standards ASTM E1321, ISO 5658-2 and IMO FTP Code Part 5. In the test, a vertical flat rectangular specimen (3) is subjected to a controlled field of radiant heat flux. A pilot flame (2) is positioned near the hotter end of the specimen, causing any volatile gases emanating from the surface to ignite. The test enables the characterization of properties related to the lateral flame. The defined field of radiant heat flux applied to the surface of the specimen is produced using a radiant panel (1) of 480 x 280 mm, inclined 15° from the sample holder. The specimen, with dimensions of 800 x 155 mm is marked with vertical lines each 50 mm horizontally to measure optically the spread of the fire in terms of the flame front (ASTM, 2018). The lift apparatus is shown in the figure 12.

According to ASTM (2018), the flame-front velocity is calculated using a least square method, as follows:

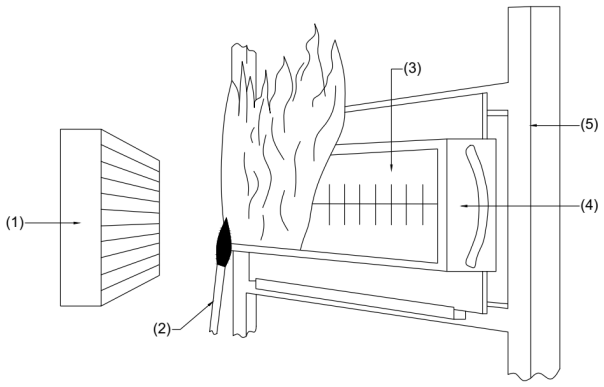

Figure 12: Sketch of the lateral ignition and flame spread test apparatus. (1) Radiant panel, (2) pilot flame burner, (3) sample, (4) sample holder and (5) frame of LIFT apparatus.

$$\mathrm{V} = \frac{\Sigma \mathrm{tx} - \dfrac{\Sigma \mathrm{t} \Sigma \mathrm{x}}{\mathrm{n}}}{\Sigma \mathrm{t}^2 - \dfrac{(\Sigma \mathrm{t})^2}{\mathrm{n}}} \tag{2}$$

where:

- V is flame-front velocity $\left[\frac{m}{s}\right]$
- x is the position along the centerline of sample where the flame-front has spreaded $[m]$
- t is the time required for the flame-front to reach the position x $[s]$
- n is the number of parameters considered to determine the flame-front velocity. These variables correspond to the position and time measurements taken during the experiment or analysis. To avoid any bias in the results caused by materials spreading further, the calculation of the flame front velocity for each material considers the same endpoint. This approach takes into account that the spread rate of the material may be slower the further it is from the radiant panel and ensures a fair comparison of the flame front velocities for all materials tested.

Considering the flame-front velocity, the thermal inertia, the temperature of ignition and the surface temperature, it is possible to obtain the pseudo material property Φ, the flame spread parameter:

$$\mathrm{V} = \frac{\Phi}{\mathrm{k} \rho \mathrm{c_p} (\mathrm{T_{ig}} - \mathrm{T_s})^2} \tag{3}$$

where:

- Φ is the flame spread parameter $\frac{kW^2}{m^3}$
- k is the thermal conductivity $\left[\frac{W}{mK}\right]$
- ρ is the density $\left[\frac{kg}{m^3}\right]$
- c_p is the heat capacity $\left[\frac{J}{kgK}\right]$
- T_{ig} is the temperature of ignition $[K]$

The temperature of ignition required in equation 3 is estimated using the results from the cone calorimeter. To model the combined convective and radiative heat transfer in the test, the assumption of linear radiation heat transfer is often made. This allows the use of a total heat transfer coefficient in equation 4. However, the value of the total heat transfer coefficient h_T can vary based on the experimental setup and apparatus configuration (Torero, 2016). Since different flow fields are used in individual tests, the convective heat transfer coefficient can also vary. In this report, a convective heat transfer coefficient value of 15 W/m^2K is used due to its frequent citation in literature. A common value for the total heat transfer coefficient is around $h_T \approx 45$ W/m^2K. It is important to note that while this assumption simplifies calculations, it can introduce errors that need to be taken into consideration.

$$q'' = h_T (T_s - T_\infty) \tag{4}$$

where:

- h_T is the total heat transfer coefficient $\left[\frac{W}{m^2K}\right]$

However, one potential concern is the use of cone calorimeter results to evaluate the flame spread parameter in this project, as the experimental setup, scale, specimen size, and orientation are all different. This makes it difficult to accurately estimate the error of the results obtained through the applied flame spread model, especially considering the limited number of repetitions. Therefore, caution should be exercised when using cone calorimeter data to evaluate flame spread parameters in this context.

3.2.4 Thermogravimetric analyzer

The thermogravimetric analysis (TGA) is a precise analytical technique that enables the measurement of the change in weight of a sample under controlled heating or cooling conditions. In TGA, a small sample of the material is subjected to a constant rate of heating, while the corresponding change in weight is continuously measured. The information derived from TGA allows for the determination of the thermal decomposition temperature, thermal stability, moisture content, sample composition, and the kinetics of chemical reactions or the rate of mass loss due to pyrolysis. It's important to note that TGA is limited in its ability to identify certain thermal events, such as phase transitions, polymorphic transformations, or reactions that do not result in changes in mass (Saadatkhah et al., 2020).

It is possible to couple TGA with a differential scanning calorimetry (DSC). In TG-DSC, the TGA measures the weight changes of the sample, while the DSC measures the corresponding changes in heat flow. This allows for the simultaneous observation of both mass loss and energy changes, providing more information about the thermal behavior of the sample (Saadatkhah et al., 2020).

A Fourier transform infrared spectroscopy (FTIR) can also be coupled with TGA-DCS to provide more detailed information about the composition of a material as it undergoes thermal degradation. During TGA-FTIR analysis, the sample is heated, and the resulting

gaseous products are carried through a transfer line to the FTIR detector. The FTIR measures the chemical composition of the gas phase using infrared radiation that passes through the sample, and the resulting spectrum of the absorbed or transmitted radiation is recorded, The absorbed or transmitted radiation is then recorded as a spectrum, which can help identify the different compounds and functional groups present in the material as it degrades (Saadatkhah et al., 2020).

The thermogravimetric (TG) curve displays the variation in mass of a sample as a function of temperature under controlled heating conditions. The derivative thermogravimetry (DTG) curve is a plot of the rate of change of the sample's mass with respect to temperature, which is derived from the TG data. The DSC curve displays the amount of heat absorbed or released by the sample as it is heated over a range of temperatures. Endothermic peaks in the DSC curve indicate that energy is being absorbed by the sample, which is usually associated with processes such as melting, glass transition, or evaporation.

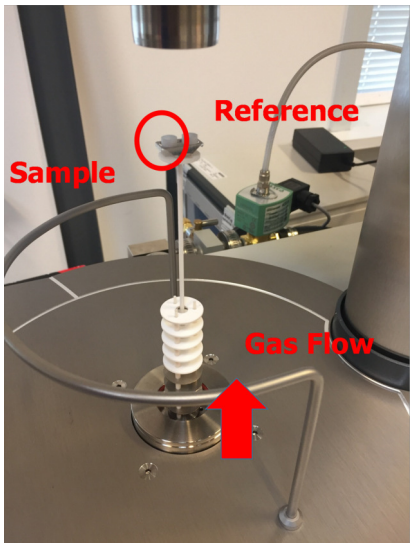

Figure 13: Simultaneous thermal analyzer model Netzsch 449 F3 open. The device is used to monitor weight loss, heat flow effects and gas analysis simultaneously upon application of thermal ramp.

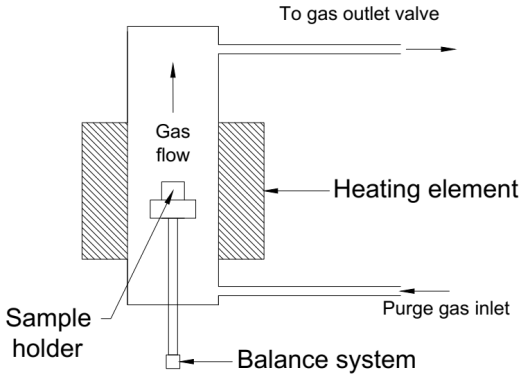

Figure 14: Simultaneous thermal analyzer model. Sketch

As part of the current project, Dr. Abhishek Bhargava, a specialist in TGA-DCS-FTIR at the Danish Institute of Fire and Security Technology (DBI), was the responsible of carrying out a series of experiments on collected samples of epoxy resins, including type 1, type 2, and fresh epoxy resin.

The TGA was performed on a a simultaneous thermal analyzer (STA) model Netzsch 449 F3. Figure 13 illustrates the TGA-DSC sample carrier, which includes a microbalance located in the bottom section of the device for continuous logging of weight change data when the sample is subjected to a heating ramp. The figure also displays the direction of the gas flow and the positions of the sample and reference type crucibles within the carrier. An sketch of the simultaneous thermal analyzer model used for the TGA is illustrated in figure 14.

4 Results and discussion

4.1 Results of the microscale combustion calorimeter

The MCC was used to conduct a total of ten tests following method A and six tests following method B.

The samples used in the tests for magnetic coil type 1 and type 2 only contained epoxy resin, without any glass fiber tape or metallic core.

The type 1 epoxy resin was collected from the edges of the magnetic coil, where the accumulation of epoxy resin resulted in a greater thickness compared to other areas. No layers of fiberglass tape had to be removed to access the epoxy resin. However, during the meticulous collection process, extra care was taken to prevent any contamination of the samples with fiberglass, which was located in close proximity to the metallic core. As a result, the collected samples were assumed to be free of any fiberglass inclusion and exhibited a transparent appearance with a smooth external surface.

The epoxy resin type 2 used for the tests was collected in the side with irregular thickness of the ring-shaped magnetic coil, which had an important accumulation of epoxy resin and is shown in the left side of figure 6. In order to collect a fresh batch of epoxy resin, it was necessary to remove the first layer of fiberglass tape. Upon inspection, it was apparent that the newly exposed epoxy resin type 2 had a different appearance than the previously used epoxy resin type 1, as well as the fresh epoxy resin. The surface of the resin was uneven, with some areas showing a jagged, fragmented texture, and visible strands covered in epoxy resin, as shown in figure 15. When the epoxy resin was cut, small shards of the material detached.

To obtain fresh epoxy resin samples, thin plates manufactured by CERN of pure epoxy resin were used to collect the samples.

Figure 15: Appearance of epoxy resin type 2 from Magnetic coil type 2, after removing the fiber glass tape

4.1.1 Results of the microscale combustion calorimeter in nitrogen atmosphere

In total, ten tests using method A were performed using the MCC. Four tests were conducted on the epoxy resin type 1, four tests on the epoxy resin type 2 and two tests on the fresh epoxy resin. The heating rate for all the experiments was 1 °C/s.

Following the internal procedure of Lund University for the MCC, for optimal testing outcomes, it is recommended to choose a sample size that leads to an oxygen level decrease of (10 ± 3)% to achieve optimal testing results when measuring heat release through oxygen-consumption calorimetry. This choice provides the best signal-to-noise ratio (Lyon et al., 2013). It is recommended to reduce the sample mass if the oxygen concentration falls below the recommended level. Conversely, increasing the sample size is necessary if the oxygen concentration is high. To further ensure the repeatability and accuracy of the tests, an additional option is to conduct the experiments multiple times and observe if consistent results are obtained. By performing repeated trials, we can assess the reliability of the findings and ascertain the consistency of the observed outcomes. In the context of the current project, we have already taken this approach by repeating the tests and increasing the mass.

The mass measurements related to each test of epoxy resin type 1 are recorded in table 9. During the initial Test 1, a sample of around 3 mg was used, but the oxygen levels did not meet the desired parameters. Subsequently, for Test 2, the mass of the sample was increased to roughly 4 mg, but the desired oxygen conditions were still not achieved. Finally, in Test 3, the sample size was further increased to approximately 6 mg, resulting in optimal oxygen levels being achieved. Consequently, for Test 4, the same sample size of 6 mg was used.

Test number	Sample name	Total initial sample mass (mg)	Remaining sample mass after test (mg)	Net pyrolyzed sample mass (mg)	Percentage of remaining sample
Test 1	A-MN-1	2.98	0.09	2.89	3%
Test 2	A-MN-2	4.09	0.16	3.93	4%
Test 3	A-MN-3	5.95	0.2	5.75	3%
Test 4	A-MN-4	6.06	0.07	5.99	1%

Table 9: Mass of samples of epoxy resin type 1 tested in nitrogen atmosphere using the MCC

For the fresh epoxy resin, the sample mass for test 5 and test 6 was approximately 6 mg, which was the same mass as the type 1 epoxy resin used to achieve the desired oxygen levels during the test. Table 10 shows the recorded mass measurements for each test of fresh epoxy resin.

Test number	Sample name	Total initial sample mass (mg)	Remaining sample mass after test (mg)	Net pyrolyzed sample mass (mg)	Percentage of remaining sample
Test 5	C-MN-1	6.06	0.21	5.85	3%
Test 6	C-MN-2	6.04	0.16	5.88	3%

Table 10: Mass of samples of fresh epoxy resin tested in nitrogen atmosphere using the MCC

The first experiment using epoxy resin type 2, Test 7, had a sample mass of approximately 6 mg, but the oxygen level drop was not optimal, and there was a significant residual sample mass after the test, as illustrated in figure 16. To rule out the possibility of including fiber glass in the sample, a new sample of roughly 6 mg was collected from a deeper location of the magnetic coil type 2. Test 8 produced similar results to Test 7, indicating that the epoxy resin type 2 contains a non-flammable filler. The sample before and after the test can be observed in figure 17 and figure 18, respectively. In Test 9 and Test 10, the initial sample mass was increased to approximately 14 mg and 16 mg, respectively, by dividing it into two pieces to increase the surface. The remaining sample mass from Test 9 can be observed in figure 19. Although the pyrolyzed sample mass of the epoxy resin was inadequate to consume the desired amount of oxygen during combustion, further tests were not conducted because the ratio between the pyrolyzed sample mass and non-flammable materials was difficult to control, resulting in inconsistent and irreproducible results. This can be seen from the net pyrolyzed sample mass of test 9 and test 10. Despite an increase in the total initial sample mass of 2 mg, the net pyrolyzed sample mass only increased by 0.19 mg. Table 11 displays the mass measurements recorded for each test of fresh epoxy resin type 2. One possible explanation for this is that the filler material may be distributed in an inhomogeneous manner within the epoxy resin.

Test number	Sample name	Total initial sample mass (mg)	Remaining sample mass after test (mg)	Net pyrolyzed sample mass (mg)	Percentage of remaining sample
Test 7	B-MN-1	6	4.11	1.89	69%
Test 8	B-MN-2	6.09	2.6	3.49	43%
Test 9	B-MN-3	13.93	7.01	6.92	50%
Test 10	B-MN-4	15.98	8.87	7.11	56%

Table 11: Mass of samples of epoxy resin type 2 tested in nitrogen atmosphere using the MCC

Table 12 shows the results the from the 10 tests conducted using the MCC. Once again, it is important to outline the results reported are based on the net pyrolyzed sample mass, which is equal to the total initial sample mass less the residual sample mass after the test. It was decided to use the net pyrolyzed sample mass to normalize the results because the magnetic coil type 2 epoxy resin contained a non-flammable filler material, resulting in a larger total initial sample mass compared to other epoxy resins, and does not allow to estimate the char yield after the test. It is worth noting that the mass of the sample has a slight effect on the MCC results, which allows for a direct comparison of results from samples of different materials with the same scale size.

The flammability of materials can be ascertained by assessing the amount of heat that is generated when they are exposed to fire. One of the most important parameters that is evaluated using an MCC experiment is the HRR (Ayoola et al., 2006). It is worth noting that the results of an MCC experiment conducted on epoxy resins can only be applied to this type of material as the samples used in the experiment do not contain the magnetic core or the glass fiber tape. Upon conducting MCC experiments on the three epoxy resin types, it was observed that the epoxy resin type 1 and fresh epoxy resin have similar flammability levels, which are higher than that of epoxy resin type 2.

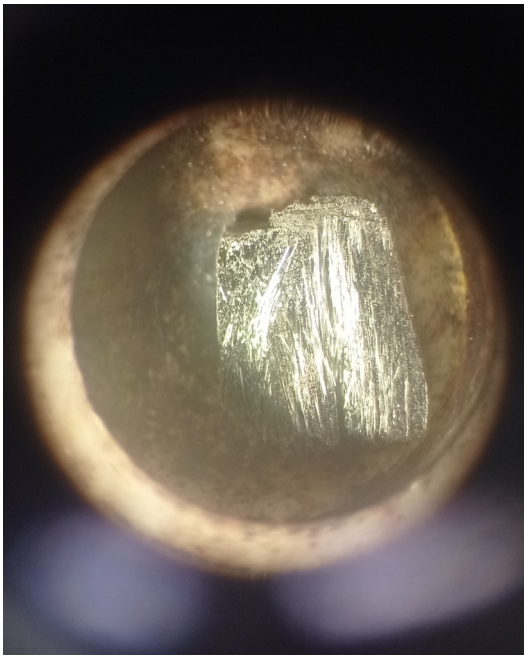

Figure 16: Sample B-MN-1 of epoxy resin type 2. Remaining material after test in MCC

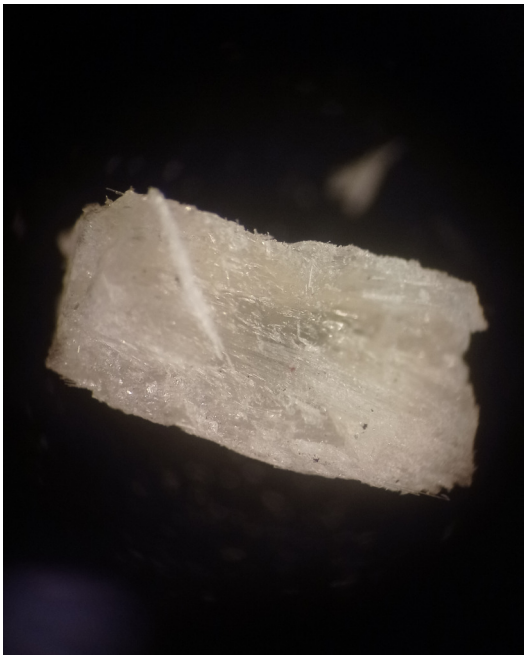

Figure 17: Sample B-MN-2 of epoxy resin type 2. Sample before test in MCC

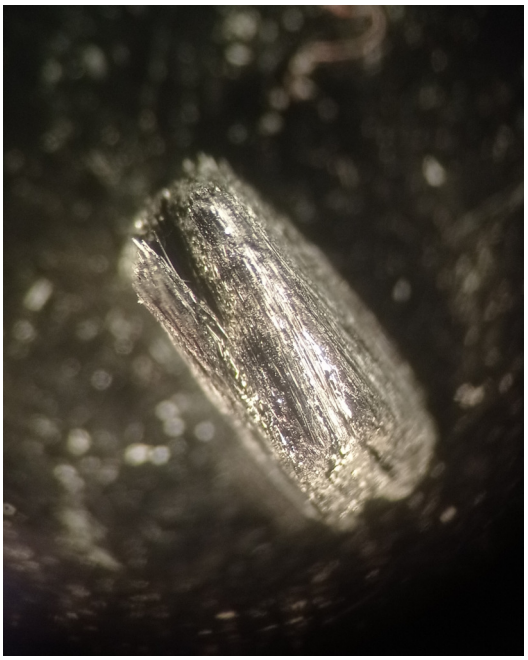

Figure 18: Sample B-MN-2 of epoxy resin type 2. Remaining material after test in MCC

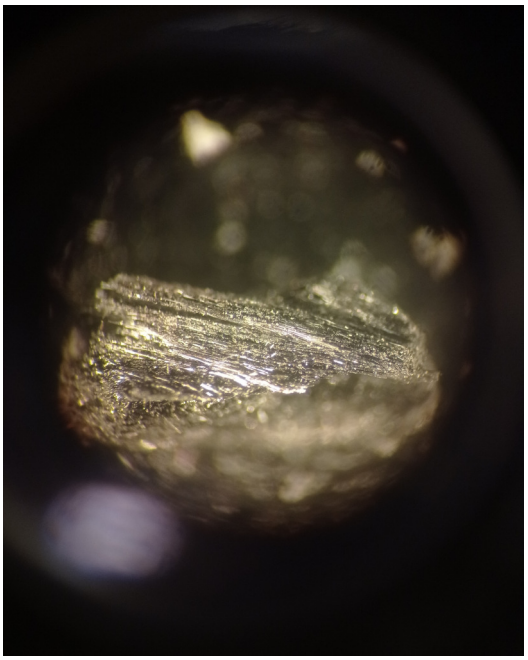

Figure 19: Sample B-MN-3 of epoxy resin type 2. Remaining material after test in MCC

Heat release capacity is a key parameter that can provide valuable information on the flammability behavior of materials. As shown in Table 12, both the type 1 epoxy resin and fresh epoxy resin exhibit comparable heat release capacities, which are higher than that of the type 2 epoxy resin. Notably, the type 2 epoxy resin begins to pyrolyze at a considerably lower temperature than the other two resins; specifically, its decomposition starts at around 200 °C, while the other two resins start decomposing at approximately 300 °C.

Sample name	Material	Heat release capacity (J/gK)	Peak heat release rate (W/g)	Total heat released by combustion of the pyrolysis gases (kJ/g)	Peak heat release temperature (°C)
A-MN-1	Epoxy resin type 1	493.62	488.03	25.43	427.71
A-MN-2	Epoxy resin type 1	514.40	507.53	28.10	425.54
A-MN-3	Epoxy resin type 1	515.46	512.65	28.10	425.50
A-MN-4	Epoxy resin type 1	463.65	462.12	27.72	426.55
C-MN-1	Fresh epoxy resin	511.18	506.84	28.96	425.70
C-MN-2	Fresh epoxy resin	507.30	504.31	28.67	427.29
B-MN-1	Epoxy resin type 2	289.65	290.51	24.85	439.92
B-MN-2	Epoxy resin type 2	329.80	315.14	28.34	428.76
B-MN-3	Epoxy resin type 2	291.92	291.17	29.16	422.03
B-MN-4	Epoxy resin type 2	280.26	279.89	29.54	438.34

Table 12: Thermal characteristics of the three epoxy resins tested in nitrogen atmosphere using the MCC. The heat release capacity, the peak heat release rate and the total heat released were normalized using the net pyrolyzed sample mass.

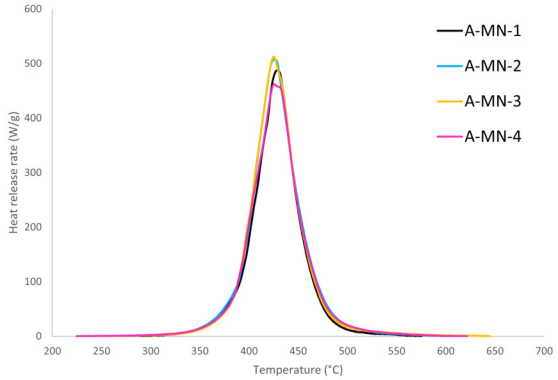

Figure 20: Heat release rate per mass unit of epoxy resin type 1 in a nitrogen atmosphere and a heating rate of 1°C/s using the MCC

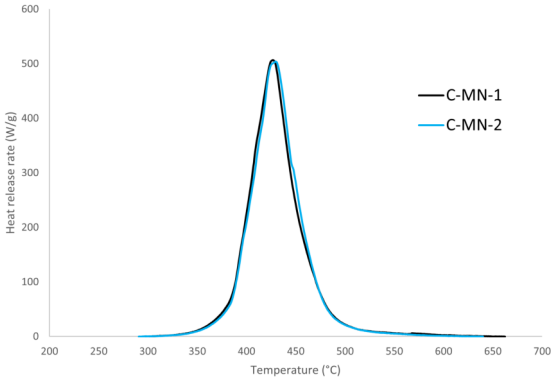

Figure 21: Heat release rate per mass unit of fresh epoxy resin in a nitrogen atmosphere and a heating rate of 1°C/s using the MCC

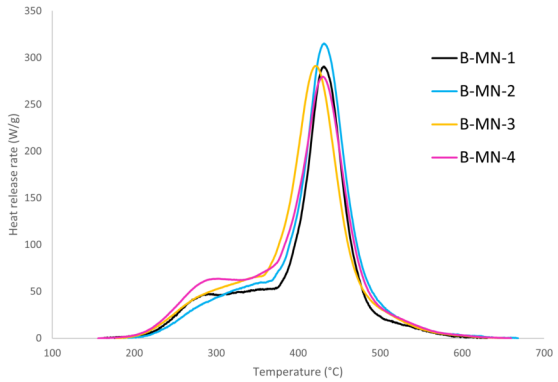

Figure 22: Heat release rate per mass unit of epoxy resin type 2 in a nitrogen atmosphere and a heating rate of 1°C/s using the MCC

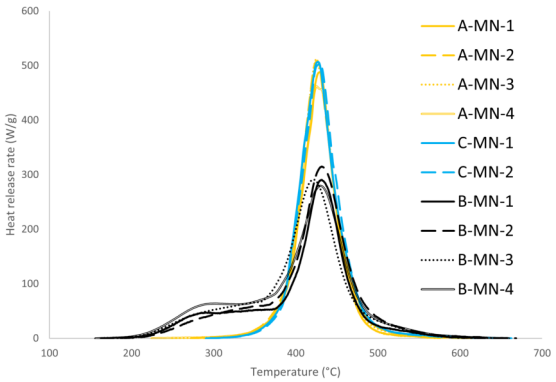

Figure 23: Heat release rate per mass unit of the three epoxy resins in a nitrogen atmosphere and a heating rate of 1°C/s using MCC

The data in the figure 23 indicates that the peak heat release rate for epoxy resin type 1 and fresh epoxy resin are comparable, while it is lower for epoxy resin type 2. This could potentially indicate that type 1 and fresh epoxy resin have a similar composition.

Although the net mass of the pyrolyzed sample was greater during tests 9 and 10 compared to the other epoxy resins, the peak heat release rate was still lower for type 2.

4.1.2 Results of the microscale combustion calorimeter in air atmosphere

A total of six MCC tests were carried out using method B. Similarly to the tests that followed method A in a nitrogen atmosphere, the tested samples of magnetic coils type 1 and type 2 were consisted solely of epoxy resin without any glass fiber tape or metallic core and followed the procedure described in the section 4.1.1. The experiments included two tests on epoxy resin type 1, two tests on epoxy resin type 2, and two tests on fresh epoxy resin, all using a heating rate of 1 °C/s.

Table 13 presents the mass measurements for the various tests. The results indicate that both the type 1 epoxy resin and fresh epoxy resin were completely oxidized during the pyrolysis process, as evidenced by their negligible remaining sample mass. In contrast, type 2 epoxy resin exhibited a substantial remaining mass similar to that observed in the nitrogen atmosphere tests.

Test number	Material	Sample name	Total initial sample mass (mg)	Remaining sample mass after test (mg)	Net pyrolyzed sample mass (mg)	Percentage of remaining sample
Test 1	Epoxy resin type 1	A-MA-1	7.4	0	7.4	0
Test 2	Epoxy resin type 1	A-MA-2	7.1	0	7.1	0
Test 3	Epoxy resin type 2	B-MA-1	12.5	7.4	5.1	59.20%
Test 4	Epoxy resin type 2	B-MA-2	13.3	8	5.3	60.15%
Test 5	Fresh epoxy resin	C-MA-1	6.9	0	6.9	0
Test 6	Fresh epoxy resin	C-MA-2	5.9	0	5.9	0

Table 13: Mass of epoxy resin tested in air atmosphere using the MCC

Table 14 provides information on the heat release capacity and peak heat release rate of the tested epoxy resins. It is evident that both the type 1 epoxy resin and fresh epoxy resin exhibit very similar heat release capacities and peak heat release rates, whereas the values for the type 2 epoxy resin are considerably lower - at least four times lower than the other two resins.

In terms of the temperature at which the sample undergoes pyrolysis, it can be observed that epoxy resin type 2 requires a lower temperature, which is consistent with its behavior in the nitrogen atmosphere.

Sample name	Material	Heat release capacity (J/gK)	Peak heat release rate (W/g)	Total heat released by combustion of the pyrolysis gases (kJ/g)	Peak heat release temperature (°C)
A-MA-1	Epoxy resin type 1	849.71	819.76	26.09	424.53
A-MA-2	Epoxy resin type 1	939.67	931.31	26.91	430.31
B-MA-1	Epoxy resin type 2	295.54	183.06	28.52	422.97
B-MA-2	Epoxy resin type 2	285.07	178.73	28.26	425.59
C-MA-1	Fresh epoxy resin	796.72	786.09	25.41	415.23
C-MA-2	Fresh epoxy resin	829.77	830.98	27.06	422.86

Table 14: Thermal characteristics of epoxy resins tested in air atmosphere using the MCC. The heat release capacity, the peak heat release rate and the total heat released were normalized using the net pyrolyzed sample mass

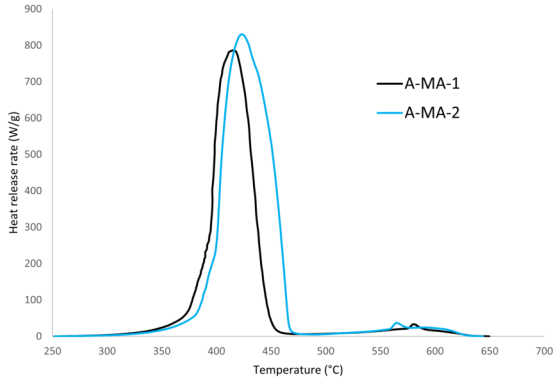

Figure 24: Heat release rate per mass unit of the epoxy resin type 1 in air atmosphere and a heating rate of 1°C/s using MCC

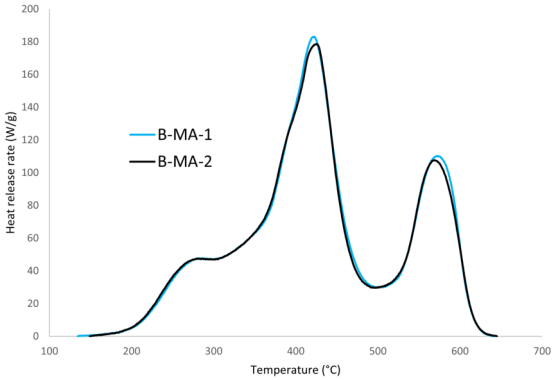

Figure 25: Heat release rate per mass unit of the epoxy resin type 2 in air atmosphere and a heating rate of 1°C/s using MCC

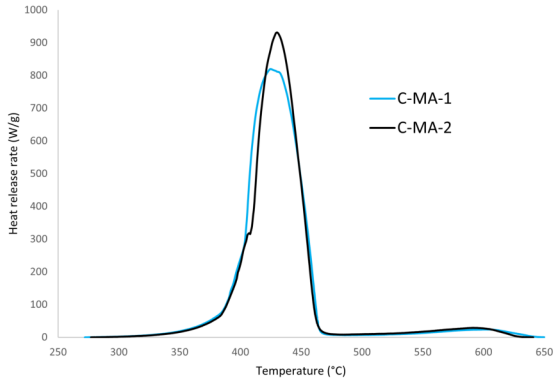

Figure 26: Heat release rate per mass unit of the fresh epoxy resin in air atmosphere and a heating rate of 1°C/s using MCC

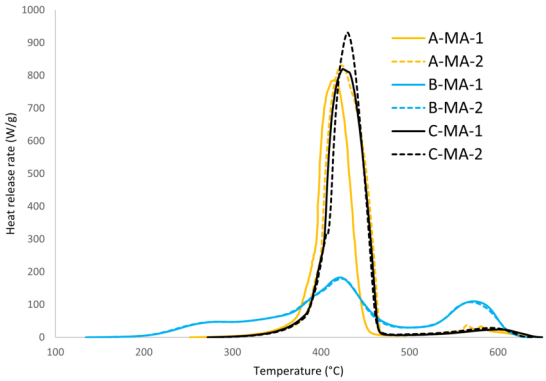

Figure 27: Heat release rate per mass unit of the three epoxy resins in air atmosphere and a heating rate of 1°C/s using MCC

A significant difference between the tests carried out using method A and method B is evident in the behavior of epoxy resin type 2. As depicted in Figure 25, two distinct combustion processes are observed, one with a peak heat release around 425°C and another around 570°C. This phenomenon can be attributed to the complete combustion of the oxidation and combustion of the char layer that remains on the surface of the non-flammable filler material after the epoxy resin has decomposed. As a result of the oxidation and combustion of the char layer left on the surface of the non-flammable filler material, the total heat released by the combustion of the pyrolysis gases was greater for epoxy resin type 2 than for the other two epoxy resins, as shown in table 14. It is worth noting that while the total heat released by the combustion of the pyrolysis gases remained fairly constant, the peak heat release rate decreased during the testing of epoxy resin type 2 in an air atmosphere.

To summarize the key takeaways from the MCC tests, the following bullets highlight the main findings:

- The flammability of epoxy resin type 1 and epoxy resin type 2 are different.
- The epoxy resin type 2 has a non-flammable filler distributed within the epoxy resin.

- The results indicate that the type 1 epoxy resin and the fresh epoxy resin exhibited comparable behaviors in both the nitrogen and air atmosphere tests in terms of flammability.
- Epoxy resin type 2 requires a lower temperature to initiate pyrolysis than epoxy resin type 1 and the fresh epoxy resin.
- The resemblance in the outcomes of epoxy resin type 1 and fresh epoxy resin using the MCC may imply that they have a comparable composition.

4.2 Results of cone calorimeter

4.2.1 Flammability

A total of twenty three samples were prepared and tested using the cone calorimeter, as described in Section 3. For the magnetic coil type 1 and magnetic coil type 2, sections were cut and used in the testing process. In the case of the epoxy composite type 2, a transversal cut was necessary due to the sample's cross-sectional thickness exceeding the cone calorimeter's sample holder. The fresh epoxy resin samples were provided by CERN and were manufactured with dimensions close to the ones indicated by the standard. Some samples can be observed in figure 28, and it is possible to observe the samples placed in the sample holder in the figures 29, 30, 31 and 32. As discussed in section 3.1, at the outset of this project, it was not known if the composition of epoxy resins of the three epoxy resins were the same or similar. Only the composition of the fresh epoxy resin was known, while the composition of the other two resins remained unknown.

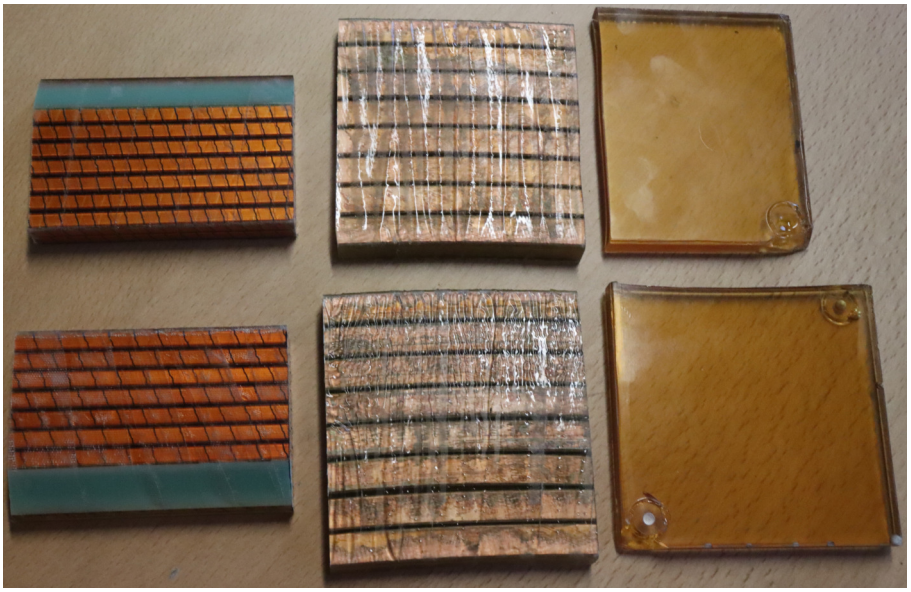

Figure 28: Samples tested using the cone calorimeter: Sample A-C-1 (Top-left), Sample B-C-2 (Top-middle), Sample C-C-2 (Top-right), Sample A-C-2 (Bottom-left), Sample B-C-1 (Bottom-middle) and Sample C-C-1 (Bottom-right)

Tables 15, 16, and 17 provide the dimensions of the samples for epoxy composite type 1, epoxy composite type 2, and fresh epoxy resin, respectively. It is worth noting that

the dimensions of the samples do not adhere to the recommended 10 cm x 10 cm size stipulated by the standard. As the exposed area to the incident heat flux is used to normalize various results, the tables list both the actual total area of the samples and the exposed area to the heat flux.

Sample name	Material	Length (mm)	Width (mm)	Exposed area to the heat flux (cm^2)	Total area (cm^2)	Thickness (cm)	Mass (g)
A-C-1	Epoxy composite type 1	94.03	64.55	60.69	60.69	15.24 ± 0.03	432.40
A-C-2	Epoxy composite type 1	94.84	64.07	60.24	60.76	15.06 ± 0.03	427.40
A-C-3	Epoxy composite type 1	94.27	64.01	60.18	60.33	15.44 ± 0.05	429.70
A-C-4	Epoxy composite type 1	94.20	64.15	60.31	60.42	14.91 ± 0.01	423.90
A-C-5	Epoxy composite type 1	94.42	64.14	60.31	60.56	14.93 ± 0.01	427.30
A-C-6	Epoxy composite type 1	94.94	64.04	60.21	60.80	15.29 ± 0.04	432.40

Table 15: Characteristics of samples of epoxy composite type 1 to be tested using the cone calorimeter

Sample name	Material	Length (mm)	Width (mm)	Exposed area to the heat flux (cm^2)	Total area (cm^2)	Thickness (cm)	Mass (g)
B-C-1	Epoxy composite type 2	98.74	91.80	86.31	90.64	13.24 ± 0.09	575.30
B-C-2	Epoxy composite type 2	97.43	91.71	86.22	89.34	13.25 ± 0.11	564.30
B-C-3	Epoxy composite type 2	97.86	95.48	88.40	93.43	11.78 ± 0.15	524.20
B-C-4	Epoxy composite type 2	97.82	93.83	88.22	91.77	12.26 ± 0.09	540.80
B-C-5	Epoxy composite type 2	97.93	94.14	88.40	92.19	11.68 ± 0.12	506.20
B-C-6	Epoxy composite type 2	97.65	95.73	88.40	93.48	13.1 ± 0.03	595.90
B-C-7	Epoxy composite type 2	98.80	90.44	85.03	89.35	12.87 ± 0.08	559.30
B-C-8	Epoxy composite type 2	97.95	90.51	85.10	88.65	13.29 ± 0.05	569.80
B-C-9	Epoxy composite type 2	97.32	91.50	86.03	89.04	13.39 ± 0.05	570.90

Table 16: Characteristics of samples of epoxy composite type 2 to be tested using the cone calorimeter

Sample name	Material	Length (mm)	Width (mm)	Exposed area to the heat flux (cm^2)	Total area (cm^2)	Thickness (cm)	Mass (g)
C-C-1	Fresh epoxy resin	99.97	95.87	88.40	95.84	10.03 ± 0.01	113.04
C-C-2	Fresh epoxy resin	99.83	78.93	74.21	78.79	10.04 ± 0.02	93.75
C-C-3	Fresh epoxy resin	99.77	96.57	88.40	96.34	9.68 ± 0.07	108.50
C-C-4	Fresh epoxy resin	99.50	97.60	88.40	97.11	8.73 ± 0.04	100.20
C-C-5	Fresh epoxy resin	99.47	98.79	88.40	98.27	10.07 ± 0.07	116.40
C-C-6	Fresh epoxy resin	99.12	98.38	88.40	97.51	10.42 ± 0.09	119.40
C-C-7	Fresh epoxy resin	99.45	96.87	88.40	96.34	10.94 ± 0.03	123.40
C-C-8	Fresh epoxy resin	99.48	97.83	88.40	97.32	9.82 ± 0.03	112.20

Table 17: Characteristics of samples of fresh epoxy resin to be tested using the cone calorimeter

Figure 33 displays the upper surface of sample A-C-1, which was exposed to an external heat flux of 50 kW/m^2 during testing. This surface appears white and is mostly clean without any signs of soot. However, in contrast, figure 34 displays the bottom side of sample A-C-1, which was positioned upside down during testing and has a noticeable layer of soot. This suggests that the bottom face was exposed to a lower heat flux than the top face, as expected due to the position of the sample during the test. The figure also shows the glass fiber tape wrapped around each individual coil, which is also covered by soot. Figure 36 presents the non-flammable material that forms part of magnetic coil type 1 after testing. Prior to testing, this material was green as shown in figure

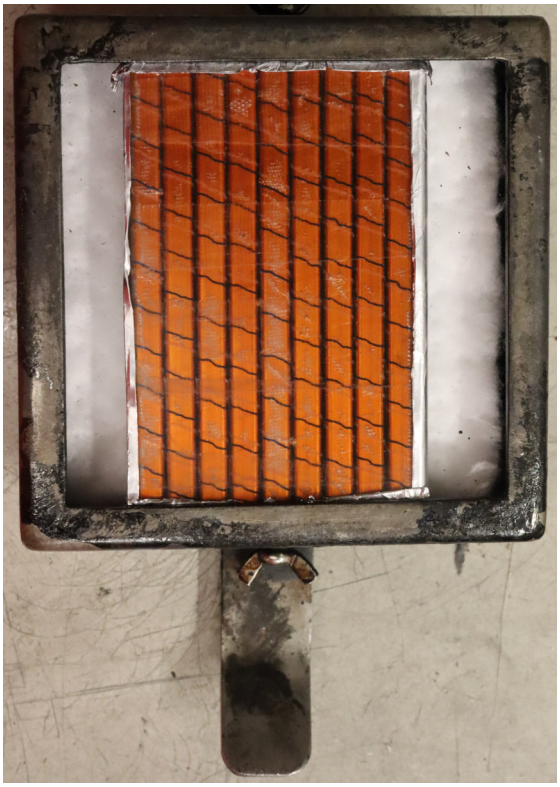

Figure 29: Sample A-C-1 of epoxy composite type 1 in sample holder for the test in the cone calorimeter

Figure 30: Sample B-C-2 of epoxy composite type 2 in sample holder for the test in the cone calorimeter

28, but after testing, it is apparent that the material has fibers which are arranged in a two-dimensional flat weave pattern and arranged in a lamellar structure.

After the test, Figure 39 displays the epoxy composite type 2 sample at 50 kW/m^2. As with the epoxy composite type 1 sample, the fiberglass tape on the composite type 2 turned white, and the upper surface was free of char.

The fresh epoxy resin had a shorter ignition time than the two epoxy composites, as expected since the fiberglass tape and metallic coils act as heat sinks, delaying the pyrolysis process. During the heating up process, the epoxy resin expanded, and the planar surface became concave. Figure 40 reveals numerous embers or burning particles of the object that has caught fire observed during the test. The mass loss rate of the fresh epoxy resin was also higher, as shown in Figure 41, where the high pyrolysis gas production may cause the flame layer to detach from the epoxy resin surface. During the test, the surface of the resin was observed to foam, indicating the release of volatile compounds as the epoxy resin underwent thermal decomposition. After the test, it is possible to observe in figure 43 that no material remained in the sample holder, and the aluminum foil wrapping the sample to preserve heat had melted.

During the experiment, samples B-C-3 and B-C-4 of epoxy composite type 2 were tested at an external heat flux of 20 kW/m^2. However, the results from Figure 46 and Table 18 show that the behavior of the two samples differed significantly. During the test of sample B-C-3, ignition occurred after 971 seconds of exposure to the external heat flux. The flame then spread throughout the sample's surface and was sustained

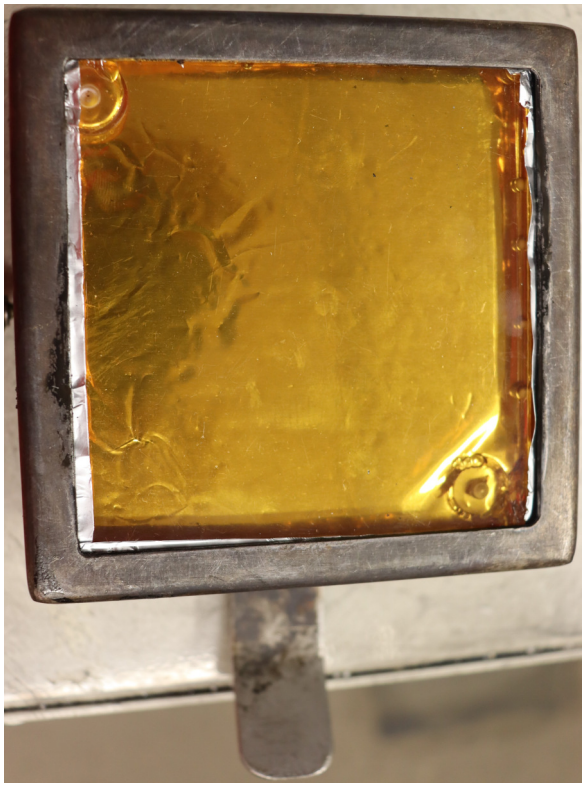

Figure 31: Sample C-C-1 of fresh epoxy resin in sample holder for the test in the cone calorimeter

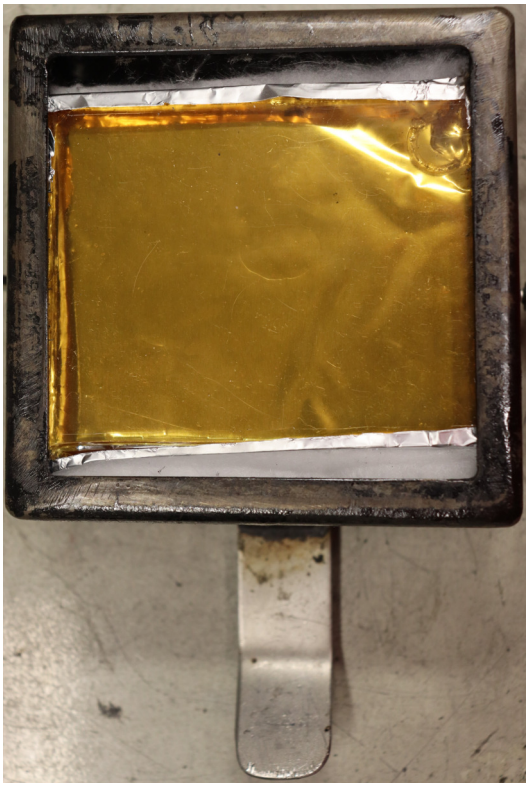

Figure 32: Sample C-C-2 of fresh epoxy resin in sample holder for the test in the cone calorimeter

Figure 33: Sample A-C-1 of epoxy composite type 1 after test in cone calorimeter. Upper face

Figure 34: Sample A-C-1 of epoxy composite type 1 after test in cone calorimeter. Bottom face

Figure 35: Sample A-C-1 of epoxy composite type 1 during test in the cone calorimeter

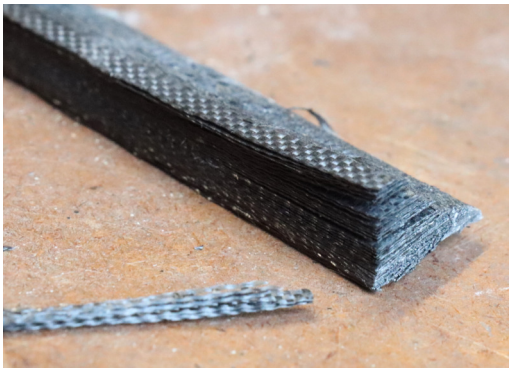

Figure 36: Sample A-C-1 of epoxy composite type 1 after test in cone calorimeter. Non-combustible filler material of magnetic coil type 1

for 652 seconds. On the other hand, sample B-C-4 exhibited a weak intermittent flame that only lasted for 116 seconds after ignition occurred before 500 seconds of starting the test, then, the sample ignited one more time after 1479 seconds of the start of the test and burned during 473 seconds. Given the contrasting results of samples B-C-3 and B-C-4, further tests were necessary. Sample B-C-5 was subjected to the same external heat flux of 20 kW/m^2. The software of the cone calorimeter stopped functioning when the sample ignited after 448 seconds, which is comparable to the ignition time of sample B-C-4. Unfortunately, no information could be obtained from this test due to the crash. Subsequently, sample B-C-6 was tested under the same conditions. It took 1200 seconds from the start of the test for ignition to occur, and the flame then spread throughout the sample's surface and lasted for 788 seconds.

The reason for testing the fresh epoxy resin at 15 15 kW/m^2 while the others were not subjected to this heat flux was due to the sequential testing order. The samples made of fresh epoxy resin were the first type to undergo testing at this specific heat flux. Sample B-C-7 of epoxy composite type 2 did not ignite during the experiment and hence was not included in Table 18. The sample was exposed to an external heat flux of 15 kW/m^2 for a duration of 1964 seconds, which is equivalent to approximately 32 minutes. The epoxy composite 1 was not tested at an external heat flux of 15 kW/m^2 because the sample B-C-7 of epoxy composite type 2 did not ignite when exposed it was exposed to that heat flux, and according to the previous tests, epoxy composite type 2 had a faster ignition time.

In a similar manner, the fresh epoxy resin was not subjected to testing using a heat flux of 30 kW/m^2. This was due to the unavailability of fresh epoxy resin samples during the testing process of epoxy composite types 1 and 2.

During the testing of fresh epoxy resin, samples C-C-1 and C-C-2 were subjected to a heat flux of 50 kW/m^2 following the standard procedure. The samples were wrapped in aluminum foil on their bottom and lateral sides and were placed over mineral wool in the sample holder. Since fresh epoxy resin lacks magnetic coils like the other two materials, samples C-C-3, C-C-4, C-C-5, and C-C-6 were tested with a layer of copper, which was part of the remainders of the samples of epoxy composite type 2, placed below

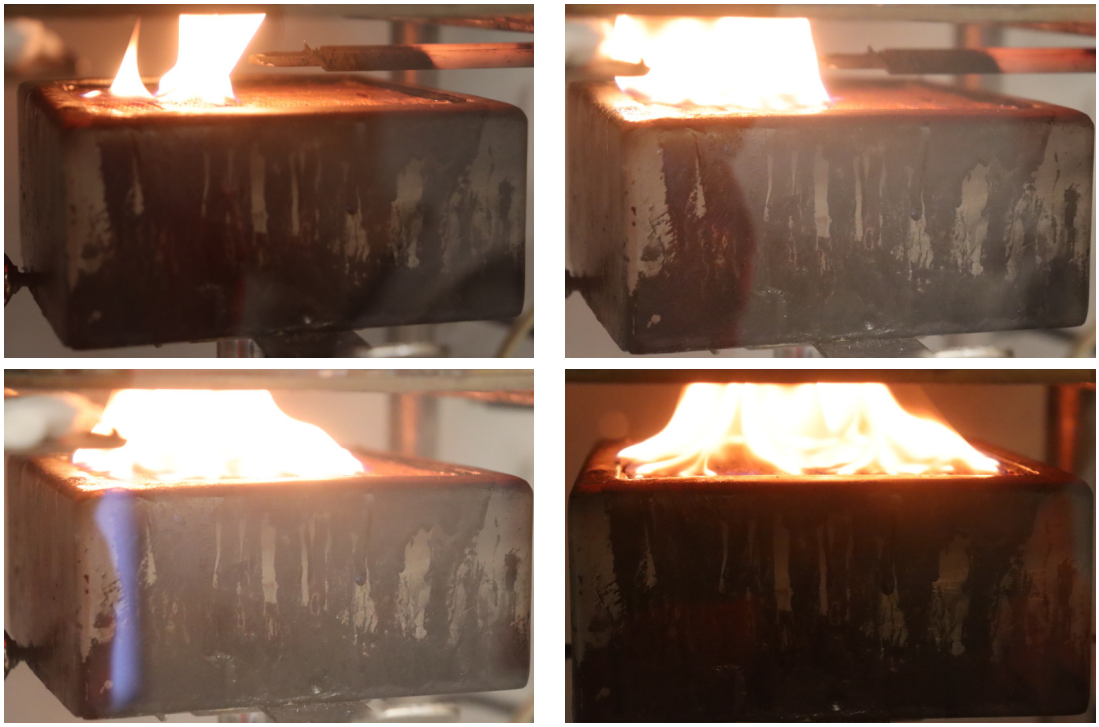

Figure 37: Sample B-C-1 during test in cone calorimeter

Figure 38: Sample B-C-1 of epoxy composite type 2 before flameout during the test in the cone calorimeter

Figure 39: Sample B-C-1 of epoxy composite type 2 after test in cone calorimeter

the aluminum foil to simulate the heat sink effect. To try to assess the effectiveness of the metallic coils, samples C-C-7 and C-C-8 were tested at 50 kW/m^2 with the copper layer placed underneath. However, the results of these tests were consistent with the results obtained from samples C-C-1 and C-C-2.

The measurement of the weight scale during the test of sample C-C-1 malfunctioned and failed to track the mass change of the sample. Consequently, it was not possible to include the mass lost during the test and the mean effective heat of combustion (EHC) in Table 18.

During the tests, non-flammable gases were released from the surface of the epoxy composite type 1 and type 2 while they were heated up, causing volatile gases to accumulate below the fiberglass tape. These volatile gas bubbles caused the tape to bend

Figure 40: Sample C-C-1 of fresh epoxy resin during the test in the cone calorimeter

Figure 41: Sample C-C-1 of epoxy composite type 2 during the test in the cone calorimeter

Figure 42: Sample C-C-1 of fresh epoxy resin during the test in the cone calorimeter

Figure 43: Sample holder after test of the sample C-C-1 of fresh epoxy resin

and move before the gases were released. This observation suggests that the composites underwent a chemical reaction, leading to the release of gases that caused the tape's movement. It is essential to note that the released gases were not flammable and did not contribute to the combustion process.

Figure 44 shows that upon exposure to external heat flux, epoxy composite type 1 displayed an initial peak in HRR immediately after ignition, followed by a significant decrease in HRR and then a second HRR peak. This behavior was observed for all three heat flux levels tested, i.e., 50, 30, and 20 kW/m^2. However, as the heat flux decreased, the peak HRR increased, and the decline in HRR between the first and second HRR peaks was less pronounced. One plausible explanation for the shape of the curve is that the first peak of the HRR curve corresponds to the ignition of the epoxy resin located above the upper layer of the fiberglass tape, after which the resulting flame and external heat flux gradually heated up the epoxy resin located below the fiberglass tape until it also ignited. This phenomenon is particularly evident in the HRR curve of the sample exposed to a heat flux of 20 kW/m^2, where the dip in HRR is less prominent because the epoxy resin was heated more uniformly. Similar behavior can also be observed in the epoxy resin type 2, as depicted in figure 46. However, the notable differences are the faster ignition time, lower mean HRR, and lower peak HRR.

The fresh epoxy resin exhibited distinct behaviors depending on the external heat flux, as illustrated in figure 48. At an external heat flux of 50 kW/m^2, it behaved like a material with an intermediate thermal thickness, without any char formation. However, at lower heat fluxes of 20 and 15 kW/m^2, the samples displayed a behavior similar to thermally thick materials with the formation of char (Schartel & Hull, 2007).

Regarding the total heat released (THR), it can be observed that epoxy resin type 1 released a greater amount of energy per unit area than epoxy resin type 2, and correspondingly, the mass loss during the test was also higher.

Sample name	Material	Heat flux (kW/m^2)	Mean HRR (kW/m^2)	Peak HRR (kW/m^2)	Mean EHC (MJ/kg)	THR (MJ/m^2)	Mass lost during test (g)
A-C-1	Epoxy composite type 1	50	114.80	207.78	19.91	87.59	26.70
A-C-2	Epoxy composite type 1	50	76.77	198.92	18.27	74.07	24.43
A-C-3	Epoxy composite type 1	30	105.28	230.81	20.72	90.86	26.39
A-C-4	Epoxy composite type 1	30	93.41	220.64	20.44	74.54	22.00
A-C-5	Epoxy composite type 1	20	68.51	265.95	20.63	68.30	19.49
A-C-6	Epoxy composite type 1	20	75.58	382.54	20.63	77.25	20.51
B-C-1	Epoxy composite type 2	50	62.36	203.88	20.86	44.83	19.00
B-C-2	Epoxy composite type 2	50	48.96	168.74	21.02	44.60	18.76
B-C-3	Epoxy composite type 2	20	49.07	218.99	21.63	31.99	13.08
B-C-4*	Epoxy composite type 2	20	45.46	159.52	5.19	19.87	12.16
B-C-6	Epoxy composite type 2	20	35.20	187.71	18.98	28.00	12.92
B-C-8	Epoxy composite type 2	30	45.40	164.47	20.63	40.83	16.83
B-C-9	Epoxy composite type 2	30	45.69	146.01	20.63	39.95	17.62
C-C-1	Fresh epoxy resin	50	278.03	1069.36	-	275.52	-
C-C-2	Fresh epoxy resin	50	377.09	925.98	21.66	273.01	93.55
C-C-3	Fresh epoxy resin	20	135.43	323.32	22.22	239.44	95.24
C-C-4	Fresh epoxy resin	20	119.40	338.81	22.58	214.95	84.16
C-C-5	Fresh epoxy resin	15	133.35	301.30	22.98	240.03	92.35
C-C-6	Fresh epoxy resin	15	143.37	311.16	24.95	258.06	91.42
C-C-7	Fresh epoxy resin	50	291.61	843.52	21.35	295.69	122.45
C-C-8	Fresh epoxy resin	50	272.81	761.72	21.79	274.17	111.24

Table 18: Flammability results from the tests on epoxy composite type 1, epoxy composite type 2 and fresh epoxy resin resins using the cone calorimeter. The sample B-C-4 is characterized by an unsteady combustion process. During the test of sample B-C-5, the software of the cone calorimeter crashed. Sample B-C-5 did not ignite

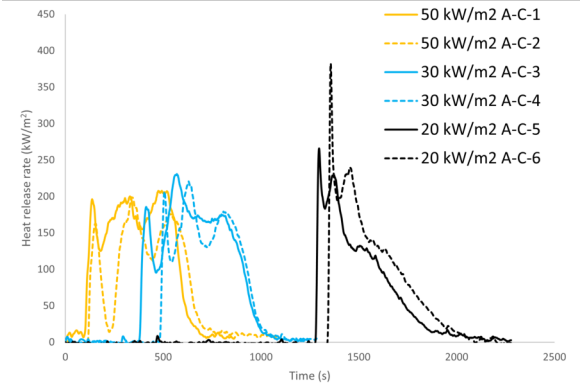

Figure 44: Heat release rate per unit area of epoxy composite type 1 using the cone calorimeter

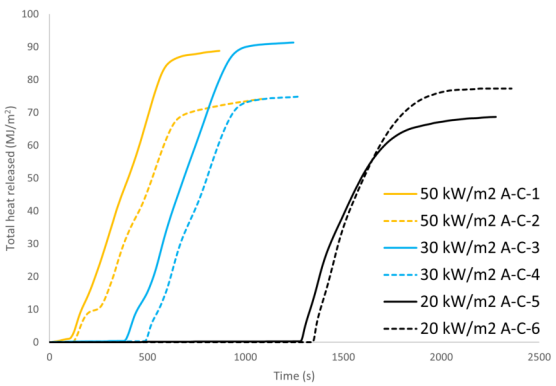

Figure 45: Total heat released per unit area of epoxy composite type 1 using the cone calorimeter

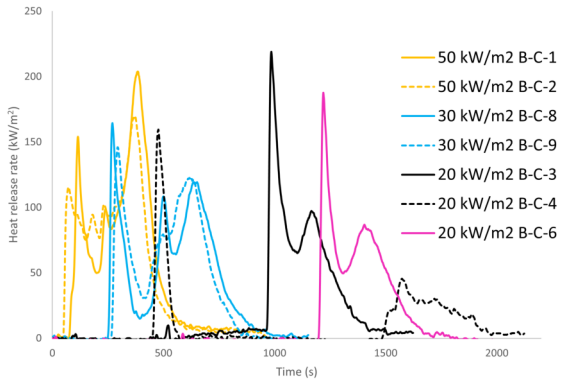

Figure 46: Heat release rate per unit area of epoxy composite type 2 using the cone calorimeter

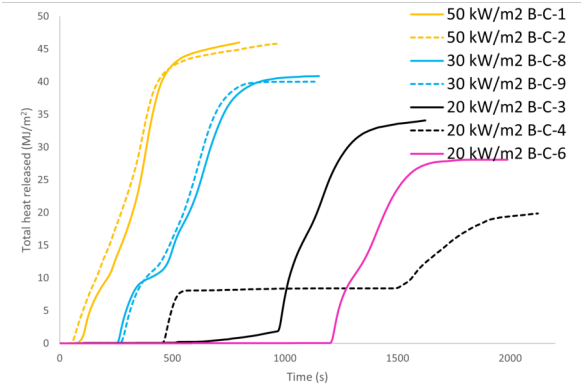

Figure 47: Total heat released per unit area of epoxy composite type 2 using the cone calorimeter

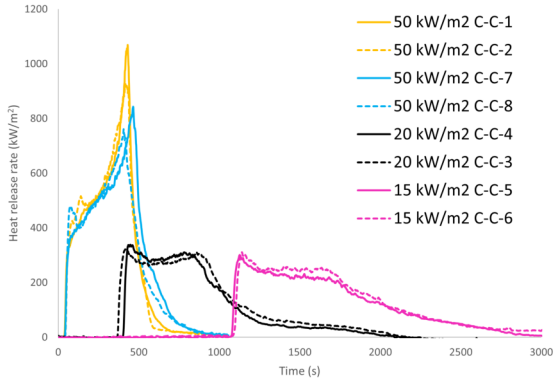

Figure 48: Heat release rate per unit area of the fresh epoxy resin using the cone calorimeter

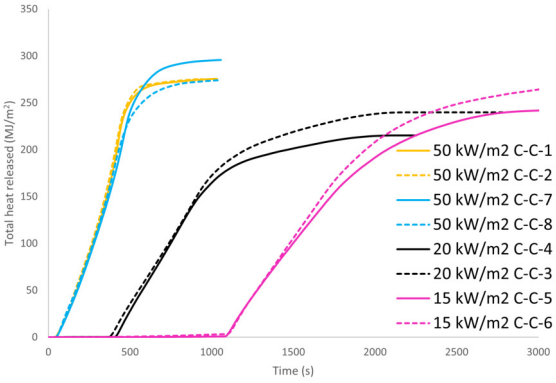

Figure 49: Total heat released per unit area of the fresh epoxy resin using the cone calorimeter

The ignition times of the tests using the cone calorimeter are presented in Table 19. Overall, the time to ignition for fresh epoxy resin was the shortest compared to the epoxy composites type 1 and type 2. One of the main reasons for this is that fresh epoxy resin does not contain the glass fiber tape, or the magnetic core found in the other samples, which act as a heat sink and delay the ignition process during heating. Furthermore, it can be observed that the time to ignition for epoxy composite type 2 is slower than that for epoxy composite type 1. The composition difference of the epoxy resins employed in the magnet coils can potentially be another factor that could impact the ignition time.

The time of ignition was plotted against eh external heat flux for each material in figures 50, 51 and 52. These plots show that as time increases, the required heat flux of ignition approaches a vertical asymptote that corresponds to the theoretical critical heat flux of ignition. To analyze the data, the ignition times and external heat flux were plotted using Equation 1, as explained in Section 3.2.2. Figures 53, 54, and 55 show these plots for the epoxy composite type 1, the epoxy composite type 2, and the fresh epoxy resin, respectively. It is also possible to observe each plot does not intercept the origin, as predicted by Equation 1. Instead, it intercepts the theoretical critical heat flux of ignition, which is the smallest amount of heat flux needed to increase the surface temperature of a solid fuel to a level where pyrolysis happens at a rate that generates a combustible mixture (Quintiere, 2016).

Sample name	Material	External heat flux (kW/m^2)	Time of ignition (s)
A-C-1	Epoxy composite type 1	50	104
A-C-2	Epoxy composite type 1	50	117
A-C-3	Epoxy composite type 1	30	382
A-C-4	Epoxy composite type 1	30	486
A-C-5	Epoxy composite type 1	20	1281
A-C-6	Epoxy composite type 1	20	1341
B-C-1	Epoxy composite type 2	50	78
B-C-2	Epoxy composite type 2	50	52
B-C-8	Epoxy composite type 2	30	252
B-C-9	Epoxy composite type 2	30	261
B-C-3	Epoxy composite type 2	20	971
B-C-4	Epoxy composite type 2	20	448
B-C-6	Epoxy composite type 2	20	1200
B-C-7	Epoxy composite type 2	15	-
C-C-1	Fresh epoxy resin	50	40
C-C-2	Fresh epoxy resin	50	45
C-C-7	Fresh epoxy resin	50	42
C-C-8	Fresh epoxy resin	50	43
C-C-3	Fresh epoxy resin	20	369
C-C-4	Fresh epoxy resin	20	403
C-C-5	Fresh epoxy resin	15	1074
C-C-6	Fresh epoxy resin	15	1085

Table 19: Time of ignition of the tests using the cone calorimeter. The critical heat flux of ignition of each one of the three materials are indicated in table 20.

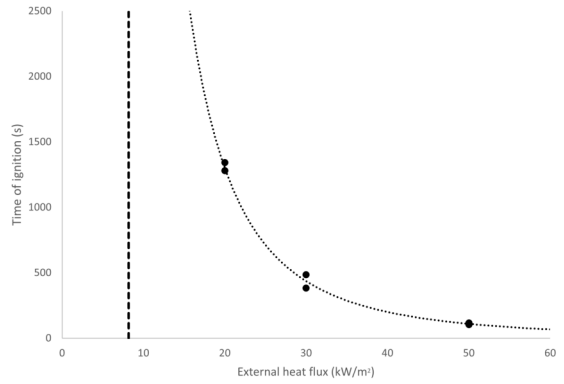

Figure 50: Time to ignition as a function of heat flux for the epoxy composite type 1. Critical heat flux of ignition of 8.18 kW/m^2

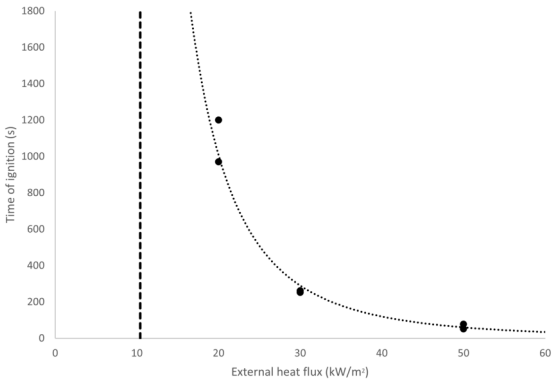

Figure 51: Time to ignition as a function of heat flux for the epoxy composite type 2. Critical heat flux of ignition of 10.40 kW/m^2

Table 20 shows the critical heat flux of ignition values for ignition of the three materials. It's important to note that this value is only theoretical and applies only if the material displays thermally thick behavior continuously. Also, critical heat flux of ignition

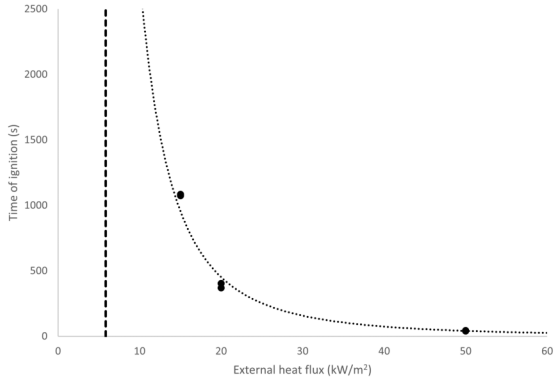

Figure 52: Time to ignition as a function of heat flux for the fresh epoxy resin. Critical heat flux of ignition of 5.84 kW/m^2

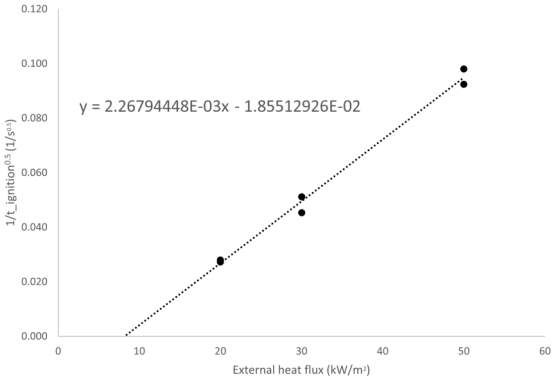

Figure 53: Time to ignition as a function of heat flux plotted according to the equation 1 for the epoxy composite type 1. Critical heat flux of ignition of 8.18 kW/m^2

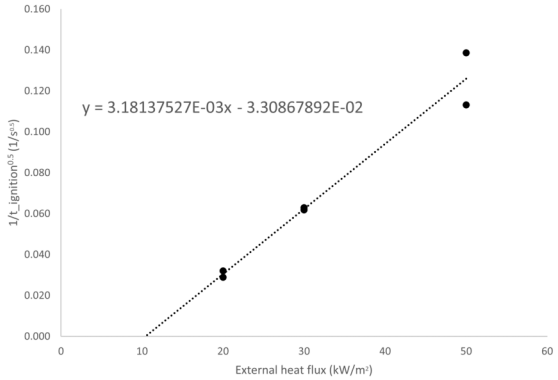

Figure 54: Time to ignition as a function of heat flux plotted according to the equation 1 for the epoxy composite type 2. Critical heat flux of ignition of 10.40 kW/m^2

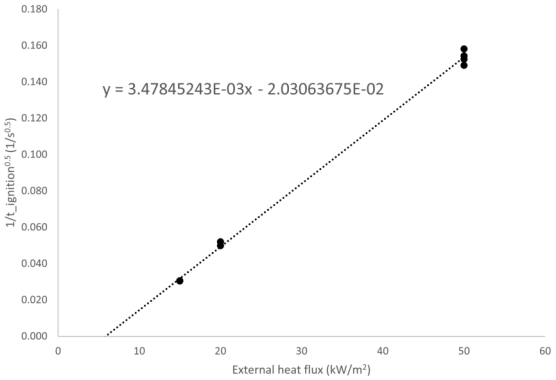

Figure 55: Time to ignition as a function of heat flux plotted according to the equation 1 for the fresh epoxy resin. Critical heat flux of ignition of 5.84 kW/m^2

Material	Critical heat flux of ignition (kW/m^2)	Heat flux of ignition at 900s (kW/m^2)	Heat flux of ignition at 1200s (kW/m^2)
Epoxy composite type 1	8.18	22.88	20.91
Epoxy composite type 2	10.40	20.88	19.47
Fresh epoxy resin	5.84	15.42	14.14

Table 20: Critical heat flux of ignition and heat flux of ignition of epoxy composite type 1, epoxy composite type 2 and fresh epoxy resin obtained from the cone calorimeter

represents the minimum heat flux required for the material to ignite if it were exposed for an indefinite period of time. However, different standards may specify different time criteria for evaluating the critical heat flux of ignition according to their test criteria. For instance, ASTM-E1321 states that tests to determine the critical heat flux of ignition can be stopped if the sample fails to ignite within 20 minutes (1200 s) (ASTM, 2018), while ISO 5660 requires the sample to be removed if no ignition occurs within 15 minutes (900 s) (ISO, 2002).

The results indicate that the minimum heat flux required for ignition of the epoxy composite type 1 is lower than that for the epoxy resin type 2, but this is only observed for exposure times longer than approximately 54 minutes (3250 s) at 15.91 kW/m^2. However, for shorter exposure times such as 20 or 15 minutes, the heat flux required for ignition is actually lower for the epoxy resin type 2. The ignition heat flux of fresh epoxy resin is generally lower compared to the epoxy composites. This is mainly attributed to metallic core, which acts as heat sink in the epoxy composites, delaying the ignition process, and the different composition of the epoxy resins.

4.2.2 Flammable material per mass unit of magnetic coils

The cone calorimeter results presented in Section 4.2 allowed to estimate the flammable material content per mass unit of the magnetic coils. For epoxy composite type 1, which was a section of the complete magnetic coil type 1, the flammable material content per mass unit was estimated by dividing the mass of the material pyrolyzed during the cone calorimeter test by the total mass of the sample, as shown in Equation 5. However, it is important to note that the absence of the filler material on the short sides of the magnetic coil type 1 and the area of the fiber glass was not considered because they are impregnated with epoxy resin. Additionally, although the magnetic coil type 1 has a smooth surface, its thickness varies slightly, as indicated in Table 15.

$$\text{Flammable material content per mass unit} = \frac{\text{Mass pyrolysis during the test}}{\text{Total mass of the sample}} \tag{5}$$

For epoxy resin type 2, two values were included for the flammable material content per mass unit of the magneteic coil. The first value pertains to the section with the same geometry as the samples tested in the cone calorimeter, as illustrated in Figure 7, and was calculated directly using Equation 5. The second value is applicable to the complete cross-section of the magnetic coil type 2 and was calculated using the ratio of the flammable material of the cone calorimeter geometry to the area of the flammable material in the entire geometry, as shown in Figure 7 and was computed using Equation 6. However, it must be noted that, similar to magnetic coil type 1, the variations in thickness in the magnetic coil could affect the results. Additionally, the transverse cut shown Figure 7 was not precise during the preparation of the cone calorimeter and LIFT samples, which may have resulted in variations in the obtained results.

$$\text{Flammable material content per mass unit} = \frac{\text{A} \cdot \text{B}}{\text{A} \cdot \text{B} + \text{C} \cdot \text{D}} \tag{6}$$

where

- A is the ratio of mass to area of flammable mass of the geometry of the samples tested in the cone calorimeter $\left[\frac{g}{m^2}\right]$
- B is the area of non-flammable mass of the complete cross section $[m^2]$

- C is the ratio of mass to area of the non-flammable mass of the geometry of the samples tested in the cone calorimeter $\left[\frac{g}{m^2}\right]$
- D is the area occupied by the non-flammable mass in the complete cross section $[m^2]$

Material	Flammable material per mass unit of magnetic coil (g/g)
Magnetic coil type 1 - Complete cross section of magnetic coil	0.054 ± 0.003
Magnetic coil type 2 - Geometry of samples tested in the cone calorimeter	0.029 ± 0.007
Magnetic coil type 2 - Complete cross section of magnetic coil	0.046 ± 0.003

Table 21: Flammable material per mass unit of magnetic coils

4.2.3 Smoke production

There are several methods to measure the soot yield value, including filter-based measurements, flame ionization detectors, and laser-induced incandescence. For the current project, the soot yield value was estimated using measurements from the helium-neon laser beam of the cone calorimeter test. In the cone calorimeter test, the total smoke obscuration of light by an aerosol, like smoke, is measured using a monochromatic light source such as a helium-neon (HeNe) laser beam. HeNe lasers emit monochromatic radiation at the red wavelength of $\lambda = 632.8$ nm, which is ideal for detecting scattered light by smoke particles and determining their concentration in the air (ISO, 2002). Mulholland and Croarkin (2000) obtained an experimental constant called the mass-specific extinction coefficient of $\sigma_s = 8.7\ \frac{m^2}{g} \pm 1.1\ \frac{m^2}{g}$, applicable to overventilated flaming. Considering this constant, it is possible to obtain the soot yield values as follows:

$$\gamma = \frac{\sigma_f}{\sigma_s} \tag{7}$$

where

- γ is the soot yield value $\left[\frac{g}{g}\right]$
- σ_f is specific extinction area $\left[\frac{m^2}{g}\right]$

According to the standard ISO 5660, the average specific extinction area can be determined by the following formula (ISO, 2002):

$$\sigma_f = \frac{\sum_{i=t_{ig}} \dot{V}_s \kappa \Delta t}{m_{ig} - m_f} \tag{8}$$

where :

- σ_f is specific extinction area $\left[\frac{m^2}{g}\right]$
- κ is the extinction coefficient $[m]$
- $\dot{V}_s$ is the volume flow rate of smoke $\left[\frac{m^3}{s}\right]$
- Δt is the period of time of the test $[s]$

- m_{ig} is the specimen mass at ignition $[g]$
- m_f is the specimen mass at the end of the test $[g]$

The estimated of the soot yield for each experiment, along the results regarding the smoke generation of the samples, is included in table 22.

Sample name	Material	Heat flux (kW/m^2)	Mean SPR (m^2/s)	Mean SPR per mass unit (m^2/s)/kg	Peak SPR (m^2/s)	Peak SPR per mass unit (m^2/s)/kg	TSP per mass unit (m^2/kg)	Mean soot yield (g/g)
A-C-1	Epoxy composite type 1	50	0.027	1.0204	0.06	2.14	779.45	0.09
A-C-2	Epoxy composite type 1	50	0.017	0.7048	0.05	2.05	680.80	0.08
A-C-3	Epoxy composite type 1	30	0.022	0.8289	0.06	2.09	716.10	0.08
A-C-4	Epoxy composite type 1	30	0.019	0.8815	0.04	1.97	704.17	0.08
A-C-5	Epoxy composite type 1	20	0.013	0.6475	0.06	2.88	646.07	0.07
A-C-6	Epoxy composite type 1	20	0.013	0.6565	0.08	3.89	668.33	0.08
B-C-1	Epoxy composite type 2	50	0.019	1.0086	0.08	4.46	726.16	0.08
B-C-2	Epoxy composite type 2	50	0.015	0.8256	0.08	4.26	752.98	0.09
B-C-3	Epoxy composite type 2	20	0.013	0.9780	0.09	6.92	637.46	0.07
B-C-4	Epoxy composite type 2	20	0.012	0.9640	0.06	4.79	577.73	0.07
B-C-6	Epoxy composite type 2	20	0.011	0.8590	0.09	6.87	677.48	0.08
B-C-8	Epoxy composite type 2	30	0.012	0.7045	0.06	3.39	634.01	0.07
B-C-9	Epoxy composite type 2	30	0.013	0.7539	0.05	2.92	656.60	0.08
C-C-1	Fresh epoxy resin	50	0.092	-	0.31	-	-	-
C-C-2	Fresh epoxy resin	50	0.106	1.1378	0.26	2.78	825.41	0.09
C-C-3	Fresh epoxy resin	20	0.037	0.3915	0.10	1.06	692.53	0.08
C-C-4	Fresh epoxy resin	20	0.032	0.3758	0.10	1.18	676.88	0.08
C-C-5	Fresh epoxy resin	15	0.034	0.3692	0.08	0.88	664.84	0.08
C-C-6	Fresh epoxy resin	15	0.034	0.3666	0.08	0.86	660.15	0.08
C-C-7	Fresh epoxy resin	50	0.093	0.7622	0.27	2.19	774.72	0.09
C-C-8	Fresh epoxy resin	50	0.085	0.7597	0.24	2.17	768.61	0.09

Table 22: Results of smoke from the tests on epoxy composites type 1 and type 2 and fresh epoxy resin using the cone calorimeter. The sample B-C-4 is characterized by an unsteady combustion process.

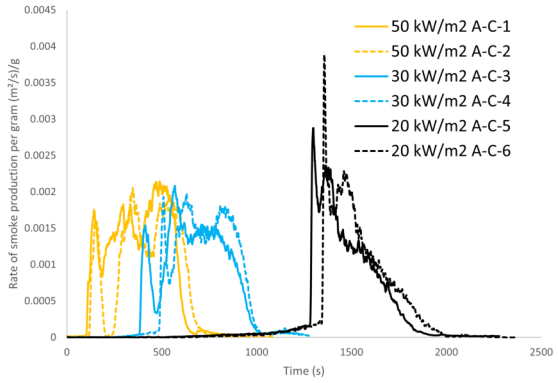

Figure 56: Rate of smoke production mass unit of epoxy composite type 1 using the cone calorimeter

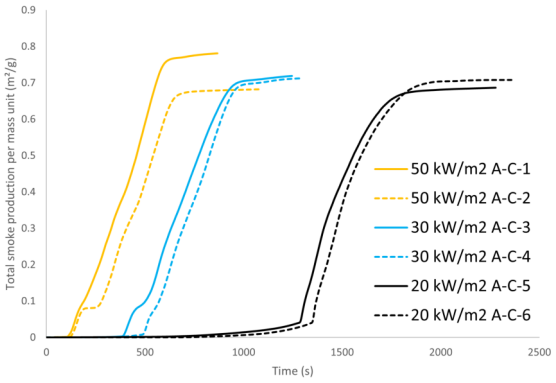

Figure 57: Total smoke production per mass unit of epoxy composite type 1 using the cone calorimeter

It can be observed from the results that the smoke production of both epoxy composite type 1 and type 2 increased as the external heat flux decreased. This behavior can be attributed to incomplete combustion of pyrolysis gases, resulting in the formation of more soot and smoke. Lower heat fluxes provide less energy to the material, which can lead to incomplete combustion and more smoke production. It is also noteworthy that the smoke production rate curves exhibit a similar trend as the HRR curves. As the material undergoes pyrolysis and combustion, volatile gases and other products are released, and as they undergo further reactions, they produce heat and smoke. The amount of smoke

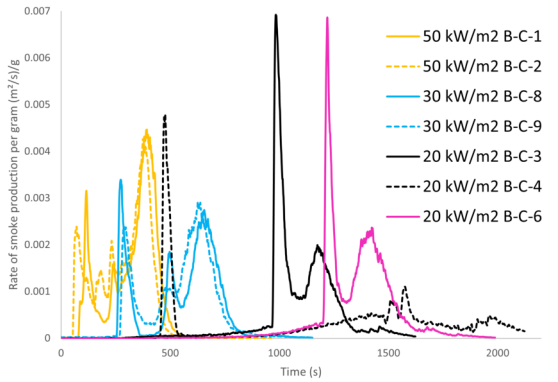

Figure 58: Rate of smoke production mass unit of epoxy composite type 2 using the cone calorimeter

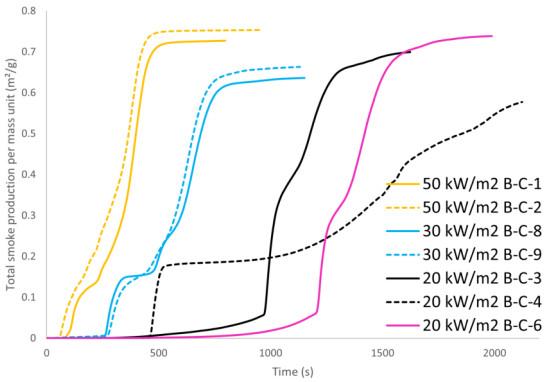

Figure 59: Total smoke production per mass unit of epoxy composite type 2 using the cone calorimeter

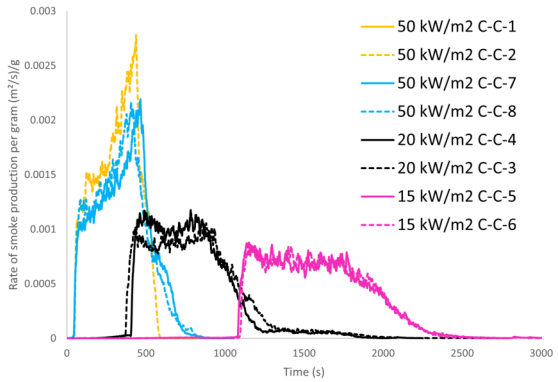

Figure 60: Rate of smoke production mass unit of the fresh epoxy resin using the cone calorimeter

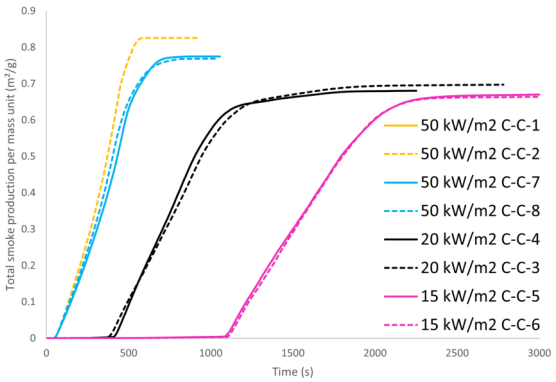

Figure 61: Total smoke production per mass unit of the fresh epoxy resin using the cone calorimeter

produced is related to the amount of fuel that is consumed and the degree of combustion, which in turn affects the HRR.

It can be observed that, in general, the total smoke production of epoxy composite type 1 was higher compared to epoxy composite type 2, while the mean soot yield value was similar for all three materials.

In summary, the following conclusions can be drawn from the results from the cone calorimeter presented in this section:

- The HRR and SRP of the epoxy composite type 1 and type 2 and fresh epoxy resin is different.
- The mean and peak HRR and the SRP of epoxy composite type 1 is higher than that of epoxy composite type 2 when ignited after exposure to an external heat flux.
- The critical heat flux of ignition is lower for epoxy composite type 1 compared to epoxy composite type 2. However, for an exposure time of less than 3250 s, the required external heat flux for ignition is higher for epoxy composite type 1.
- Epoxy composite type 1 has a longer time of ignition than epoxy composite 2 when they are ignited after being exposed to an external heat flux.

- The soot yield value for the three materials is very similar

4.3 Results of the lateral ignition and flame spread test

Unfortunately, it proved impossible to obtain a sample of the required dimensions from the magnetic coils of 80 cm x 15 cm, according to the standard (ASTM, 2018). In order to obtain samples of epoxy composite type 1 that met the necessary specifications, the long sections of the ring-shaped magnetic coil type 1 were cut to obtain the largest continuous samples possible. The resulting samples were approximately 68 cm long, and an additional piece of epoxy composite type 1 was cut, measuring 12 cm in length, to create a sample of the required 80 cm length. Therefore, there was a gap between the two segments that was positioned at the farthest end of the sample holder from the radiant panel and the external flame source. Careful attention was given during the placement of the segments in the sample holder to minimize this gap. To ensure that the samples were securely held in place, a calcium silicate board was used as a base and fixed the parts with bolts, nuts, and washers. These measures ensured that the samples remained stable and secure during testing. Notably, the samples of magnetic coil type 2 were tested with its complete thickness. The samples of epoxy composite type 1 can be observed in figures 62 and 63

The magnetic coil type 2 features mostly straight small sides, but its longer sides are bent and covered with epoxy resin, making it impossible to obtain a long, straight piece. Therefore, it was opted to cut the magnetic coil into shorter segments to form the complete sample. In total, the magnetic coil was cut into five pieces, with lengths of 20 cm, 15 cm, 15 cm, 15 cm, and 15 cm respectively. By using these shorter segments, it was possible to create a sample of the required dimensions while ensuring its straightness. Nevertheless, since the segments were not continuous and the cutting process was imperfect, the segments did not fit together perfectly, resulting in gaps between them when assembled into a sample. To minimize these gaps, care was taken during the placement of the segments in the sample holder. It should be noted that magnetic coil type 2 was not tested in its full thickness due to sample size limitations, and instead, it was cut in half to meet the requirements of the LIFT experiments. This could have had a slight impact on the results obtained. The samples of epoxy composite type 2 can be seen in the figures 64 and 65.

The standard ASTM (2018) states this test method may not be applicable to products and assemblies in which physical performance such as joint separation and fastening methods can have a significant impact on flame propagation in actual fire conditions. Nonetheless, given the limitations of the samples, the expectation was that the tested samples may exhibit behavior consistent with a continuous sample.

The measurements of the external heat flux at five different positions along the sample were taken before each test using a water cooled heat flux sensor model SBG03-O50, and they are shown in table 24. As shown in figures 66 and 67, the heat flux at any position along the sample was estimated using polynomial regression.

Test number	Sample name	Thickness (mm)	Width (mm)
Test 1	A-L-1	15.13 ± 0.06	64.01
Test 3	A-L-2	15.28 ± 0.03	64.69
Test 2	B-L-1	31.46 ± 0.36	98.61
Test 4	B-L-2	31.2 ± 0.17	98.99

Table 23: Dimensions of the samples of epoxy composite type 1 and epoxy composite type 2 tested in the LIFT apparatus

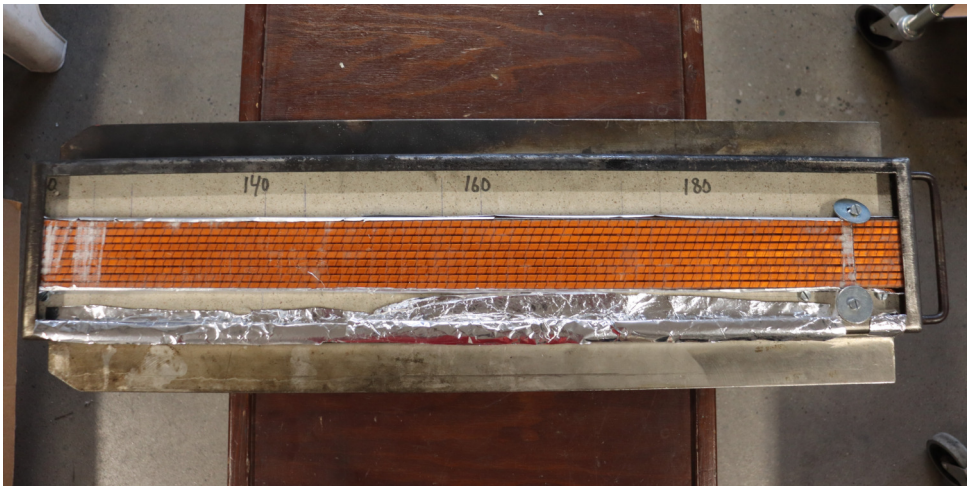

Figure 62: Sample A-L-1 for test 1 of epoxy composite type 1 in the sample holder for the LIFT. The gap between the two segments was located at the farthest end of the sample holder from the radiant panel and the external flame source

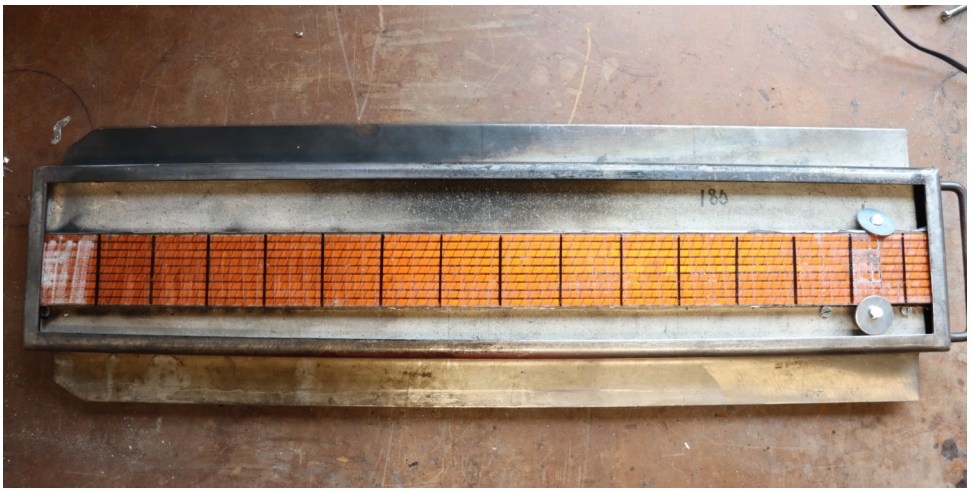

Figure 63: Sample A-L-2 for test 3 of epoxy composite type 1 in the sample holder for the LIFT. The gap between the two segments was located at the farthest end of the sample holder from the radiant panel and the external flame source

Measured incident heat flux at each position during tests of samples A-L-1 and B-L-1					
Position (cm)	5	20	35	50	65
Measured incident heat flux (kW/m^2)	49.59	39.37	22.24	9.48	3.65

Measured incident heat flux at each position during tests of samples A-L-2 and B-L-2					
Position (cm)	5	20	35	50	65
Measured incident heat flux (kW/m^2)	49.36	39.35	21.92	9.33	3.62

Table 24: Measured incident heat flux at each position along the sample in the LIFT apparatus

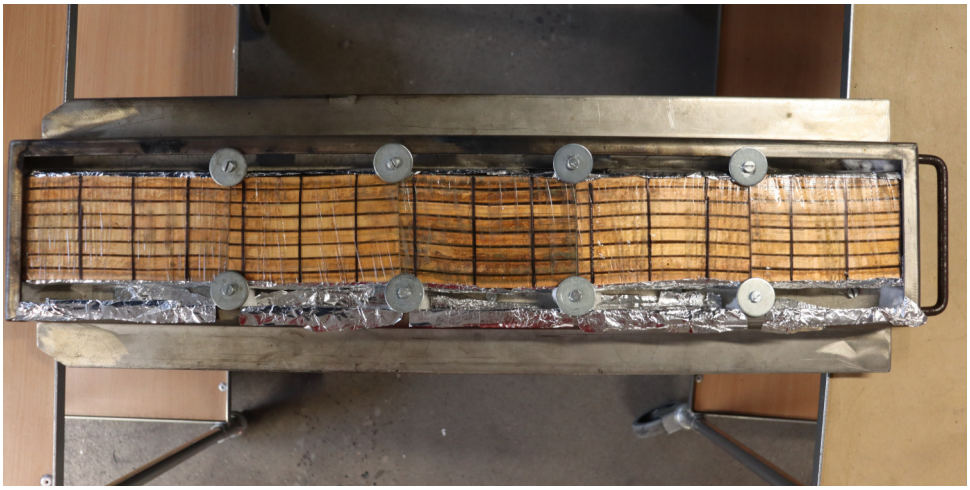

Figure 64: Sample B-L-1 for test 2 of epoxy composite type 2 in the sample holder for the LIFT. The sample consists of five segments with gaps between them.

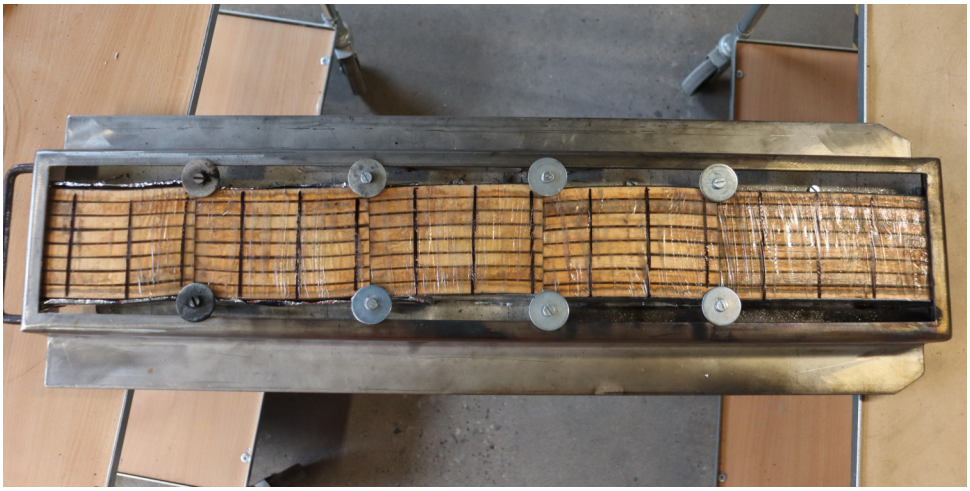

Figure 65: Sample B-L-2 for test 4 of epoxy composite type 2 in the sample holder for the LIFT. The sample consists of five segments with gaps between them.

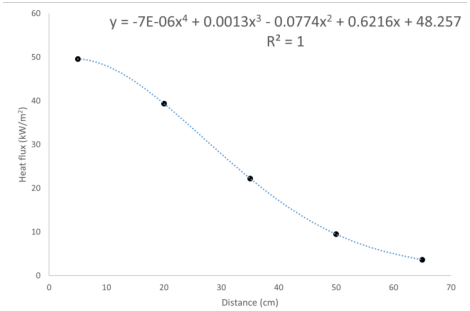

Figure 66: Measured incident heat flux at each position during tests of samples A-L-1 and B-L-1.

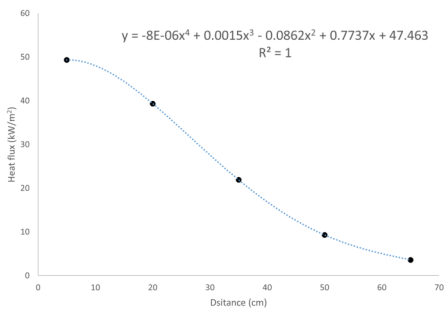

Figure 67: Measured incident heat flux at each position during tests of samples A-L-2 and B-L-2.

Figures 68 and 69 depict the position of the flame-front and the corresponding time required to reach it. The LIFT results for the epoxy composite type 1 were consistent between both tests, as confirmed by the flame front velocity calculated using equation 3. However, the LIFT results for the epoxy composite type 2 were inconsistent between the

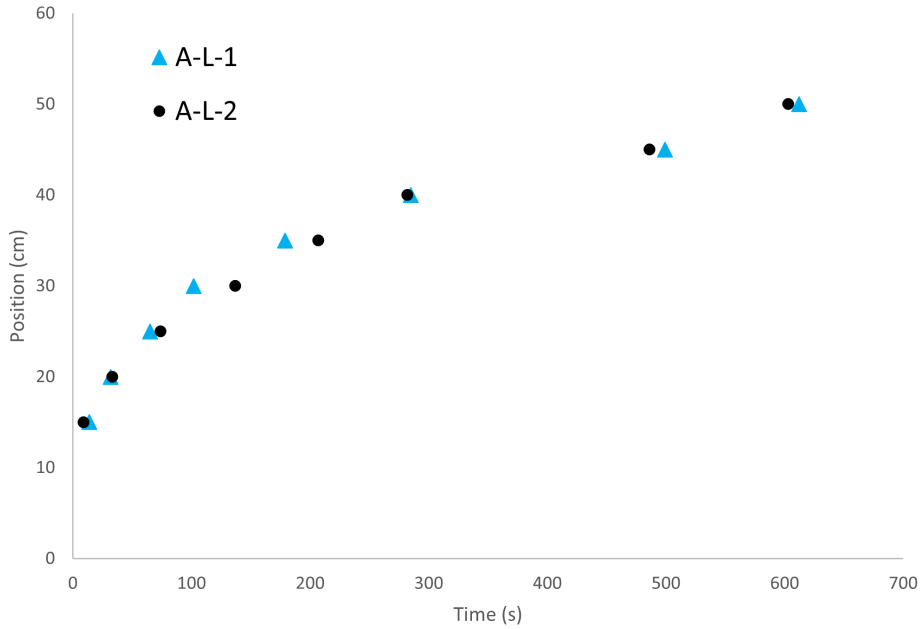

Figure 68: Measured position and time of the flame front of epoxy composite type 1 using the LIFT apparatus

two tests. In test 4, the gap between the first and second pieces of the sample influenced the results and lead to a longer time required for the flame to spread from the first to the second piece, thus causing a significant difference in behavior compared to test 2 where the influence of the gap was not significant. Consequently, the flame front velocity obtained for both tests was also different, as shown in the table 27. Therefore, it has been decided to exclude the results of test 4 of epoxy composite type 2. However, it is noteworthy that during test 4, the flame spread behavior after spreading to the second piece was similar to that observed in test 2, as shown in Figure 69. Additionally, both samples of epoxy composite type 2 in test 2 and test 4 exhibited a comparable maximum distance of flame spread.

Table 25 shows that the maximum travel distance was observed at the edge of the samples. However, this is attributed to the edge effect that can affect the LIFT results. The edge effect refers to the phenomenon where the flame front at the edges of the sample experiences different conditions compared to the flame front in the center of the sample. In the edge region, the react zone is not heated from one side, but instead is heated by the flame from the front of the sample and above the sample. Moreover, there is more air flow available in the edge region, which can lead to a longer flame spread. To mitigate the edge effect, a commonly adopted method is to cover the sides and back of the specimen with aluminum foil. This helps to reduce heat loss and air flow from the sides and back of the specimen, thereby creating more uniform conditions for the flame front across the surface of the sample.

It is worth noting that there is a tendency for longer flame travel distances to occur on the upper part of the samples, which can be attributed to the buoyancy of the flame. As the flame moves upwards, the upper surface of the sample is exposed to more heat compared to the lower part, resulting in a longer flame spread distance.

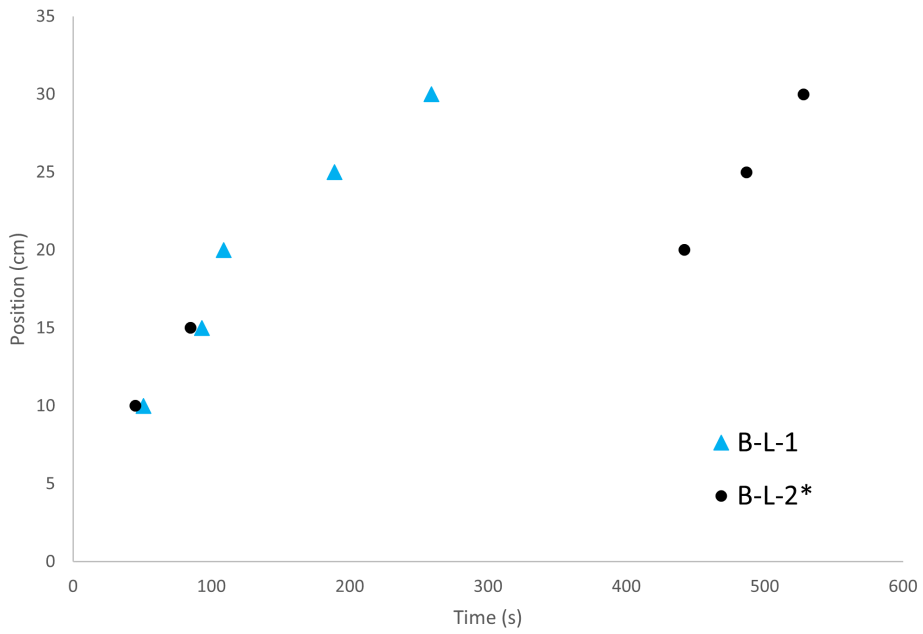

Figure 69: Measured position and time of the flame front of epoxy composite type 2 using the LIFT apparatus. The results from test 4 of sample B-L-2 will be disregarded as the gap between the first and second pieces of the sample significantly affected the accuracy and reliability of the results.

Test number	Sample	Material	Distance of flame spread (cm)			
			Maximum travel distance Upper edge	Upper part of the sample	Middle part of the sample	Lower part of the sample
Test 1	A-L-1	Epoxy composite type 1	56.5	53.8	45	40
Test 3	A-L-2	Epoxy composite type 1	55.5	44.2	44.5	44
Test 2	B-L-1	Epoxy composite type 2	34.9	34.9	34.7	33.1
Test 4	B-L-2	Epoxy composite type 2	34.7	34.7	34.8	33.7

Table 25: Maximum travel distance of the flame-front of the epoxy composite type 1 and type 2 using the LIFT apparatus

During the tests, it was observed that epoxy composite type 1 ignited within the first 15 cm of the exposed surface and exhibited non-uniform flame propagation. In contrast, epoxy composite type 2 underwent ignition within the initial 10 cm and showed uniform flame spread. However, it is crucial to ensure that the flame is mainly driven by the external heat flux, rather than being just ignited due to the external heat flux. Therefore, it is necessary to check that the heat flux of ignition is higher than the external heat flux required to sustain the flame spread, which is expressed as $q_{ig} - q_e \geq 0$. This condition ensures that the obtained data is a result of the flame spread rather than ignition. Table 26 presents the minimum external heat flux values required to sustain flame spread for both epoxy composite types.For epoxy composite type 1, it can be observed from table 26 that the minimum external heat flux required to sustain the flame spread at the position of maximum flame spread was 10.35 kW/m^2, which is lower than the critical heat flux of ignition obtained from the cone calorimeter as reported in table 20. However, for epoxy composite type 2, the minimum external heat flux required to sustain flame spread at the position of maximum flame spread was approximately 22.30 kW/m^2, which is higher than the critical heat flux of ignition reported in Table 20. As shown in Figure 69, it

took 259 s to reach the maximum flame spread for epoxy composite type 2 during test 2. By using the equation obtained from the cone calorimeter experiment shown in Figure 54, it is possible to estimate that the required external heat flux of ignition at 259 s is around 29.93 kW/m^2, which is higher than the minimum external heat flux required to sustain flame spread of 22.30 kW/m^2. Therefore, it is confirmed that the flame spread for epoxy composite type 2 was mainly driven by the external heat flux. However, it is important to note that the presence of gaps in the epoxy composite type 2 samples may have significantly affected the results obtained from the LIFT tests. As can be seen in Figures 73 and 72, the flame spread was halted just after the gap between the second and third segments of the sample. This creates a high level of uncertainty when comparing the results obtained from the LIFT with those obtained from other methods. Despite the external heat flux being higher than the critical heat flux of ignition at the maximum distance of flame spread, a significant portion of this result may be attributed to the presence of the gaps.

Test number	Sample	Material	External heat flux at the maximum distance of flame spread (kW/m^2)			
			Maximum travel distance Upper edge	Upper part of the sample	Middle part of the sample	Lower part of the sample
Test 1	A-L-1	Epoxy composite type 1	6.26	7.44	12.91	17.19
Test 3	A-L-2	Epoxy composite type 1	6.65	13.26	13.03	13.42
Test 2	B-L-1	Epoxy composite type 2	22.35	22.35	22.56	24.32
Test 4	B-L-2	Epoxy composite type 2	22.24	22.24	22.13	23.34

Table 26: External heat flux at the maximum distance of flame spread using the LIFT apparatus. Average external heat flux at the maximum distance of flame spread for epoxy composite type 1 is 10.30 kW/m^2, and for epoxy composite type 2 is 22.30 kW/m^2.

Figure 70: Sample A-L-1 after test 1 of epoxy composite type 1 in the LIFT

Table 27 shows that the epoxy composite type 1 has a higher estimated flame front velocity than the epoxy composite type 2, but a higher flame spread parameter. It is important to note that the flame front velocity is the speed at which the flame front moves through the material surface, while the flame spread parameter represents the relationship between the heat flux applied to the material and the rate of flame spread over the material's surface. A higher flame spread parameter indicates that the material being tested has a greater potential to spread flames laterally. This means that the

Figure 71: Sample A-L-2 after test 3 of epoxy composite type 1 in the LIFT

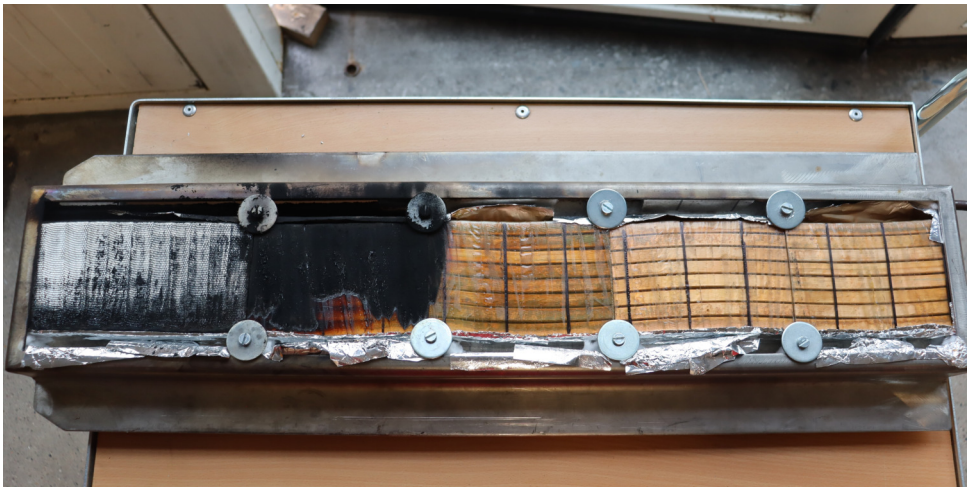

Figure 72: Sample B-L-1 after test 1 of epoxy composite type 1 in the LIFT

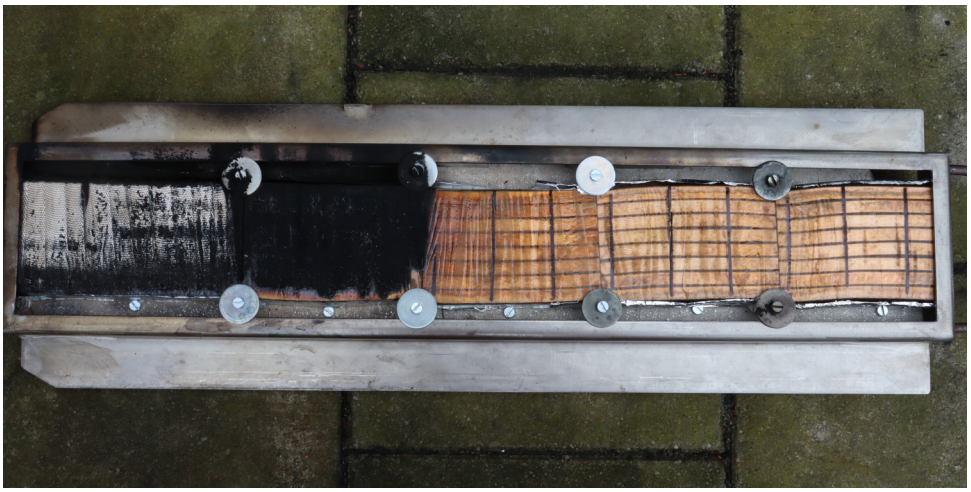

Figure 73: Sample B-L-2 after test 4 of epoxy composite type 2 in the LIFT

material is more likely to ignite and continue burning in the presence of a flame, which could pose a significant fire hazard (Hurley et al., 2015).

Test number	Sample name	Material	Flame front velocity (cm/s)	Flame spread parameter (kW^2/m^3)
Test 1	A-L-1	Epoxy composite type 1	0.165	522.29
Test 3	A-L-2	Epoxy composite type 1	0.113	529.62
Test 2	B-L-1	Epoxy composite type 2	0.093	313.21
Test 4	B-L-2*	Epoxy composite type 2	0.032	19.76

Table 27: Results for the epoxy composite type 1 and type 2 using the LIFT apparatus. The results from test 4 were disregarded as the gap between the first and second pieces of the sample significantly affected the accuracy and reliability of the results. The average flame front velocity of epoxy composite type 1 is 0.139 m/s. For epoxy composite type 2, it is considered to be 0.093 m/s.

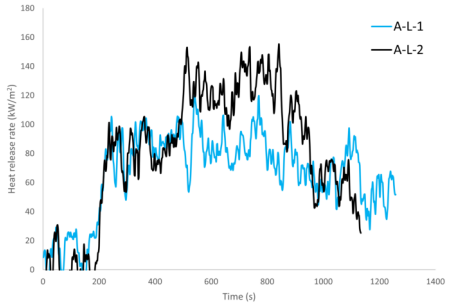

Figure 74: Heat release rate per unit area of samples A-L-1 and A-L-2 using the LIFT apparatus. The time t=0 s corresponds to the moment when the sample was placed in the LIFT apparatus and exposed to the external heat flux field and external flame source.

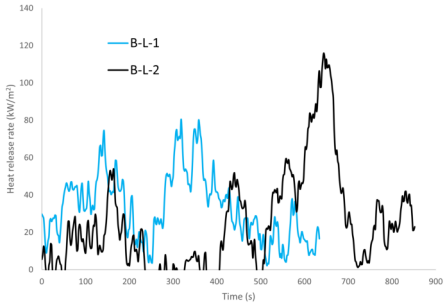

Figure 75: Heat release rate per unit area of samples B-L-1 and B-L-2 using the LIFT apparatus.The time t=0 s corresponds to the moment when the sample was placed in the LIFT apparatus and exposed to the external heat flux field and external flame source.

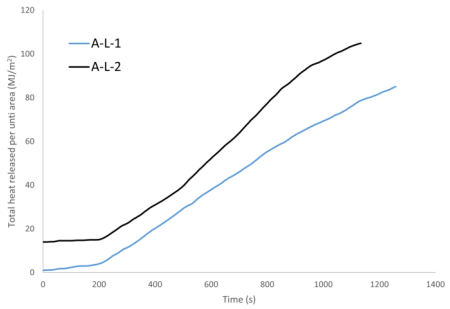

Figure 76: Total heat released during tests 1 and 2 in LIFT. The time t=0 s corresponds to the moment when the sample was placed in the LIFT apparatus and exposed to the external heat flux field and external flame source.

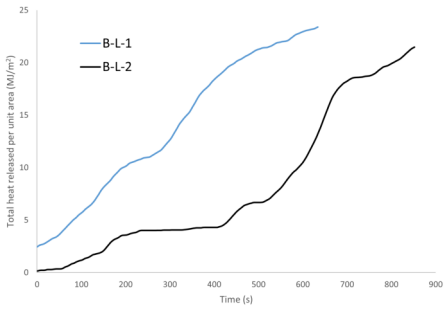

Figure 77: Total heat released during tests 3 and 4 in LIFT. The time t=0 s corresponds to the moment when the sample was placed in the LIFT apparatus and exposed to the external heat flux field and external flame source.

By comparing figure 74, which illustrates the HRR during the LIFT of epoxy composite type 1, against figure 44, which shows the HRR during the cone calorimeter test, it is possible to observe that the HRR was lower during the LIFT. The reason for this is the difference in the testing procedures. In the cone calorimeter, the sample is subjected to a constant heat flux until it produces enough pyrolysis gases to reach ignition and then the complete sample burns. On the other hand, in the LIFT, the sample is ignited using

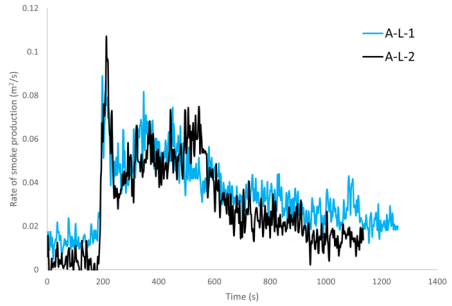

Figure 78: Rate of smoke production during tests 1 and 2 in LIFT. The time t=0 s corresponds to the moment when the sample was placed in the LIFT apparatus and exposed to the external heat flux field and external flame source.

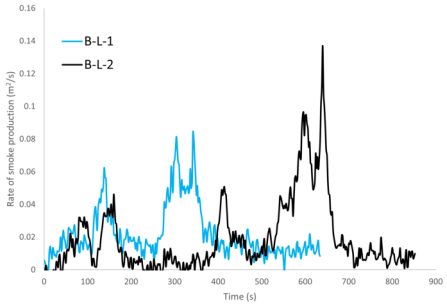

Figure 79: Rate of smoke production during tests 3 and 4 in LIFT. The time t=0 s corresponds to the moment when the sample was placed in the LIFT apparatus and exposed to the external heat flux field and external flame source.

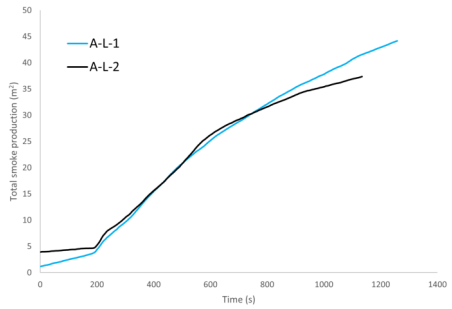

Figure 80: Total smoke produced during tests 1 and 2 in LIFT. The time t=0 s corresponds to the moment when the sample was placed in the LIFT apparatus and exposed to the external heat flux field and external flame source.

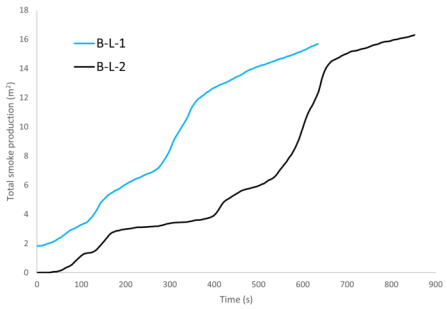

Figure 81: Total smoke produced during tests 3 and 4 in LIFT. The time t=0 s corresponds to the moment when the sample was placed in the LIFT apparatus and exposed to the external heat flux field and external flame source.

an external flame and only the flame spread on one surface is measured. This behavior is also observed for the HRR of epoxy composite type 2 and the smoke production rate of both materials.

Additionally, there was no evidence of the samples dripping during the testing. During the cone calorimeter tests, it was observed that the surface of the fresh epoxy resin appeared to foam. According to Mouritz and Gibson (2007), this phenomenon occurred due to the accumulation of volatile compounds generated by the thermal degradation of the epoxy resin, which causes the char layer to foam and swell. Although the possibility of the production of liquid compounds as part of the thermal degradation of epoxy resin cannot be ruled out due to the uncertainty regarding the exact composition of the epoxy compounds and the possibility that they vaporize before flowing, it can be concluded that the risk of a pool fire resulting from the dripping of epoxy resin in the magnetic coils is negligible, given the low concentration of flammable epoxy resin present.

In summary, the following are the main conclusions drawn from LIFT:

- The epoxy composite type 1 has a shorter time of ignition compared to the epoxy composite type 2 when it is exposed to an external flame source and heated up by an external heat flux.

		Material			
Purge gas Atmosphere	Type of test	Epoxy resin type 1	Epoxy resin type 2	Fresh epoxy resin	Total
100% N2	TGA-DSC-FTIR	2 Tests	2 Tests	-	4
Air	TGA – DSC	2 Tests	2 Tests	1 Tests	5

Table 28: Experimental test plan for thermal decomposition analysis of epoxy resins using TGA

- The time of ignition for epoxy composite type 1 was faster when exposed to an external flame source and heated up by an external heat flux compared to the time of ignition for the same material observed in the cone calorimeter test.
- Epoxy composite type 1 requires a lower external heat flux to sustain the flame spread than epoxy composite type 2.
- Epoxy composite type 1 has a higher flame front velocity than epoxy composite type 2.
- Epoxy composite type 1 has a higher resistance to flame spread than epoxy composite type 2.
- When exposed to an external flame source and heated up by an external heat flux, epoxy composite type 1 exhibits higher HRR and SPR compared to composite type 2, which is consistent with the results obtained from the cone calorimeter experiments.
- For epoxy compounds with the geometry, material, and shape of the tested samples, it was observed that the likelihood of a pool fire caused by the dripping of epoxy resin in the magnetic coils is negligible.

4.4 Results of the thermogravimetric analyzer

The tests were carried out by heating samples with a relatively small mass (5-10 mg) in an 85 µl alumina crucible at a rate of 20K/min up to 750°C, using a TGA-DSC type sample carrier in Netzsch 449 F3 (Jupiter) STA. The crucible lids had a hole, and no pre-treatment was performed on the samples prior to testing. Baseline correction was applied before the test to ensure accurate results.

Table 28 shows the designed test plan that was part of the current project. Unfortunately, experiments on fresh epoxy resin could not be conducted due to a malfunction in the STA.

4.4.1 Results of the thermogravimetric analyzer in air atmosphere

For the epoxy resin type 1 in air atmosphere, the degradation process of the samples comprised two distinct stages. The first stage, characterized by a rapid mass loss, occurred between 350 °C and 370 °C, with a total mass loss of 75%, and lasted until 440 °C. The second stage, involving a slower mass loss, occurred between 440 °C and 620 °C, where the remaining 20% of the mass was lost. As shown in figure 82, the maximum rate of mass loss during the first stage was observed at temperatures of 419.3 °C and 411.4 °C for tests 1 and 2, respectively. No residue was observed when the samples were heated to 750 °C. During the test, the DSC curve exhibits a broad, concave endothermic peak,

indicative of an endothermic reaction. Notably, this peak begins after the maximum mass loss rate, and persists until complete pyrolysis of the sample.

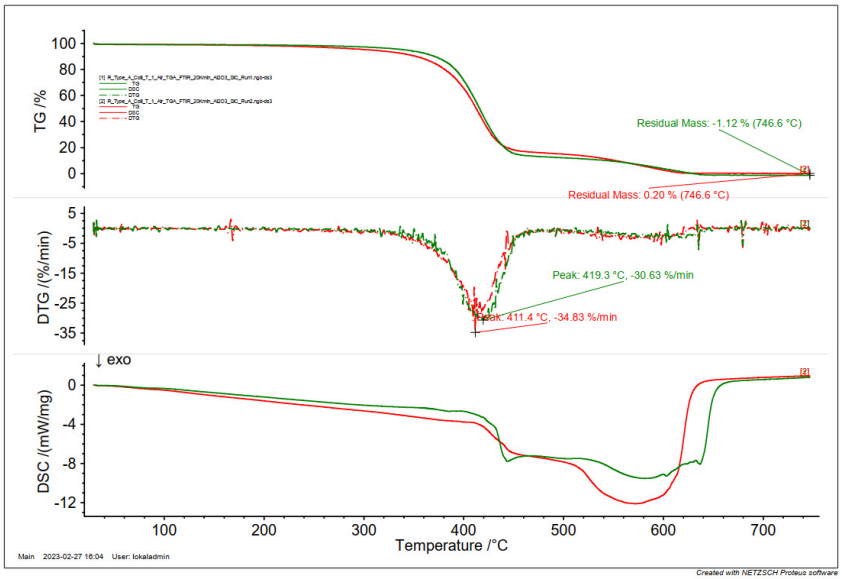

Figure 82: TG curve, DTG curve and DSC curve of the two tests epoxy resin type 1 using the TGA -DSC with a heating rate of 20K/min in air atmosphere. Test 1 and test 2

For epoxy resin type 2 in air atmosphere, the mass loss rate of the two tests differed noticeably, as shown in figure 83. In test 3, the degradation process involved three distinct stages. The first stage, marked by a rapid mass loss rate, commenced at 280 °C and ended at 440 °C. This was followed by a second stage with a slower mass loss rate, extending from 440 °C to approximately 530 °C. The final stage, also characterized by a fast mass loss rate, occurred from about 530 °C to 580 °C. Each stage of rapid mass loss was accompanied by a peak in the mass loss rate. The first fast stage exhibited a peak at 427.9 °C, while the second fast stage showed a peak at 547.3 °C. In contrast, test 4 displayed only one peak in the mass loss rate, occurring at 428.4 °C. The rapid mass loss in test 4 began at around 340 °C and ended at 560 °C. The TG curve revealed that after tests 3 and 4, there was a residual mass of 48.98% and 54.35%, respectively, when the samples reached a temperature of 750 °C.

The DCS curve for test 4 revealed the presence of two distinct endothermic peaks, suggesting that the sample underwent two different stages of melting, crystallization, or glass transitions. In contrast, test 3 only showed a single peak. To fully understand the significance of these findings, additional research would be necessary. The interpretation of the peaks would be highly dependent on the unique properties of the epoxy resin and non-flammable material used in the sample. Therefore, a comprehensive investigation is needed to provide a more definitive explanation for this behavior.

For the fresh epoxy resin in air atmosphere, similar to the epoxy resin type 1 sample, the TG curve for this sample exhibited a single stage of mass loss. The onset of decomposition was observed to be 370°C and continued until approximately 480°C. The peak of mass loss rate occurred at 426.8 °C. Upon reaching 750 °C, a residual mass of 6.28% was observed in the TG curve.

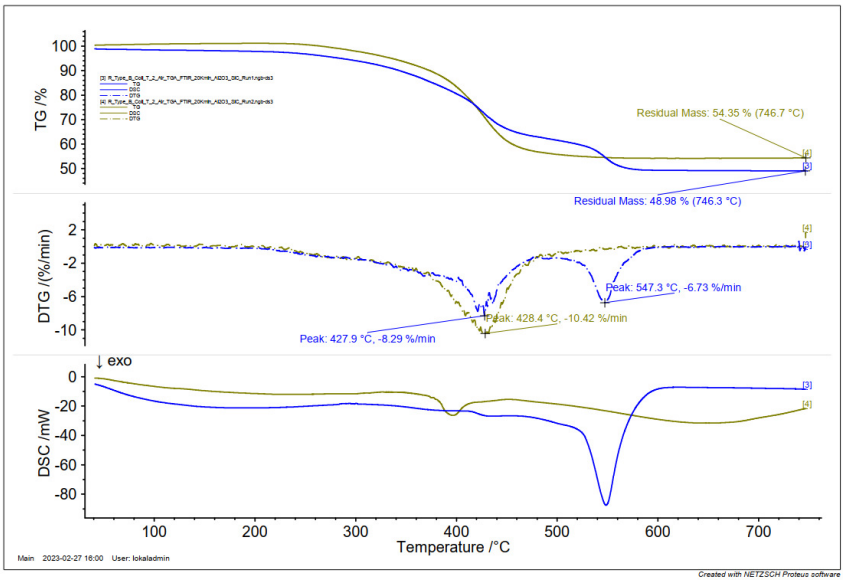

Figure 83: TG curve, DTG curve and DSC curve of the two tests epoxy resin type 2 using the TGA -DSC with a heating rate of 20K/min in air atmosphere. Test 3 and test 4

The DSC curve for the sample is not available for reporting, as the test was performed in an open crucible. Previous attempts to conduct the test in a sealed aluminum crucible were unsuccessful, as the seal broke, and tar liquid leaked out. Following this incident, a crucible lid with a hole was not available, and the test had to be carried out in an open crucible.

Material	Onset temperature (°C)	Temperature at peak mass loss rate (°C)	Residual mass
Epoxy Resin Type 1	350-370	411.4 - 419	0.2%, -1.12%
Epoxy Resin Type 2 Test 3	280	427.9, 547.3	48.98%
Epoxy Resin Type 2 Test 4	340	428.4	54.35%
Fresh Epoxy Resin	370	426.8	6.28%

Table 29: Results of the tests of the three material using the TGA-DSC-FTIR in air atmosphere using TGA

As a result of the tests of the three epoxy resins in air atmosphere, it is possible to observe the epoxy resin type 2 shows an inconsistent behavior in air atmosphere. Even though both tests have the first peak of mass loss rate at very similar temperatures, the sample of test 3 had a second peak. The different behavior is also appreciated in the DCS curve, where their behavior does not match. To understand the behavior of epoxy resin type 2, more tests would be necessary.

The volatiles generated during the combustion process of the pyrolysis gases of the epoxy resin type 1 and type in air atmosphere were analyzed using FTIR. However, since the tests were conducted in an air atmosphere, the obtained signal was primarily

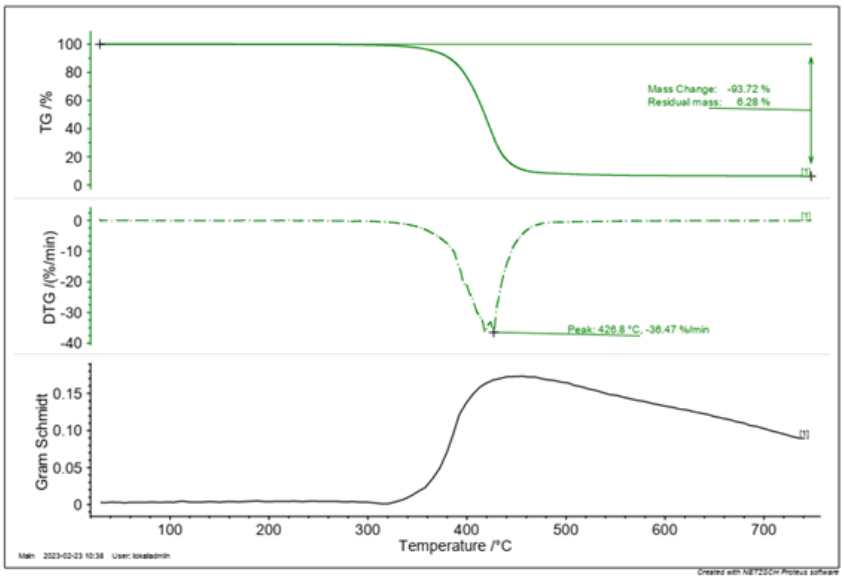

Figure 84: TG curve, DTG curve and DSC curve of the test of the fresh epoxy resin using the TGA -DSC with a heating rate of 20K/min in air atmosphere.

dominated by CO2 for all three samples. Therefore, it was decided not to include the graphs.

Comparing the thermal behavior of the fresh epoxy resin and epoxy resin type 1, it is noticeable that their onset temperatures are similar, and the temperature at which the first peak mass loss rate occurs is also similar among the three materials. Despite these similarities, each TG, DTG, and DSC curve displays distinctive characteristics, indicating differences in the thermal behavior of the materials.

4.4.2 Results of the thermogravimetric analyzer in nitrogen atmosphere

For epoxy resin type 1 in nitrogen atmosphere, the thermogravimetric (TG) curve exhibits a single primary stage of mass loss, which is characterized by a rapid rate of weight loss. This stage initiates at approximately 350°C-370°C and terminates at 470°C. Notably, the highest rate of mass loss is observed at a temperature of 418°C, as depicted in figures 85 and 86 . The TG curve also reveals a residual mass of 6.26% for test 1 and 5.42% for test 2, indicative of the remaining solid material after the mass loss event.

The FTIR absorbance spectra obtained during the thermal scan underwent analysis using a standard library. The analysis revealed that the primary compound detected was 2-Octenyl succinic anhydride (C12H18O3, molecular weight 210.27).

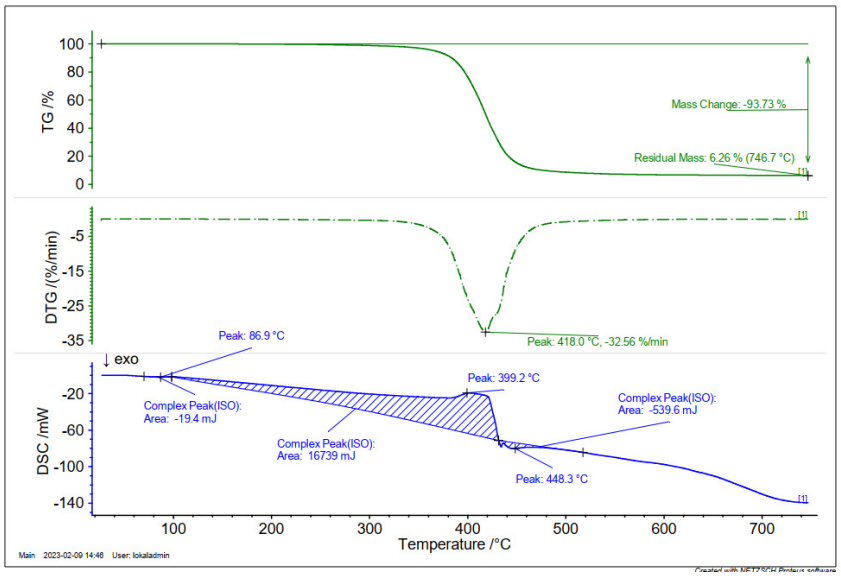

Figure 85: TG curve, DTG curve and DSC curve of two tests of epoxy resin type 1 using the TGA - DSC - FTIR with a heating rate of 20K/min in nitrogen atmosphere. Test 1.

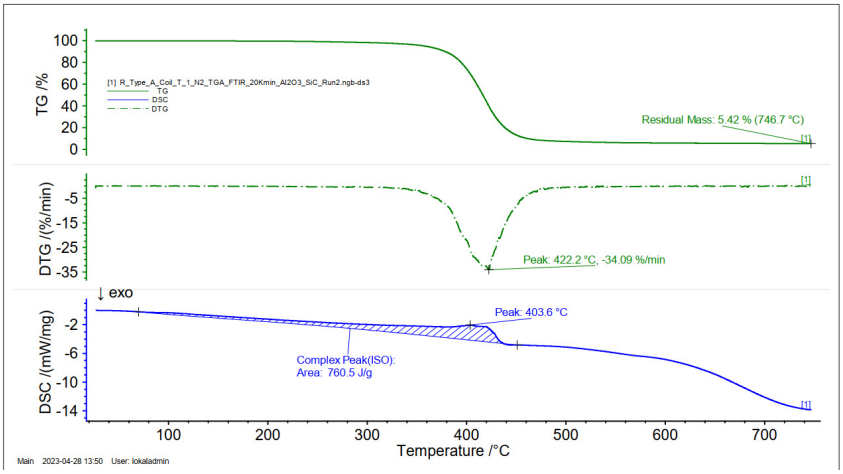

Figure 86: TG curve, DTG curve and DSC curve of two tests of epoxy resin type 1 using the TGA - DSC - FTIR with a heating rate of 20K/min in nitrogen atmosphere. Test 2.

For epoxy resin type 2 in nitrogen atmosphere, tests 3 and 4 both exhibit an onset temperature of approximately 310°C, which terminates at 470°C. Figures 89 and 90 illustrate that the maximum mass loss rate for samples in test 3 and test 4 occurs at 423.1°C and 420°C, respectively. As observed in previous tests conducted in an air atmosphere, residual mass is also present after these tests. For test 3, the residual mass is measured to be 44.07%, while for test 4, it is 44.69%.

Figure 92 displays the FTIR absorbance spectra obtained during the thermal scan, which were subsequently analyzed using a standard library. The results of the analysis indicated that the dominant compound detected in the spectra was cyanoacetic acid (C3H3NO2, molecular weight 85.06).

As a result of the tests in nitrogen, it is possible to conclude the thermal stability, that is the ability of a material to resist changes in its properties or structure when exposed

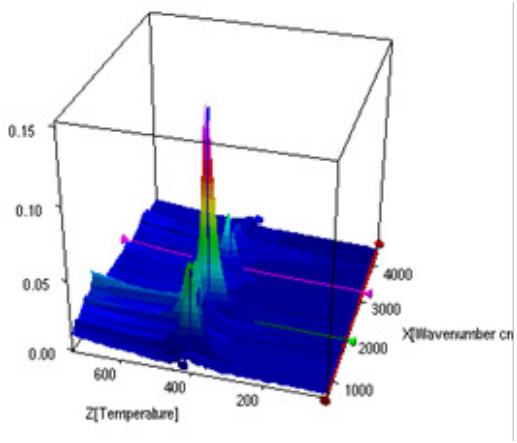

Figure 87: Overall FTIR absorbance spectra during the thermal scan in TGA. Epoxy Resin Type 1

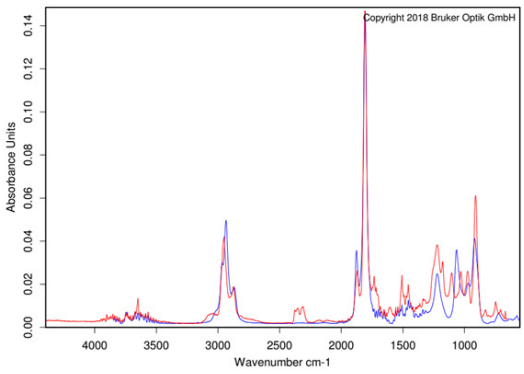

Figure 88: Extracted spectrum of the peak at around 400 °C showing match of the query spectra with the library one. Epoxy Resin Type 1. 2-Octenyl succinic anhydride was detected

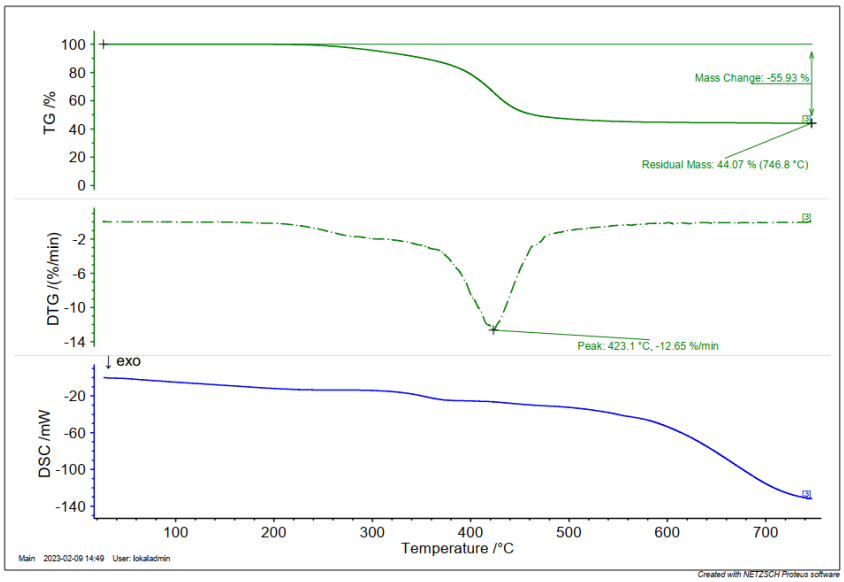

Figure 89: TG curve, DTG curve and DSC curve of two tests of epoxy resin type 2 using the TGA - DSC - FTIR with a heating rate of 20K/min in nitrogen atmosphere. Test 3.

Material	Onset temperature (°C)	Temperature at peak mass loss rate (°C)	Residual mass
Epoxy Resin Type 1	360	418, 422.2	6.26%, 5.42%
Epoxy Resin Type 2	310	423.1, 420	44.07%, 44.69%.

Table 30: Results of the tests of the three material using the TGA – DSC in nitrogen atmosphere.

to high temperatures, of the epoxy resin type 2 is lower than for epoxy resin type 1, as its onset temperature is lower.

Similar to the tests in air atmosphere, the tests show the epoxy resin type 2 contains a non-flammable material that is approximately 44% of the total mass of the sample.

After analyzing the data from the FTIR in nitrogen atmosphere, it was found that the primary compound detected during the TGA-DCS-FTIR test of epoxy resin type 1

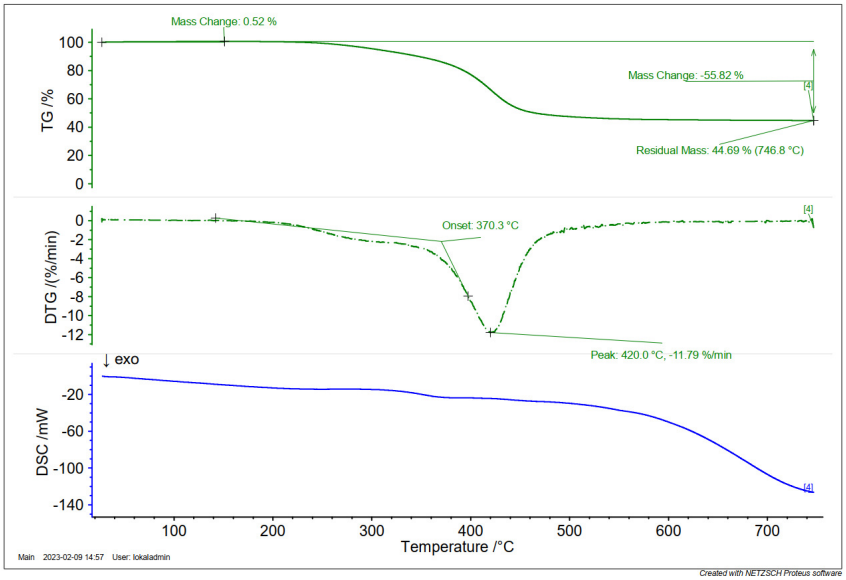

Figure 90: TG curve, DTG curve and DSC curve of two tests of epoxy resin type 2 using the TGA - DSC - FTIR with a heating rate of 20K/min in nitrogen atmosphere. Test 4.

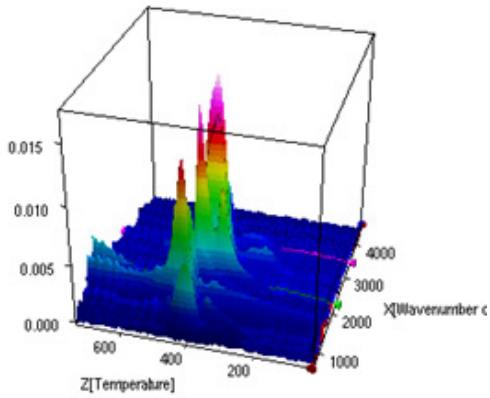

Figure 91: Overall FTIR absorbance spectra during the thermal scan in TGA. Epoxy Resin Type 2

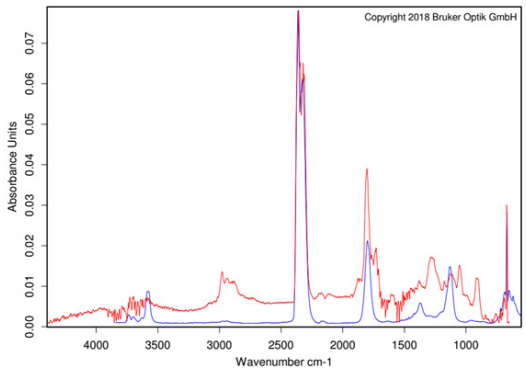

Figure 92: Extracted spectrum of the peak at around 400°C showing match of the query spectra with the library one. Epoxy Resin Type 2. Cyanoacetic acid was detected.

is 2-Octenyl succinic anhydride. As discussed in section 2.1, anhydrides are commonly used as hardeners in epoxy resin formulations. By comparing the hardener used in the production of the fresh epoxy resin with the one used in epoxy resin type 1, it can be inferred that the two formulations have similar compositions. This is also suggested by the results from the MCC, as seen in figures 23 and 27.

The following list presents the key findings of this section:

- The composition of epoxy resin type 1 and epoxy resin type 2 are different.
- The analysis revealed that the hardener used in epoxy resin type 1 is a anhydride, which is also the same curing agent utilized in the production of fresh epoxy resin with a known composition.
- Upon analysis, it was discovered that the curing agent utilized in epoxy resin type 2 is a carboxylic acid.
- Epoxy resin type 2 contains a non-flammable filler material.

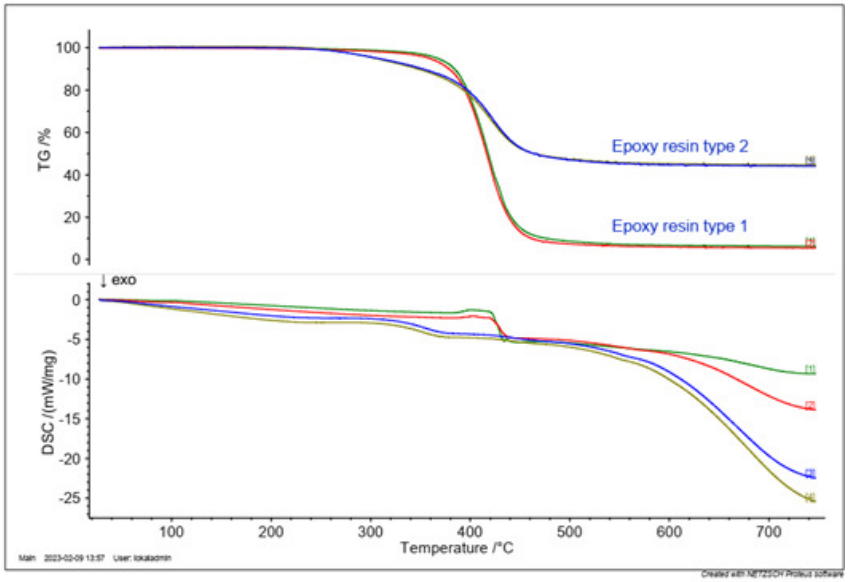

Figure 93: TG curve and DSC curve of two tests of epoxy resin type 1 and two test of epoxy resin type 2 using the TGA - DSC - FTIR with a heating rate of 20K/min in nitrogen atmosphere.

- The peak mass loss temperature obtained in the TGA analysis is comparable to the peak heat release temperature obtained in the MCC test. However, minor variations in the values can be attributed to the different heating rates utilized in each experiment.

5 Discussion

Based on the findings derived from the MCC and TGA tests, it is clear that there are discernible variations in composition and flammability between epoxy resin type 1 and epoxy resin type 2. Moreover, the bench-scale tests conducted on epoxy composite type 1 and epoxy composite type 2 also demonstrate distinct behaviors. Conversely, the micro-scale tests indicate a similarity in composition and flammability between epoxy resin type 1 and fresh epoxy resin, meaning the effects of radiation and aging on the flammability of the epoxy resin may not be significant.

For comparison purposes, it is worth comparing the results with the the flammability properties of polymethyl methacrylate (PMMA), a material that is well-known for its characteristics in this regard. When subjected to the same heating rate of 1 K/s using nitrogen and with a mass of 6 mg, PMMA displays a peak heat release rate of 364.4 W/g, an HRC of 364.4 J/gK, a peak heat release temperature of 387.2 °C and an onset temperature of pyrolysis of 297.9 °C(Q. Xu et al., 2016). Another polymer that can be compared is polyurethane (PU). When tested in the MCC with a heating rate of 1 K/s and a nitrogen atmosphere, PU shows a peak heat release rate of 393.4 W/g and a peak heat release temperature of 368.9 °C (Song et al., 2020). The HRC and peak heat release rate of PMMA are higher than those of epoxy resin type 2, but lower than those of epoxy resin type 1 and fresh epoxy resin. The peak heat release temperature of PMMA and PU are lower than that of the three types of epoxy resins. In terms of the onset temperature of pyrolysis, PMMA shares similarities with epoxy resin type 1 and fresh epoxy resin, but it is considerably lower than that of epoxy resin type 2.

In the experiments carried out by Scudamore et al. (1991) in the cone calorimeter, it was noted that the addition of fiberglass to the epoxy resin resulted in a decrease of the time of ignition. However, in the present study, when testing the epoxy composite using the cone calorimeter, Table 19 shows that the time of ignition increased. One possible explanation for this phenomenon is that the metallic core of the magnetic coil, which is wrapped in an epoxy composite, serves as a heat sink, causing a delay in the ignition time. Another possible explanation is the different composition of the epoxy resins used to manufacture the fresh epoxy resin samples and the magnet coils. Comparing the ignition times reported in Zhang et al. (2011) with those observed in this study, it is apparent that the ignition time for the fresh epoxy resin used in both studies is similar. However, the use of glass fiber tape and metallic core in the magnetic coil tested in this study appears to delay the ignition time, as evidenced by the difference in ignition times between the fresh epoxy resin and the samples of epoxy composite type 1 and type 2.

The results from the cone calorimeter tests conducted on epoxy composite type 1, type 2, and fresh epoxy resins were compared to those obtained by Scudamore et al. (1991), Zhang et al. (2011), Y. Xu et al. (2020), and (Wang & Zhang, 2019), but no clear relationship was found between the mean HRR, peak HRR, and EHC values. In some cases, the values obtained in this study were lower, while in others they were higher than those reported in the literature. It would be advised to conduct further investigation by reviewing existing literature and identifying the key parameters that may affect these

results. This can help to develop a more comprehensive understanding of the behavior of the materials under.

As discussed in section 3.2.2, the critical heat fluxes of ignition of the epoxy composite type 1, epoxy composite type 2 and fresh epoxy resin are 8.18, 10.40 and 5.84 kW/m^2 respectively. These values are lower than the critical heat flux of ignition of 12.12 kW/m^2 found from literature in section 2.2. This outcome indicates that all three epoxy resins tested, even when reinforced with fiberglass and forming part of the magnetic coil, exhibit a higher susceptibility to catching fire or igniting at lower levels of heat exposure. This finding shows the high flammability characteristics of these epoxy resins, emphasizing their increased fire risk.

To gain further insights, it is worthwhile to compare the obtained results with the critical heat flux values of other materials. For instance, in the case of PMMA, rigid PVC, and flexible PVC, the critical heat fluxes of ignition are reported as 10, 15, and 10 kW/m^2, respectively (Hurley et al., 2015). These critical heat flux values are comparable to the critical heat flux of the epoxy composite type 2 but higher than those of the other samples. However, it is crucial to note that the samples of epoxy composite type 2 include fiberglass and metallic coils, which may influence the overall flammability characteristics.

A more extensive range of tests would be required to provide a more conclusive understanding of their flammability characteristics. As discussed in section 3.2.4, the TGA results suggest that the curing agent of the epoxy resin type 1 and the fresh epoxy resin are similar. Additionally, it may be possible to assume the epoxy resin used to manufacture epoxy resin type 1 can be bisphenol A, meaning the composition of both resins are similar. However, the results from the MCC and the TGA do not show a significant difference in their flammability. It should be noted that these tests were limited in number, preventing us from reaching a conclusive statement. It is plausible that the flammability of the epoxy resins may vary significantly at higher temperatures or when exposed to the working conditions at CERN. Another area out of the scope of this thesis is the likelihood that the mechanical properties have been degraded, which could represent a ignition source, as stated in section 2.4. Further investigation and a more extensive range of tests would be required to provide a more conclusive understanding of their flammability characteristics.

The experiments conducted by McBride (1991) and Tarrio-Saavedra et al. (2008) suggest that the addition of filler materials and increasing their contents do not significantly affect the flammability values of epoxy resin. Considering that in figures 29, 30, 14, and 12, the onset temperature at which epoxy resin type 2 began pyrolyzing was faster than for epoxy resin type 1 and the fresh epoxy resin, it can be concluded that epoxy resin type 2 in the magnetic coil type 2 requires less heat to start pyrolyzing.

As part of the current thesis project, one of the objectives was to assess the relationship between results obtained from tests conducted on different scales. However, it was not possible to establish a numerical relationship between the micro-scale tests, such as MCC and TGA, and the macro-scale tests, such as the cone calorimeter and the LIFT, mainly due to the differences in the composition of the samples tested. The micro-scale tests only involved the testing of epoxy resins, while the macro-scale tests included glass fiber

reinforcement and metallic core, which inevitably affected the behavior of the epoxy resin. Nevertheless, qualitative consistency in the results was observed. For example, the peak heat release temperature from MCC and the peak mass loss temperature from the TGA were found to be similar for all three epoxy resins. Additionally, the order of classification regarding the heat released by each magnetic coil obtained using the MCC and cone calorimeter was consistent.

Based on the results obtained from the LIFT apparatus, it has been determined that in the event of an existing fire, the surface of magnetic coil type 2 would experience fire spread only when exposed to a minimum external heat flux of approximately 22.30 kW/m^2. In contrast, magnetic coil type 1 would require a minimum external heat flux of approximately 10.35 kW/m^2 for flame spread to occur. However, because flame spread also can also be influenced by other factors such as the object's geometry and orientation, the environmental and ventilation, it cannot be guaranteed that sustained burning would not occur if the minimum heat fluxes mentioned are not present.

A comparison of the values obtained from the LIFT with the parameters of other materials would give a better insight. For instance, the flame spread parameter for PMMA, fiberboard, and plywood is reported as 14, 2.3, and 13 kW^2/m^3, respectively (Quintiere, 2006). Overall, the results for the two epoxy composites exhibit significantly higher values. These elevated values can be attributed to the high thermal inertia associated with the epoxy composites and the low flame spread velocity even under high heat fluxes contributes. In summary, the epoxy composites demonstrate remarkable resistance to flame spread. According to Quintiere (2016), a typical range of lateral or downward spread on thick solids is 0.1 to 1 cm/s. Referring to Table 27, the flame spread velocity of epoxy composite type 1 can be regarded as relatively low, while the flame spread velocity of epoxy composite type 2 is significantly lower than the lower limit of this range.

Regrettably, no recommendations or findings could be derived on the impact of thickness and shape on the flammability of the epoxy resin. This is due to the fact that the samples obtained for the different tests were similar in terms of their thickness and/or size, despite the magnetic coils having different cross sections and geometries.

To prevent the magnetic coils from igniting due to exposure to an external heat flux from burning flammable materials, it is possible to estimate a safety distance between the coils and the materials. One approach could be to calculate the heat flux reaching the surface of the magnetic coil through radiation from the flames resulting from the ignition of the flammable material using view factors (Drysdale, 2011). However, due to the unique operational conditions of the facilities at CERN, any safety distance assessment must take into account the specific flammable materials in the area close to the magnetic coils. The reason is because the safety distance is dependent on the geometry and temperature of the flame produced by the flammable material, as these factors ultimately determine the heat flux that would reach the magnetic coil surface and cause ignition. To illustrate, it can be considered that magnetic coils of type 1 and type 2 are exposed to flames generated by the combustion of methane, which has a flame temperature of 1440 K, through a square window that measures 2 m x 2 m. The minimum distance required between the window and the magnetic coils to prevent ignition can be estimated based on the critical heat flux of ignition of the epoxy resin of each type of magnetic coil. To maintain a safe distance

between the magnetic coils and flammable materials, the critical heat flux of ignition for magnetic coil type 1 (8.18 kW/m^2) requires a minimum distance of 6.1 m from the window, whereas magnetic coil type 2, with a critical heat flux of ignition10.40 kW/m^2, needs a minimum distance of 5.32 m. However, it is possible to reduce the distance from the window to the magnetic coil by limiting the exposure time to the radiant heat flux. For instance, restricting the exposure time to 20 minutes (1200 s) increases the minimum heat flux of ignition for magnetic coil type 1 to 20.91 kW/m^2, reducing the minimum distance to 3.77 m. Similarly, for magnetic coil type 2, the minimum heat flux of ignition would be 19.47 kW/m^2, allowing for a minimum distance of 3.90 m from the window.

The subsequent list presents a summary of the primary results obtained in this section:

- The reviewed literature suggests that incorporating glass fiber laminates as reinforcement can reduce the ignition time of epoxy resin in comparison to unreinforced materials. However, the results of this thesis project indicate that the presence of a metallic core in magnetic coils leads to a substantial delay in the ignition time of epoxy resin, even when the resin is reinforced with glass fiber.
- The magnetic coil type 1 contains a higher amount of flammable material compared to magnetic coil type 2.
- The findings from the micro-scale and bench-scale tests clearly demonstrate a distinction in the composition of epoxy resin type 1 and type 2. Conversely, the micro-scale tests reveal a similarity in both composition and flammability between epoxy resin type 1 and the fresh epoxy resin.
- When exposed to the same external heat flux, the ignition time of epoxy resin type 1 is shorter compared to that of epoxy resin type 2, as suggested by the findings of the study.
- Despite the lack of a direct relationship between the micro-scale tests and the macro-scale tests, the flammability behavior of the samples showed qualitative consistency.
- No conclusions or recommendations were made regarding the influence of thickness and shape on the flammability of epoxy resins in magnetic coils due to the uniformity of the samples used in the tests, despite the magnetic coils having diverse cross sections and geometries.
- The safety distance between magnetic coils and flammable materials can be estimated by considering the geometry and temperature of the flames produced by the flammable material, as well as the critical heat flux of ignition for the epoxy resin of the magnetic coil. At CERN, due to unique operational conditions, any safety distance assessment must account for specific flammable materials in the surrounding area of the magnetic coil. In addition, the expected exposure time to external heat flux can impact the minimum safe distance required.
- The critical heat flux of ignition for the tested materials was found to be lower than the values reported in the literature for epoxy resins and epoxy compounds.

6 Recommendations

Certain characteristics that may help minimize fire risk were identified in magnetic coils during the current project. These characteristics can be taken into consideration while designing magnetic coil assemblies.

The results of the lateral ignition and flame spread test indicated that creating small gaps between segments of a magnetic coil can limit flame spread. This is because during flame spread, the area near the flame front is heated by radiation and heat conduction to a temperature that generates sufficient fuel gas for ignition and sustains the flame. However, the presence of gaps reduces the heat transfer through conduction. Although it may not be feasible to apply this to magnetic coils since they need a continuous surface to conduct electrical current, it could be useful for preventing flame propagation between magnetic coils. Therefore, this characteristic could be considered in designing magnetic coil assemblies to minimize fire risk.

Based on the test results, it can be inferred that epoxy resin type 1 exhibits higher flammability compared to epoxy resin type 2, particularly in terms of HRR. Epoxy resin type 1 would contribute more significantly to the intensity and spread of a fire, enabling fire propagation across its surface to a greater extent. Furthermore, epoxy resin type 1 demonstrates a lower critical heat flux of ignition when subjected to an external heat flux exceeding a certain threshold for a duration of over 54 minutes. This indicates that it requires less heat exposure to ignite and initiate sustained combustion compared to epoxy resin type 2. Meaning it would be recommended to use epoxy resins in the manufacturing of new magnetic coils similar to epoxy resin type 2.

An additional suggestion is to raise the proportion of the metallic core in relation to the thickness of the glass fiber-reinforced epoxy composite. This is based on the findings of the present study, which indicate that the metallic core has a retarding effect on ignition time.

To further enhance safety measures at CERN, it is recommended to assess the irradiation levels and total operation time of the magnetic coils. According to the literature, radiation and aging can deteriorate the properties of epoxy resins. Hence, it can be inferred that areas with lower radiation doses are relatively safer, whereas those with radiation doses greater than 10 MGy pose a higher risk of fire hazards, necessitating the implementation of supplementary precautions to ensure fire safety. Furthermore, it can be deduced that the safety of newly installed magnetic coils is higher than that of the ones which have been in operation for a longer period. The latter may require more attention to be paid to their maintenance in order to ensure their safety.

Lastly, it has been suggested by the literature by (Mouritz & Gibson, 2007) that adding flame retardant fillers during the production of epoxy resin could be a potential recommendation. However, it would be necessary to further investigate their performance as part of magnetic coils, under the influence of the radiation environment at CERN and their susceptibility to aging effects.

7 Future work

To conduct a more comprehensive study of the flammability of magnetic coils used at CERN, further tests on more epoxy resins and epoxy composites would be required. As described in the current project, the choice of test method depends on the scale of the samples being tested. To evaluate the flammability of epoxy resin with or without fillers, it would be suggested to carry out experiments in the MCC. It is important to note that the behavior of epoxy resin may vary depending on the type of atmosphere used to pyrolyze the samples. However, based on the project results, it can be concluded that the flammability classification and behavior of each epoxy resin would remain in the same order when compared to others. Alternatively, if the aim is to evaluate the flammability of epoxy compounds in the magnetic coil, it would be more appropriate to use the cone calorimeter or the LIFT, given that the interaction between the epoxy and magnetic core can affect the results. To assess the flammability using the cone calorimeter, it is recommended to perform the test at three different heat fluxes to analyze the ignition behavior of each sample. On the other hand, in the case of the LIFT, it is advisable to produce continuous samples to avoid interruptions in flame spread.

Ideally, if further tests are conducted to evaluate the flammability of epoxy resins using bench-scale tests, it would be highly desirable to manufacture standardized samples. This approach would facilitate easier comparison of the test results and enhance the overall reliability of the findings. However, it is important to acknowledge that this suggestion may not be feasible due to the high cost associated with the production of magnetic coils.

The literature review indicates that the effects of radiation and aging on epoxy compounds are influenced by the initial properties of the resin and environmental factors. Therefore, for a comprehensive evaluation of the epoxy compounds in this study, it is recommended to test samples of recently produced magnetic coils and compare their flammability with the findings of this project. Moreover, testing the mechanical properties of epoxy resins exposed to operational conditions and comparing them with new ones will help evaluate the potential for mechanical failure, which could represent a potential ignition source.

As a part of future tasks, performing a chemical characterization of the samples and their residues analyzed in the current project could also be beneficial to identify the constituents of the epoxy resin and non-combustible fillers used in the magnetic coils.

In order to explore potential future actions, it is highly recommended to compare the operating conditions of the magnetic coils at CERN with those mentioned in this report. This comparative analysis would provide valuable insights into the extent to which the testing conditions align with the actual operational conditions.

8 Conclusions

As part of the current thesis project, an assessment was conducted on the flammability of three epoxy resins that are commonly used in magnetic coils at CERN. The assessment involved subjecting representative epoxy resins and epoxy resin composites to four standardized test methods: the MCC, the cone calorimeter, the LIFT, and the TGA+FTIR. Additionally, a literature review of the characterization of epoxy resins and their composition was conducted, and the factors that affect the flammability of epoxy resins were identified.

The relationship between micro-scale tests (MCC and TGA) and bench-scale tests (cone calorimeter and LIFT) could not be directly established due to differences in the composition of the tested samples. However, it was noted that the qualitative behavior of the samples regarding flammability was consistent across the different tests.

The impact of radiation on epoxy resins was investigated, and it was determined that chain scission and crosslinking are the primary destructive mechanisms, causing a reduction in properties and an increase in flammability. Epoxy resins may also become brittle when exposed to high radiation doses, typically above 10 MGy. However, the effects of radiation on epoxy resins over an extended exposure period are still not well understood, and further research would be needed to explore this area. Similarly, the flammability of epoxy resins can also be affected by aging, as polymers tend to become more flammable over time. However, in order to assess the effects of aging on the magnetic coils, new samples would need to be tested.

According to the literature review, adding glass fiber reinforcement to epoxy resin tends to decrease ignition time. However, the experiments conducted in this project found that the presence of a metallic core in magnetic coils led to a delay in ignition time, even when using epoxy composites made of glass fiber-reinforced epoxy resin.

Acknowledgements

Firstly, I wish to extend my profound gratitude to my supervisors Konrad Wilkens Flecknoe-Brown and Patrick Van Hees for their unwavering support and guidance throughout the entirety of the semester. Their dedication and mentorship helped me navigate the challenges and complexities of my research.

I would like to express my heartfelt gratitude to Dan Madsen for his indispensable role in facilitating my access to Lund University's laboratory and assisting me in organizing the extensive number of tests that formed a vital part of this thesis.

I am deeply grateful to Darko Perović, my co-supervisor from CERN, for his invaluable guidance and insightful suggestions throughout the process of writing this thesis. Without his help, this work would not have been possible.

Many thanks to Martin Gunder. His generous support, availability, and kindness have enabled me to complete my work efficiently and safely.

I am immensely grateful to DBI for their invaluable contribution to the completion of this project by conducting the TGA+FTIR analysis. I would also like to extend my heartfelt appreciation to Dr. Abhishek Bhargava, whose unwavering support and guidance have been instrumental in bringing this thesis to fruition. His contributions have played an essential role in ensuring its successful completion, and for that, I owe him a debt of gratitude.

Finally, I want to emphasize the profound significance of my family's unwavering support throughout my academic journey, which I hold dear to my heart. In particular, I would like to express my heartfelt appreciation and love to my mother, who has been a constant source of love, encouragement, and limitless support. Her unwavering dedication has been an immense source of inspiration and strength for me.

References

ASTM. (2018). *E1321 - standard test method for determining material ignition and flame spread propertie* (ASTM International). American Society for Testing and Materials. West Conshohocken, Pennsylvania, The United States of America.

ASTM. (2021). *D7309 - standard test method for determining flammability characteristics of plastics and other solid materials using microscale combustion calorimetry* (ASTM International). American Society for Testing and Materials. West Conshohocken, Pennsylvania, The United States of America.

Ayoola, B., Balachandran, R., Frank, J., Mastorakos, E., & Kaminski, C. (2006). Spatially resolved heat release rate measurements in turbulent premixed flames. *Combustion and flame*, *144*(1-2), 1–16.

Brugner, F., & Jonnatti, A. (1983). An air pyrolysis study of cast bisphenol a epoxy transformer coils. *IEEE Transactions on Power Apparatus and Systems*, (7), 2203–2207.

Dao, D. Q., Luche, J., Richard, F., Rogaume, T., Bourhy-Weber, C., & Ruban, S. (2013). Determination of characteristic parameters for the thermal decomposition of epoxy resin/carbon fibre composites in cone calorimeter. *International journal of hydrogen energy*, *38*(19), 8167–8178.

Debré, O., Nsouli, B., Thomas, J.-P., Stevenson, I., Colombini, D., & Romero, M.-A. (1997). Gamma irradiation-induced modifications of polymers found in nuclear waste embedding processes part i: The epoxy/amine resin. *Nuclear Instruments and Methods in Physics Research Section B: Beam Interactions with Materials and Atoms*, *131*(1-4), 313–320.

Drysdale, D. (2011). *An introduction to fire dynamics*. John wiley & sons.

Ellis, B., et al. (1993). *Chemistry and technology of epoxy resins*. Springer.

Guarino, F., Tavlet, M., & Hauviller, C. (2001). *Compilation of radiation damage test data*. CERN.

Hurley, M. J., Gottuk, D. T., Hall Jr, J. R., Harada, K., Kuligowski, E. D., Puchovsky, M., Watts Jr, J. M., WIECZOREK, C. J., et al. (2015). *Sfpe handbook of fire protection engineering*. Springer.

ISO. (2002). *5660-2:2002(e) reaction-to-fire tests — heat release, smoke production and mass loss rate* (ISO). The International Organization for Standardization. Geneva, Switzerland.

Kacem, I., Daoudi, M., Dridi, W., Sellemi, H., Harzli, K., De Izzara, G., Geslot, B., Guermazi, H., Blaise, P., Hosni, F., et al. (2019). Effects of neutron–gamma radiation on the free radical contents in epoxy resin: Upconversion luminescence and structural stabilization. *Applied Physics A*, *125*, 1–9.

Kong, E. S.-W. (2005). Physical aging in epoxy matrices and composites. In *Epoxy resins and composites iv* (pp. 125–171). Springer.

Longiéras, N., Sebban, M., Palmas, P., Rivaton, A., & Gardette, J.-L. (2007). Degradation of epoxy resins under high energy electron beam irradiation: Radio-oxidation. *Polymer Degradation and Stability*, *92*(12), 2190–2197.

Lyon, R., Walters, R., Stoliarov, S., & Safronava, N. (2013). Principles and practice of microscale combustion calorimetry. *Federal Aviation Administration: Atlantic City International Airport, NJ, USA*, 1–80.

McBride, S. (1991). *Cast coil transformer fire susceptibility and reliability study* (tech. rep.). EG and G IDAHO INC IDAHO FALLS.

McKenna, S. T., Jones, N., Peck, G., Dickens, K., Pawelec, W., Oradei, S., Harris, S., Stec, A. A., & Hull, T. R. (2019). Fire behaviour of modern façade materials–understanding the grenfell tower fire. *Journal of hazardous materials*, *368*, 115–123.

Montserrat, S. (1994). Physical aging studies in epoxy resins. i. kinetics of the enthalpy relaxation process in a fully cured epoxy resin. *Journal of Polymer Science Part B: Polymer Physics*, *32*(3), 509–522.

Mouritz, A. P., & Gibson, A. G. (2007). *Fire properties of polymer composite materials* (Vol. 143). Springer Science & Business Media.

Mulholland, G. W., & Croarkin, C. (2000). Specific extinction coefficient of flame generated smoke. *Fire and Materials*, *24*(5), 227–230.

Odegard, G., & Bandyopadhyay, A. (2011). Physical aging of epoxy polymers and their composites. *Journal of polymer science Part B: Polymer physics*, *49*(24), 1695–1716.

Ovsik, M., Manas, M., Stanek, M., Dockal, A., Vanek, J., Mizera, A., Adamek, M., & Stoklasek, P. (2020). Polyamide surface layer nano-indentation and thermal properties modified by irradiation. *Materials*, *13*(13), 2915.

Oyanguren, P. A., & Williams, R. J. (1992). Analysis of the epoxidation of bisphenol a and phenolic novolacs with epichlorohydrin. *Polymer*, *33*(11), 2376–2381.

Quintiere, J. G. (2006). Fundamentals of fire phenomena.

Quintiere, J. G. (2016). *Principles of fire behavior*. CRC Press.

Saadatkhah, N., Carillo Garcia, A., Ackermann, S., Leclerc, P., Latifi, M., Samih, S., Patience, G. S., & Chaouki, J. (2020). Experimental methods in chemical engineering: Thermogravimetric analysis—tga. *The Canadian Journal of Chemical Engineering*, *98*(1), 34–43.

Schartel, B., & Hull, T. R. (2007). Development of fire-retarded materials—interpretation of cone calorimeter data. *Fire and Materials: An International Journal*, *31*(5), 327–354.

Schönbacher, H., & Van de Voorde, M. H. (1975). *Radiation and fire resistance of cable-insulating materials used in accelerator engineering* (tech. rep.). CERN.

Scudamore, M., Briggs, P., & Prager, F. (1991). Cone calorimetry—a review of tests carried out on plastics for the association of plastic manufacturers in europe. *Fire and Materials*, *15*(2), 65–84.

Song, X., Chi, H., Li, Z., Li, T., & Wang, F. (2020). Star-shaped crosslinker for multifunctional shape memory polyurethane. *Polymers*, *12*(4), 740.

Spindel, A. (1993). *Report on the program of 4 k irradiation of insulating materials for the superconducting super collider* (tech. rep.). Superconducting Super Collider Lab., Dallas, TX (United States).

Tarrio-Saavedra, J., López-Beceiro, J., Naya, S., & Artiaga, R. (2008). Effect of silica content on thermal stability of fumed silica/epoxy composites. *Polymer Degradation and Stability*, *93*(12), 2133–2137.

Torero, J. (2016). Flaming ignition of solid fuels. *SFPE handbook of fire protection engineering*, 633–661.

Wang, H., & Zhang, L. (2019). Pyrolysis and combustion characteristics and reaction kinetics of carbon fiber/epoxy composites. *AIP Advances*, *9*(12), 125110.

Weil, E. D., Patel, N. G., Said, M., Hirschler, M. M., & Shakir, S. (1992). Oxygen index: Correlations to other fire tests. *Fire and materials*, *16*(4), 159–167.

Wood, A. W., & Karipidis, K. (2017). Non-ionizing radiation protection: Summary of research and policy options.

Wu, Z., Li, J., Huang, C., Huang, R., & Li, L. (2013). Effect of gamma irradiation on the mechanical behavior, thermal properties and structure of epoxy/glass-fiber composite. *Journal of nuclear materials*, *441*(1-3), 67–72.

Xie, Q., Zhang, H., & Tong, L. (2010). Experimental study on the fire protection properties of pvc sheath for old and new cables. *Journal of hazardous materials*, *179*(1-3), 373–381.

Xu, Q., Jin, C., Griffin, G. J., Matala, A., & Hostikka, S. (2016). A pmma flammability analysis using the mcc: Effect of specimen mass. *Journal of Thermal Analysis and Calorimetry*, *126*, 1831–1840.

Xu, Q., Jin, C., Majlingova, A., & Restas, A. (2018). Discuss the heat release capacity of polymer derived from microscale combustion calorimeter. *Journal of Thermal Analysis and Calorimetry*, *133*, 649–657.

Xu, Y., Lv, C., Shen, R., Wang, Z., & Wang, Q. (2020). Comparison of thermal and fire properties of carbon/epoxy laminate composites manufactured using two forming processes. *Polymer Composites*, *41*(9), 3778–3786.

Zhang, W., Li, X., & Yang, R. (2011). Pyrolysis and fire behaviour of epoxy resin composites based on a phosphorus-containing polyhedral oligomeric silsesquioxane (dopoposs). *Polymer Degradation and Stability*, *96*(10), 1821–1832.